Cape Peninsula
University of Technology

DESIGN AND OPERATION OF A STAND-ALONE SOLAR PATHWAY FOR PUBLIC PARK LIGHTING

by

ABDULRAUF AHMED ASWAY ABAID

Thesis submitted in fulfilment of the requirements for the degree

Master of Engineering: Electrical Engineering

**in the
Faculty of Engineering at the
Cape Peninsula University of Technology**

Supervisor: **Prof. MTE Kahn**

Bellville
January 2017

DECLARATION

I, Abdulrauf Ahmed Asway Abaid, declare that the content of this thesis represents my own unaided work, and that the thesis has not previously been submitted for academic examination towards any qualification. Furthermore, it represents my own opinions and not necessarily those of the Cape Peninsula University of Technology.

Signed   Date

ABSTRACT

The development of solar roads to convert insolation on vast stretches of land to electrical energy, otherwise dedicated solely for transportation, is in its nascent stage. A great potential is seen for PV application with the maturing of solar road technology. Apart from increasing the versatility by smart utilization of land resources, widening the cover of renewable energy generation will lead to a sustainable, secure energy future. A stand-alone solar pathway for public park lighting or area lighting system, completely independent of the power grid, was designed and operated. Public lighting for 65 m stretch of walkway located next to the Electrical, Electronic and Computer Engineering Department building, was chosen as a case study in this study. The case study presented simplified method for sizing, performance evaluation and simulation of a stand-alone solar pathway to power public lighting on the Bellville Campus of the Cape Peninsula University of Technology.

Depending on the requirements of the electrical, the quantity and quality of lighting, as well as the required duration of the lighting were calculated. Battery storage capacity, based on the desired autonomy period, and maximum and average daily depth of discharge, were sized. PV array size, based on the type and specifications of PV module, the time of year with the highest average daily lighting load and minimum solar radiation, were selected and measured. Control strategies for battery protection and lighting control conditions were determined, and the control set points were specified. The operating efficiency of solar pathway was evaluated and showed excellent performance compared to the expected with annual average value of the monthly performance ratio and system efficiency. A stand-alone solar pathway system was programmed using MATLAB, in order to size a PV system to the supply public lighting for the walkway. The computer program used, can be applied to any site with different weather conditions.

ACKNOWLEDGEMENTS

First and foremost, all praise be to ALLAH for giving me the opportunity to complete my research work successfully.

My sincere gratitude and appreciation to my supervisor, Professor MTE Kahn, for his invaluable guidance, enthusiastic help, and consistent encouragement throughout the entire research project.

Special thanks to Dr. Ali Almaktoof for his help and encouragement throughout this journey.

Thanks to all my friends and colleagues in the Department of Electrical Electronic and Computer Engineering, support and encouragement during my study.

I acknowledge Mr. Niels Wieffering; his intensive editing work is highly appreciated. And also, I thank Dr. Atanda Raji

For all the unconditional love and support and patience, for all the encouragement and sacrifices, I dedicate this thesis to my parents, my wife Siham, my three daughters Janait, Retal and Braah, and my brothers and my sisters.

ABDULRAUF AHMED ASWAY ABAID

Table of Contents

LIST OF FIGURES

LIST OF TABLES

ABBREVIATIONS and NOMENCLATURE

α	temperature coefficient of power(per ^{o}C)
A	temperature modification factor
AC	alternating current
As	active cell area
BIPV	building integrated PV
C	required capacity
C	longest days without Sunlight
CdTe	cadmium telluride
CIGS	copper-indium-gallium-diselenide
CPV	concentrator photovoltaic
D	solar declination (degrees)
DC	direct current
D_j	diode impedance
DOD	depth of discharge
Ea	array output energy (kWh/d)
EPV	PV energy consumed (kWh).
FF	fill factor
GSTC	reference irradiation at STC = 1 (kW/m^2)
Gt	average daily of hours sunshine (solar rad. / 1000 W.m^{-2})
H	solar hour angle (degrees)
H_i	mean radiation in the plan of array (kWh/m^2.d)
I	load current (A)
I_j	current flow
I_L	Current
I_L	daily required capacity, (Ah)

I_{mp}	current at maximum power point
I_{sc}	short circuit current
L	latitude (degrees)
L_C	capture losses
LED	light-emitting diode
L_S	system losses
mc-Si	multi crystalline silicon
MPPT	maximum power point tracker
N	Julian day number (1-365)
NASA	National Aeronautics and Space Administration
NASA SSE	NASA surface meteorology and solar energy
N_{PV}	number of PV panels.
NREL	National Renewable Energy Laboratory
Pa, max	peak array power (kW)
P_{in}	input power of the cell
P_m	maximum power under standard condition (watt)
P_{mx}	maximum output power from one PV module (watt)
P_o	peak power (Wp)
P_{out}	electrical output power of the cell
PR	performance ratio
P_s	solar radiation level per unit area
PSH	peak sun hours
PV	photovoltaic
R	overall efficient circuit modification factor
RES	renewable energy system
R_L	resistive load
R_s	series resistance
R_{sh}	shunt resistance

sc-Si	single crystal silicon
SHS	solar home systems
SSE	surface meteorology and solar energy
SSP	stand-alone solar pathway
STC	standard tests conditions
T	night hours (sunset to sunrise)
T	daily use time, (hours)
T_a	the average ambient temperature (^oC)
TL	total system losses (per unit).
U	discharge depth
V	Voltage
V_{mp}	voltage at maximum power point
V_{oc}	open circuit voltage
VRLA	valve-regulated lead-acid
Y_A	array yield
Y_F	final yield
Y_R	reference yield
ηA, mean	mean array efficiency
ηsys	system efficiency
ηtot	total efficiency

CHAPTER ONE

INTRODUCTION

1.1 Background

The current world population of 7.2 billion is projected to reach 9.6 billion by 2050, according to a United Nations report which points out that growth will be mainly in developing countries, with more than half in Africa (UN News, 2013) . In order to provide this growing population with a reasonable standard of living, sustained economic development is essential; such development will require a corresponding increase in the production of energy. The extra energy required will have to be provided from sources other than the traditional ones. Furthermore, when taking the concept of sustainable development into account, consideration must be given to environmentally friendly energy sources. These energy sources are also known as renewable or sustainable energy sources. Renewable energy is understood as energy that is obtained from the continuing flows of energy occurring in the natural environment, such as solar energy(Zeman, 2003). In recent years the use of renewable energy systems (RESs) has become very important due to environmental concerns and the increased demand for energy. Using RESs can substantially reduce harmful emissions from polluting the environment, while also offering inexhaustible resources of primary energy.

The conversion of solar energy into electricity takes place in a solar cell, which is a semiconductor device. Commercially available solar cells typically deliver a relatively small quantity of power. To use solar electricity for practical devices requires a particular voltage or current for their operation; a number of solar cells have to be connected together to form a solar panel, also called a PV module. For large-scale generation of solar electricity the solar panels are connected together into a solar array (Zeman, 1998).

Photovoltaic conversion is the direct conversion of sunlight into electricity with no intervening heat engine. Photovoltaic devices are solid state, making them rugged, simple in design, and low-maintenance. Perhaps the biggest advantage of solar photovoltaic devices is that they can be constructed as stand-alone systems to give outputs ranging from microwatts to megawatts, which is why they are used as a power source for calculators, watches, water pumps, remote buildings, communications, and street lighting (Goswami et al., 2007).

Cells are configured into panels (or modules) resulting in wide range of commercially available panels with differing outputs. The panels are in turn connected to form arrays, these panels, or arrays can be used to charge batteries, operate motors, and to power any number of electrical loads. With appropriate power conversion equipment, PV installations can produce alternating current compatible with any conventional appliances, and can be operated in parallel with a utility grid.

Direct conversion of solar energy using PVs to provide electricity in small quantities for stand-alone solar pathway (SSP) applications is competitive when compared to alternatives such as diesel, or a grid extension; these alternatives need continuous maintenance and are associated with high costs (Markvart, 2000).

A literature survey was conducted to establish what types of lighting system configurations exist for PV operation, the performance of each of these configurations, and how the efficient each of the components is . Components typically used in a PV-powered lighting system may include PV panel, battery, electricity grid, power conditioning unit (to provide DC output), AC load centre (to provide AC output), DC-DC converter, AC-DC converter (LED AC driver), DC current regulator, and luminaires. Depending on the light source and the different application requirements, the system configuration will not necessarily include all these components.

Three major types of system configuration exist for PV-powered lighting systems; they are the stand-alone system, the utility grid-connected system, and the hybrid system (Patel et al., 2011). Stand-alone systems are mostly seen as residential pathway markers, parking lot luminaires, and off-grid lighting networks for facilities. These stand-alone systems normally require batteries, which introduces high storage-retrieval losses and high maintenance costs (Patel et al., 2011). Grid-connected systems do not require batteries; instead they are connected to an electricity grid and draw power from the grid when the solar power provided by the PV panels is insufficient for the intended application.

Depending on the type of load, a power conditioning unit or an AC load centre is needed in grid-connected systems to adjust the input power from the utility grid. Optionally, some grid-connected systems can feed power back to the grid when the PV panels generate more energy than needed. Hybrid systems combine a number of electricity production and storage elements to meet the energy demand — for example, a grid-connected system with a battery backup. These systems are complicated and expensive but are more reliable, especially when connected to a utility grid.

Utilising a sectionalised, controlled luminaire provides a solution to the energy and pollution problems associated with current roadway lighting technology. In order to advocate the necessary development in off-grid lighting, the overall luminaire system will address the excessive costs, robustness, and energy efficiencies of existing street lights. By effectively limiting operational time and creating a self-sustaining system, the design will reduce the amount of excess lighting during the night and eliminate the need for grid-connected roadway lighting.

If our transportation infrastructure, being all the highways, pathways and roads in a country, were solar panelled, it would produce enough electricity to fulfil the needs of every home and industry in the country. This will however, not get rid of electricity bills, there will still be a cost to distribute electricity to homes and businesses, but that cost could be reduced by 90%, which means cheaper consumer goods and commodities. Additionally such solar-panelled transport infrastructure would mean greater opportunities for indoor agriculture, which would increase food production and reduce food prices, as well as ending famine and food crises worldwide, and it would further create new industries and improve our environment by a hundred fold (VASSILI GROUP, 2016) .

It will encourage the increased manufacture of electric vehicles, which if all fossil-fuelled vehicles are replaced by electric vehicles, will transform our planet, our vegetation will improve by 100%, our clean air levels will improve by 50%, greenhouse damage will improve by 100% and global warming will go back to normal, all within 5 years (VASSILI GROUP, 2016) .

SolaRoad is a new concept for the generation of sustainable energy. It is a commercial venture specifically aimed at utilizing road surfaces for the harvesting of solar energy by integrating solar panels into the roadway surface. The generated electrical energy can be used for various applications, such as road lighting, public park lighting and traffic systems; households may benefit as well. In time, electric cars might possibly be able to make use of this energy as well. Part of the SolaRoad concept is that the energy will actually be generated at the place where it is needed; this is a big step towards an energy-neutral mobility system.

The first solar roadway opened in Amsterdam, the Netherlands, in November 2014; it was a 70-metre stretch of cycle path running between two suburbs of the city (Hruska, 2014b; Shekhar et al., 2015). The SolaRoad, as it has been named by the Netherlands Organization for Applied Scientific Research, is made up of rows of crystalline silicon solar cells. The surface of the road has been treated with a special non-adhesive coating, and the road itself was built to sit at a slight tilt in an effort to keep dust and dirt from accumulating and obscuring the solar cells.

The path cost about USD 4.3 million. The path was created as the first step in a project, to be extended to 100 meters, with the local authority initiating a first phase of 70 metres — so by 2016 (which is now) they will have added another 30 metres (Hruska, 2014b; Schmidt, 2014; Shekhar et al., 2015). One reason why these solar panels were installed on a cycle path is that the lighter loading will effect substantially less wear-and-tear than the traffic consisting of cars and trucks. According to studies, one reasonable method of estimating road wear is the so-called fourth-power law, which states that the damage a vehicle causes to a road surface is related to the fourth power of its axle weight. Speed and tire pressure also play a part, but the end result is that cars cause damage to the road surface which is at least several thousand times higher than what bicycles do; trucks in turn, cause damage which is thousands of times more than what cars do. A solar road surface for a cycle path is therefore subject to stresses which are several orders of magnitude less than that expected for a vehicular road surface (Hruska, 2014b; Shekhar et al., 2015)

1.2 Stand-alone Photovoltaic Pathway Technologies for Public Park Lighting

Solar energy is one of the most important clean energy technologies. Mounting solar panels which forms the roadway surface is a fairly recent development. The Netherlands Organization for Applied Scientific Research Institute in the Netherlands developed a concept by which solar cells could be laid out on a road surface using prefabricated slabs and then covering with a tempered glass. The glass must be very strong. and withstand a heavy weight. An added safety feature is that the glass surface is skid-resistant. A cycle lane that connects the suburbs of Krommenie and Wormerveer in the Netherlands has been built using this concept. It is a busy cycle lane with over 2000 cyclists passing over it on a daily basis. The path is only a 70 metre stretch but the concept is slated to also be extended to roadways. This will enable the Netherlands to harness solar energy through almost 20% of its roadways, which is making a good contribution towards greener energy solutions in the world (Shekhar et al., 2015)

For a self-cleaning method there are nano coatings with self-cleaning and hydrophobic properties especially for photovoltaic (PV) panels. The self-cleaning properties stop dust and bird faeces from sticking to PV panels, keeping them clean, maintaining their efficiency, and ensuring the maximum amount of electricity is produced. Figure 1.1 shows the solar PV Self-Cleaning Solar Panel Coating. These coating benefits are easy-to-apply, hydrophobic panel coatings which can last up to 5 years and greatly reducing the need for expensive cleaning of the surfaces (NanoShell, 2016).

Figure 1.1: Solar PV Self-Cleaning Solar Panel Coating, (NanoShell, 2016).

Such paths can be used to power many things whether they are electric cars or the traffic signals, and while the idea is still in its nascent stages, it is a truly a wonderful direction to a greener future. Figure 1.2 depicts cyclists riding over a stretch of a new cycle path in the Netherlands, surfaced entirely with solar panels (Hruska, 2014a).

Figure 1.2: Cyclists ride over a stretch of a new cycle path surfaced entirely with solar panels in the Netherlands. (Hruska, 2014a)

With the benefits of no noise, no distribution wiring, a lower maintenance cost, and no electricity bills, the use of solar electric power has become very popular. Its application for lighting is just one of the applications. For a lighting application, the system consists of solar cells, a battery, lighting fixtures and with a connection to utility in general.

For a system which is backed up by the utility grid, design considerations do usually not include deliberation on how to achieve the best choice of capacities for the solar panels and the battery, nor are quantity and quality of the load for a system considered. However, in such places such as highways, pathways and roads, a stand-alone solar power system for lighting is very attractive and suitable, since it is cost effective. But a stand-alone solar power system for these places needs special consideration. The irradiation of sun changes with the seasons, the time of day, the location and the weather conditions; therefore, a good design of a stand-alone solar system must be considered and then take account of the capacities of battery and solar cell for a particular load. This project presents a design method and the procedure to calculate the required battery capacity for an SSP for public park lighting.

1.3 Statement of research problem

The main research problems can be stated as:

- Is it possible to develop a sustainable stand-alone solar pathway for public park lighting using an optimum mix of low cost PV modules designed for light loading, with embedded battery packs and associated electronics to achieve the objective?

- To evaluate by simulation and selection, the best convertor, battery sizing and PV system array deployment to achieve the objective.

- A secondary problem would be assessing the choices in public lighting to fulfil the above objective with the best efficiency.

1.4 Objectives of the Research

The main focus of this project is to determine the options that are available to replace grid-powered street lamps with a stand-alone system that has the reliability to work under the worst conditions. The renewable energy source selected for this project is a photovoltaic pathway technology. The study was undertaken to determine the capabilities of stand-alone systems and to determine if the long-term saving of electricity warrants the conversion to new lamps powered off-grid by public park lighting.

The objectives of this research are to present a simplified method for sizing and performance evaluation of an SSP for public park lighting. A MATLAB/Simulink program was developed for the sizing and simulation of an SSP for public park lighting.

Simulations were carried out using MATLAB software to size and assess the performance of an SSP system. The computer program can be applied to any site with different weather conditions.

1.5 Significance of the research

A pathway for public park lighting is more practical as a pilot site (than for example a highway) for various reasons. A pedestrian path is less heavily loaded. It is also easier to make adjustments and to implement improvements to a pedestrian path..

1.6 Research Outlines

Research outlines are used to clearly define the activity needed to meet the research objectives; as mentioned earlier, the research objective is to size and assess the performance of an SSP system for public park lighting. Figure 1.3 shows the research outlines.

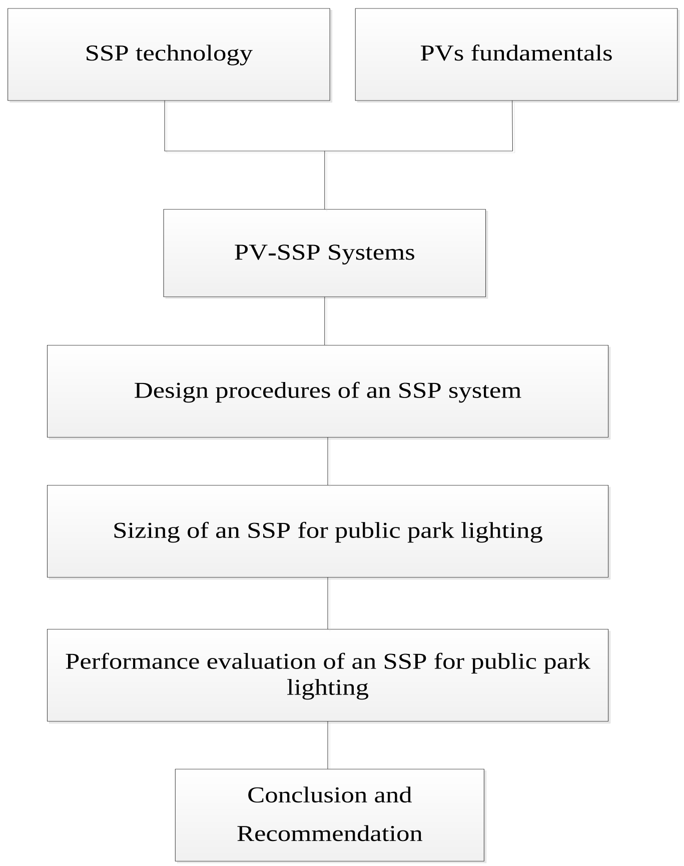

Figure 1.3: Research outlines.

1.7 Organization of the thesis

This thesis contains five chapters which are summarized as follows:

CHAPTER ONE provides an introduction to the thesis. It starts with a theoretical background on PV systems, after which the photovoltaic pathway technology system for public park lighting is highlighted. A statement of research problem and objectives of the research are presented. Next the research and research outlines are presented

CHAPTER TWO begins with a history of photovoltaics and the principles of solar PV cell operation, solar irradiation, and the effects of temperature and solar radiation on solar cells are discussed. Next, types of PV systems, highlighting their advantages and disadvantages, photovoltaic applications are presented, and an overview of commercially available PV systems is given. This followed by a presentation of PV lighting components. A summary is presented in the last section. The objective of this chapter is to provide interested readers with a general background of PV systems, and PV system components and their applications.

CHAPTER THREE provides an overview of PV lighting components, system design principles and existing quantities for system performance assessment and their limitations. This information is intended for those individuals who specify PV lighting equipment and evaluate system designs, as well as those who design and integrate systems. The methodology used for sizing and design of stand-alone PV lighting systems is presented. All the components that have been used in the design of the SSP are fully described in this chapter. The fundamentals and selection criteria for the major PV lighting system components — the PV array, batteries, controls and luminaires are presented in this chapter. Furthermore this chapter discusses the procedures in determining product sizing and provides justification for the selection of each component, as well as the parameters that were used to evaluate the SSP technology for pathway public lighting, from the generation stage to the load. This chapter also contains a detailed explanation of methodology that was implemented to make this project functional.

CHAPTER FOUR presents the modelling and simulation of a stand-alone solar pathway for public park lighting. The model is composed of a PV array designed for public park lighting, charge controller, and batteries connected to the load power. The remaining part of this chapter is organised as follows: a selected case study to study sizing, and performance analysis of an SSP system to power public park lighting, is chosen and illustrated. Then, the modelling of SSP system to supply a public park lighting is executed by computer program on the selected site.

When the evaluation of load needs "quantity and quality of lighting and duration of the lighting electrical load" are calculated. Battery storage size based on the desired autonomy period and maximum and average daily depth of discharge is estimated. PV array size based on the type and specifications of PV module, the time of year with the highest average daily lighting load and minimum solar radiation are selected and measured respectively. Control strategy for battery protection and lighting control and specify the control set points and conditions are determined.

CHAPTER FIVE is the final chapter and presents a brief summary of the research work undertaken for this thesis. The chapter highlights significant contributions made as a result this study. The chapter concludes with a discussion of possible future research work identified during the production of this thesis.

APPENDICES:

Appendix A: Specification data sheets luminaire chosen

Appendix B: Product specification sheet of Aspen 24S-83 battery

Appendix C: NASA Surface meteorology and Solar Energy

C1: Available Tables for the selected site.

C2: Parameters Definitions

Appendix D: Global irradiation of South Africa

CHAPTER TWO

LITERATURE REVIEW

2.1 Introduction
2.2 History of Photovoltaics
2.3 Stand-alone Solar Pathway Technology System.
2.4 PV- Cell Operation
2.4.1 Equivalent circuit of solar cell
2.4.2 Current–voltage characteristics
2.4.3 Power losses in solar cells
2.5 Solar Irradiation
2.5.1 Considerations affecting the amount of solar irradiation received on a surface at any given location.
2.5.2 The difference between solar irradiance and insolation.
2.6 The Effects of Temperature and Solar Radiation on Solar Cells.
2.6.1 Effects of temperature
2.6.2 Effect of irradiance
2.7 Types of PV System
2.7.1 Stand-alone PV systems
2.7.2 Grid-connected PV systems
2.8 Advantages and Disadvantages of PV systems
2.9 PV Lighting Applications
2.10 Market Overview of PVs
2.11 PV Lighting System Components
2.11.1 Luminaires
2.11.2 PV cells, modules and arrays
2.11.3 Balance of system equipment
2.11.3.1 PV Lighting System Controllers
2.11.3.2 Battery
2.12 Summary

2.1 Introduction

Electrical power is a very important factor for industrialization, urbanization, and financial growth of every region around the world. There are different types of conventional and non-conventional energy sources used to generate electricity. Renewable energy such as solar energy systems is one of the most important sources of energy. The utilization of solar energy systems has become increasingly popular due to its modular and environment friendly nature. The field of solar has experienced remarkable growth over past two decades in its widespread application, ranging from stand-alone to utility-interactive solar systems (Khare et al., 2016). The technological advances made in the photovoltaic industry have led to a vast exploration of self-sustaining systems. Increasing populations will increase the demand for electricity, and existing technologies will not be able to meet this demand; new approaches to the design of systems will have to be developed to relieve the impact on the electrical grid.

Solar energy systems function either in stand-alone or grid-connected mode. Due to nature of solar power as a resource, the efficiency of solar technology is less than that of conventional energy sources. A solar energy system is considered a sustainable energy source, and can be combined with other renewable energy topologies to provide electricity either concurrently, or alternately in sequential mode (Khare et al., 2016).

Although lighting systems powered by PV cells have existed for many years, they are not widely used in lighting for buildings and highways due to their high initial cost and their low conversion efficiency. One of the technical challenges facing PV-powered lighting systems has been converting the DC power generated by the PV module, to energize common light sources that are designed to operate efficiently under AC power. Usually, the efficiency of the DC light sources is very poor compared to AC light sources. Rapid developments in LED lighting systems have made this technology a potential candidate for PV-powered lighting systems.

In this chapter information on PV systems relating to the principles of PV-cell operation, solar irradiation, and the effects of temperature and solar radiation on the solar cells are presented. Thereafter the types of PV system, advantages and disadvantages, photovoltaic applications and a market overview of PV components, are discussed. Finally, PV lighting system components are introduced.

2.2 History of Photovoltaics

French physicist Edmond Becquerel first described the photovoltaic effect in 1839, but it remained a curiosity of science for a half century. At the age of 19, Becquerel found that certain materials would produce small amounts of electric current when exposed to light. In the 1870s William Adams and Richard Day showed that light could produce an electric current in selenium. In 1883 Charles Fritts invented the first PV cell using selenium and gold leaf; his cell converted light to electricity at an efficiency of about one percent. The conversion efficiency of a PV cell is the ratio of the amount of radiant energy striking the PV cell to the amount of electrical energy obtained from the conversion. This is very important when discussing PV devices, because improving this efficiency is vital to making PV energy competitive with more traditional sources of energy such as fossil fuels. During the second half of the twentieth century, PV science was refined and the process was more fully developed. Major steps toward commercialising photovoltaics were taken in the 1940s and 1950s, when the Czochralski process was developed for producing highly pure crystalline silicon(National Energy Education Project, 2015).

The first conventional PV cells were produced in the late 1950s, and throughout the 1960s were principally used to provide electrical power for earth-orbiting satellites. In the 1970s, improvements in manufacturing, performance and quality of PV modules helped to reduce costs and opened up a number of opportunities for powering remote terrestrial applications, including battery charging for navigational aids, signals, telecommunications equipment and low-power needs. In the 1980s PVs became a popular power source for consumer electronic devices, including calculators, watches, radios, lanterns and other small battery charging applications. Following the energy crises of the 1970s, significant efforts also began to develop PV power systems for residential and commercial uses, both for stand-alone remote power, as well as for utility-connected applications. During the same period, international the application for PVs to power rural health clinics, refrigeration, water pumping, telecommunications, and off-grid households, increased dramatically, and remain a major portion of the present world market for PV products (Energy.gov, 2013; Luque & Hegedus, 2011).

2.3 Stand-alone solar pathway technology system

Direct conversion of solar energy to electricity for providing small quantities of electrical energy to such applications as SSP through the use of PVs is competitive to the alternatives such diesel, or a grid extension; the latter alternatives need continuous maintenance and have high running costs (Markvart, 2000) .

If all the highways, pathways and roads were solar panelled, it would produce sufficient free energy for every residential and industrial use in that country. This will not get rid of electricity bills; there will still be a cost to distribute electricity to homes and businesses. However, that cost could be reduced by 90%, because lower electricity cost means cheaper consumer goods, commodities, greater opportunity for indoor agriculture which increases food production and reduces food prices as well as ending famine and food crises worldwide; and it create new industries and clean environment.

A solar road is a new concept for the generation of sustainable energy. Here, the road surface also acts as a solar panel. The generated electrical energy can be used for various applications, such as road lighting, public park lighting and traffic systems. Households may benefit from it as well. Electric cars might be able to make use of the energy. This energy will then actually be generated at the place where it is needed; this is a big step towards an energy-neutral mobility system.

The first solar roadway opened in Amsterdam, the Netherlands, in November, 2014; it is part of a 100-metre stretch of cycle path between two suburbs of the city; electricity is generated by rugged, textured glass-covered photovoltaic cells exposed to solar irradiation (Hruska, 2014b). SolaRoad, as it has been named by the Netherlands Organization for Applied Scientific Research, is made up of rows of crystalline silicon solar cells. The cells are fully embedded into the surface of the concrete of the path, and then covered with a layer of translucent, tempered glass as shown in Figure 2.1(a). The surface of the road has been treated with a special non-adhesive coating as shown in Figure 2.2, and the road itself was built to sit at a slight tilt in an effort to keep dust and dirt from accumulating and obscuring the solar cells.

(a) (b)

Figure 2.1: The first solar roadway opened in Amsterdam, the Netherlands:
(a) close up; (b) showing the width of the path

Figure 2.2: Solar roadway covered with a layer of translucent, tempered glass with a special non-adhesive coating

The path opened to the public in November 2014, and cost about USD 4.3 million. The path was created as the first step in a project, which is to be extended to 100 meters. The local authority initiated a first phase of 70 meters — so by 2016 (which is now) they will have added another 30 meters. Photos of the solar roadway which was made of the SolaRoad are shown in Figure 2.3. There are additional photos of the solar roadway available in the publications of Hruska (2014b) and Shekhar et al.(2015).

Figure 2.3: The world's first solar-paneled road in the Netherlands

One reason installing these solar panels on a bike path makes more sense than a traditional road is the wear-and-tear expected on the road itself. According to studies, one reasonable method of estimating road wear is the so-called fourth-power law, which states that the damage a vehicle causes to a road surface is related to the fourth power of its axle weight. Speed and tire pressure play a part, as a result cars can be several thousand times more damaging to a road surface than bikes, and trucks are thousands of times more damaging than cars. A solar road surface for a bike path is thus under orders of magnitude less stress than a vehicular road surface (Hruska, 2014b)

The entire project is a proof-of-concept demonstration. Many people who are otherwise enthusiastic proponents of solar power, are dubious of embedding panels into roadways, and it remains to be seen how this solution performs under real-world conditions before conclusions can be drawn; it is impossible to draw conclusions until tests have been performed (Hruska, 2014b; Schmidt, 2014)

Community members have readily accepted the new road, and they are excited about the future plans the government has for powering everything from traffic lights to electric cars with solar technology. It is a step in the right direction, and a step to be followed by other countries and neighbourhoods looking to pave their own solar-panelled paths and roads (Schmidt, 2014). The conceptual independent solar road lighting system design and its equivalent circuit for this study, is shown in Figure 2.4.

(a) Conceptual PV road lighting

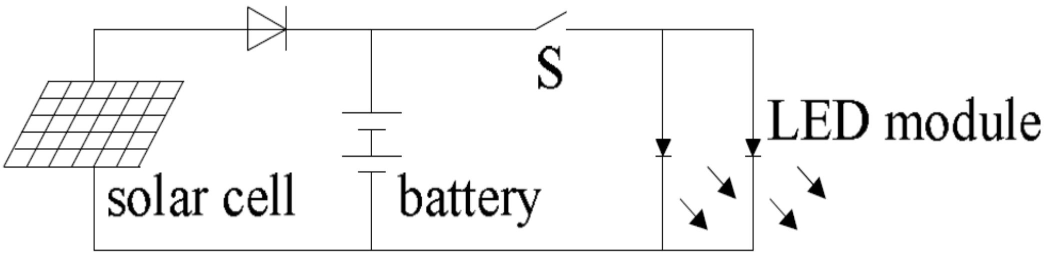

(b) Equivalent circuit

Figure 2.4: A stand-alone solar lighting system

2.4 PV Cell Operation

PV cells are made of semiconductor materials that can generate electricity electromagnetically when exposed to sunlight. If a minority electron-hole pair generated by the absorption of photons in the semiconductor material (the holes in n-regions, and the electrons in p-regions), diffuses into a boundary region in which there is an electric filed; the electron will be accelerated into the n-region, and the hole into the p-region. This causes the n-region to accumulate a negative charge and the p-region to build up a positive charge, resulting in a photovoltage. If there is a closed external circuit, a photocurrent and photovoltage can be measured by the external resistance. The working of PV cells is illustrated in Figure 2.5.

The balance of electrons and holes in a silicon crystal lattice can be shifted by doping it with other atoms. Atoms with one more valance electron than silicon are used to produce n-type semiconductor materials. Atoms with one less valence electron result in p-type material. Once the n- and p-type semiconductor materials are reached, the process will produce photovoltage. The most common materials used in forming n- and p-type semiconductor materials are phosphorus and boron (Markvart, 2000). A p-n junction can be formed either through a high temperature diffusion process or an ion implantation process. Diffusion can be created either from a vapour phase or a solid phase. Crystalline silicon and amorphous silicon are the most dominant semiconductor materials for commercial PV cells (Markvart, 2000).

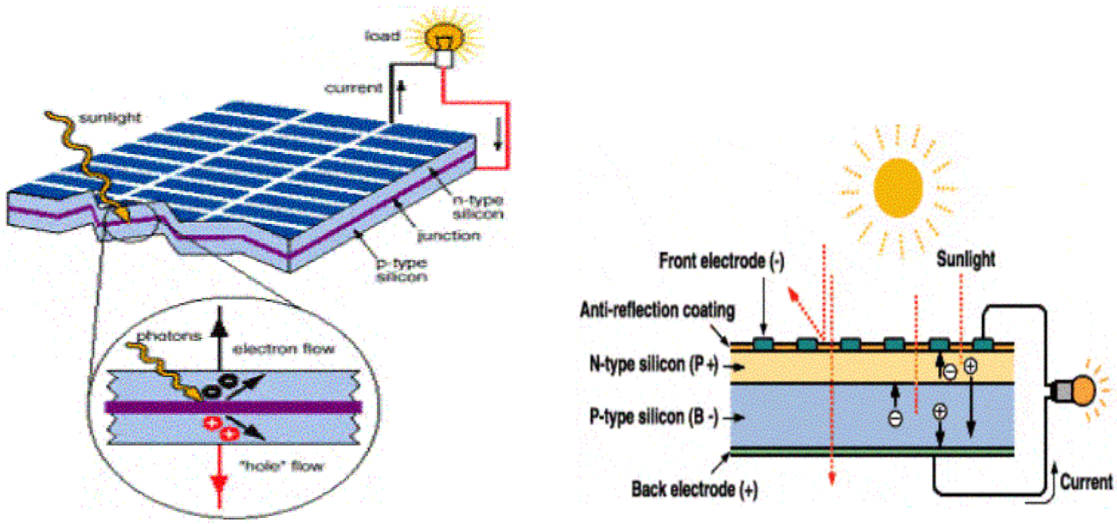

(a) (b)

Figure 2.5: (a) and (b): PV cell operation diagram

2.4.1 Equivalent circuit of solar cell.

The equivalent circuit of a solar cell consists of: a constant current source, I_{sc} ; a nonlinear function diode impedance, D_j ; a shunt resistance, R_{sh} due to leakage near the edges and corners of the cell; a series resistance, R_s due to the resistance of the cell material; the resistance encountered when electrons travel along the thin top sheet of n- or p-type doped material; the contact resistance, and finally; a resistive load, R_L (Heavens, 1991). In Figure 2.6 the equivalent circuit is shown.

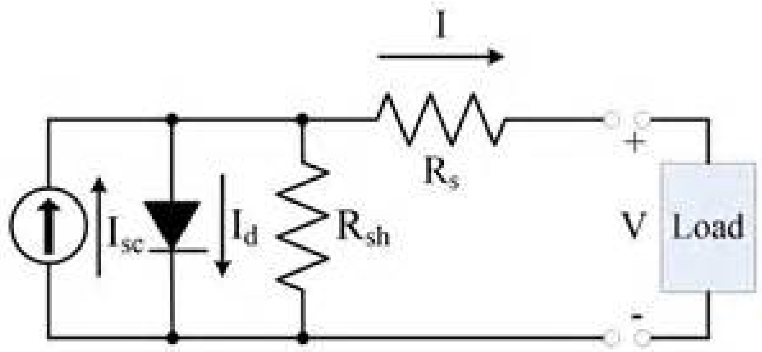

Figure 2.6: Diagram of the equivalent circuit of a solar cell, including a resistive load

2.4.2 Current-voltage characteristics

When a solar cell is exposed to light, a constant current, I_{sc} is generated which causes a current, I_L to flow in a load with resistance, R_L. Figure 2.7 shows an I-V characteristic together with the power curve. At zero voltage, the current flow, I_j through the junction is zero and $I_L = I_{sc}$ (short circuit current). For a small increase in the voltage, I_j remains effectively zero and the slope of I-V curve depends only on the cell shunt resistance. If R_{sh} is infinite, the curve would be horizontal in this region (Markvart, 2000).

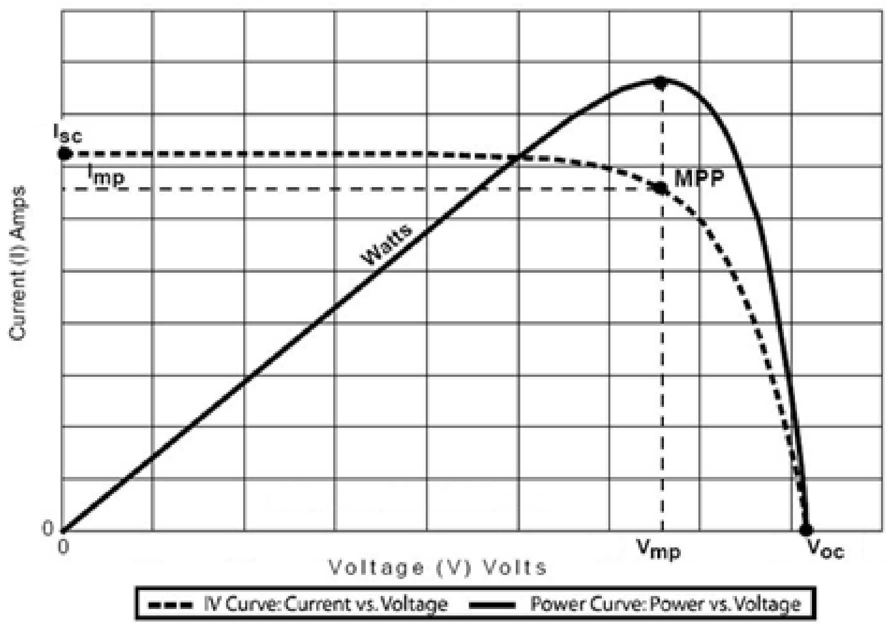

Figure 2.7: Current-voltage characteristic together with the power curve of solar cell

At a certain potential however the junction begins to conduct current, increasing exponentially with voltage, causing I_L to decrease rapidly.

At V_{oc} (open circuit voltage), I_j effectively equals I_{sc} and no current flows through the load. In the region from the knee of the curve up to V_{oc}, the slope of the I-V curve is governed by Rs; high values of R_s lead to steep slopes. The power delivered to the load at any point on the I-V curve is I x V.

Efficiency and fill factor:

The efficiency of a solar cell is defined as:

$$\eta = \frac{P_{out}}{P_{in}} \tag{2.1}$$

$$= \frac{P_{out}}{P_s . A_s} \tag{2.2}$$

where:

P_{out} = the electrical output power of the cell.

P_{in} = the input power of the cell.

P_s = the solar radiation level per unit area.

A_s = the active cell area.

The maximum cell efficiency can be defined as:

$$\eta_{\max} = \frac{I_{mp}.V_{mp}}{P_{in}} \tag{2.3}$$

where:

I_{mp} = current at maximum power point.

V_{mp} = voltage at maximum power point.

To optimize the cell efficiency, I_{mp} and V_{mp} have to be optimised.

The maximum voltage and current achievable are respectively V_{oc} and I_{sc}. Therefore ratio $\frac{I_{mp}.V_{mp}}{I_{sc}.V_{oc}}$ is a useful measure of realizable power. The fill factor (FF) is defined as:

$$FF = \frac{I_{mp}.V_{mp}}{I_{sc}.V_{oc}} \tag{2.4}$$

The value of the FF is always less than unity and typically between 0.6 and 0.8 and η = 6 – 20%.

The fill factor is a practical quantity to use when comparing different solar cells under the same conditions.

2.4.3 Power losses in solar cells

The energy conversion process in solar cells is very different from the operation of the classical heat engine, and it is instructive to consider the limitations and losses that occur in more detail. The fundamental mechanisms responsible for losses in solar cells are apparent from the discussion of solar cell operation earlier in this chapter: heat is produced on carrier generation in the semiconductor by photons with an energy in excess of the bandgap, and a considerable part of the solar spectrum is not utilized because of the inability of a semiconductor to absorb the below-bandgap light. These losses can be reduced, but only by going over to more complex structures based on several semiconductors with different bandgaps.

A device called a tandem cell, for example, is effectively represented by a stack of several cells, each operating according to the principles described above. The top cell is made of a high-bandgap semiconductor, and converts the short-wavelength radiation. The transmitted light is then converted by the bottom cell. This arrangement considerably increases the achievable efficiency: high efficiency space cells operating at close to 30% efficiency, are now commercially available. There are also amorphous silicon cells where a double or triple stack is used to boost the low efficiencies of single-junction devices and reduce the degradation which is observed in these materials (Markvart, 2000).

Other losses reduce the typical efficiency of commercial devices to roughly 50% of the achievable maximum (see Figure 2.8), and somewhat less in thin film devices. An ubiquitous loss mechanism present in all practical devices, is non-radiative recombination of the photogenerated electron-hole pairs. Such recombination is most common at impurities and defects of the crystal structure, or at the surface of the semiconductor where energy levels within the range of the energy gap may be introduced.

The loss of current resulting from recombination is usually grouped under the term collection efficiency, which is the ratio between the number of carriers generated by light and the number of carriers that reach the junction.

Consideration of the collection efficiency affects the design of a solar cell. In crystalline materials, the transport properties are usually good, and carrier transport by simple diffusion is sufficiently effective. In amorphous and polycrystalline thin films however, electric fields are needed to pull the carriers. The junction region is then made wider to absorb the main part of the photon flux.

Other losses of current produced by the cell, arise from light reflection from the top surface, shading of the cell by the top contacts, and incomplete absorption of light. The last-mentioned loss source can be particularly significant for crystalline silicon cells, which is an indirect-gap semiconductor, and has poor light absorption properties. Another common loss in commercial cells involves ohmic losses in the transmission of electric current produced by a solar cell; these losses are usually grouped together as a series resistance, and reduce the fill factor of the cell (Markvart, 2000) .

Table 2.1: Solar cell efficiencies achieved by the most popular solar cell technologies (energyinformative.org, 2013)

material	Monocrystalline	Polycrystalline	Amorphous
Typical module efficiency	15–20%	13–16%	6–8%
Best research cell efficiency	25.0%	20.4%	13.4%

The losses which were discussed in this section are summarized in Figure 2.8. It is seen that the fundamental losses reduce the maximum theoretical efficiency of a silicon cell to about 48%. Additional voltage losses (~36%), current losses (~10%), and losses associated with the fill factor (~20%) then explain the efficiency of about 23% for the best silicon cell today. Higher efficiencies have been obtained under concentrated sunlight, in devices made from other materials, and in tandem structures. The typical production silicon cell has an efficiency of about 14%. However, new devices with efficiency approaching 18% are beginning to appear on the market. Solar cell efficiencies achieved by the most popular solar cell technologies are shown in Table 2.1 (Energyinformative.org, 2013).

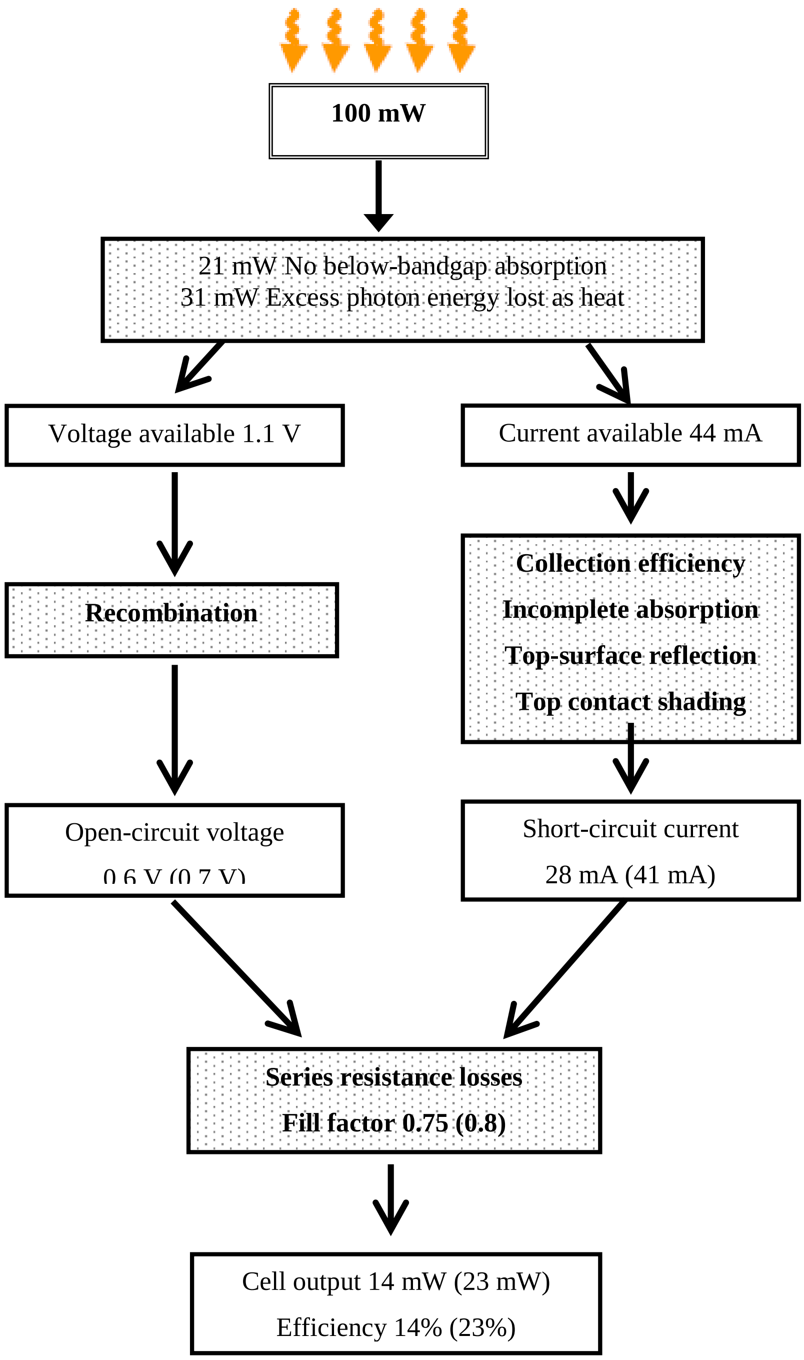

Figure 2.8: The power losses in silicon solar cells (polycrystalline). The figures are per square centimeter for production cells and the figures in brackets are applicable to laboratory cells.

2.5 Solar irradiation

The amount of solar energy which reaches the surface of the Earth, varies over the year, from an average of less than 0.8 kWh/m^2 per day during winter in northern Europe, to more than 4 kWh/m^2 per day during summer in this same region. The difference decreases for the regions closer to the equator. The obtainability of solar energy varies with the geographical location of a site and is the highest in regions closest to the equator. Thus the average annual global radiation impinging on a horizontal surface amounts to approximately: a 1000 kWh/m^2 in Central Europe, Central Asia, and Canada; approximately 1700 kWh/m^2 in the Mediterranian region, and; approximately 2200 kWh/m^2 in most equatorial regions in Africa, the Orient, and the Australian desert areas. Overall, seasonal and geographical differences in irradiation are considerable and must be taken into account for all solar energy applications in order to get the average solar radiation levels; the world solar irradiation map is shown in Figure 2.9 (Holding, 2011)

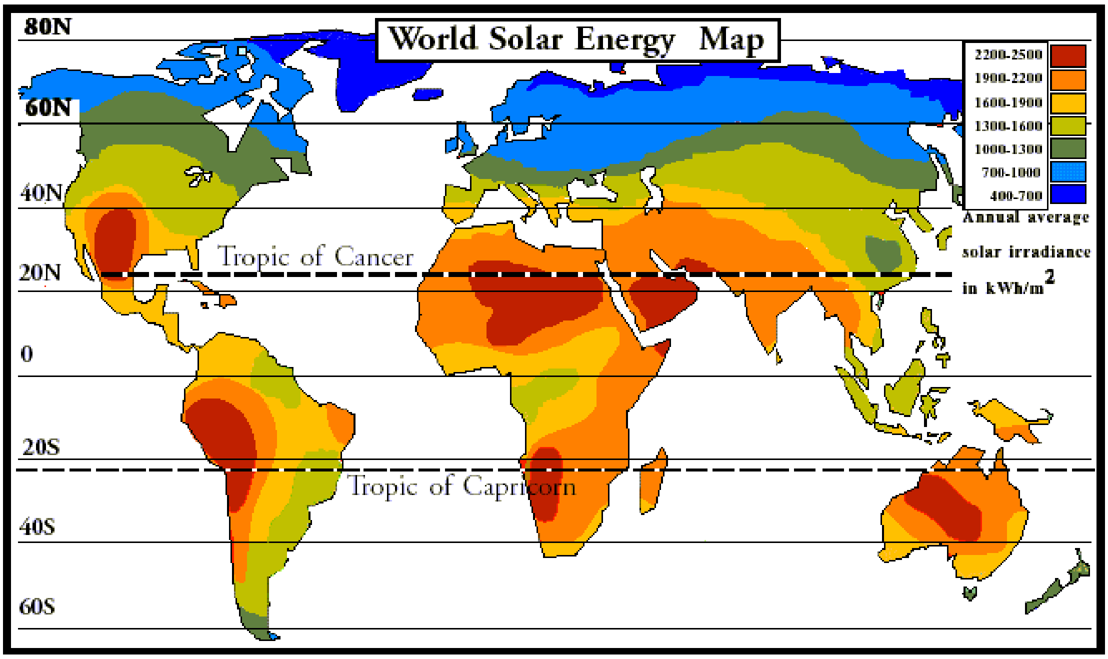

Figure 2.9: World solar irradiation map (Holding, 2011)

2.5.1 Considerations affecting the amount of solar irradiation received on a surface at any given location.

The amount of solar energy received on a surface at any given location depends on the altitude, latitude, time of day and year, local weather patterns and atmospheric effects, and orientation of the surface with respect to the sun.

2.5.2 The difference between solar irradiance and insolation.

Solar irradiance is an instantaneous quantity describing the rate or flux of solar radiation (power) incident on a surface; it is commonly expressed in units of kilowatts per square meter (kW/m^2). Outside the atmosphere of the Earth, the solar irradiance on a surface which is perpendicular to the rays of the Sun is essentially constant at 1.36 kW/m^2. Due to atmospheric effects, the peak solar irradiance incident on a terrestrial surface oriented normal to the sun, at noon on a clear day is on the order 1 kW/m^2. A solar irradiance level of 1 kW/m^2 is often called a *peak sun* and is the reference condition commonly used to rate the peak electrical output of photovoltaic modules and arrays.

Solar insolation is an amount of solar energy received on a surface, commonly expressed in units of kilowatt-hours per square meter (kWh/m^2). Solar insolation (energy) is essentially the average solar irradiance (power), integrated with respect to time. When solar insolation data is represented on an average daily basis, the value is often called *peak sun hours* (PSH), and can be thought of as the number of equivalent hours per day that solar irradiance is at its peak level of 1 kW/m^2. The worldwide average daily value of solar insolation on optimally oriented surfaces is approximately 5 kWh/m^2, or 5 PSH. Figure 2.10 shows the relationship between solar irradiance and insolation (Center, 1999) .

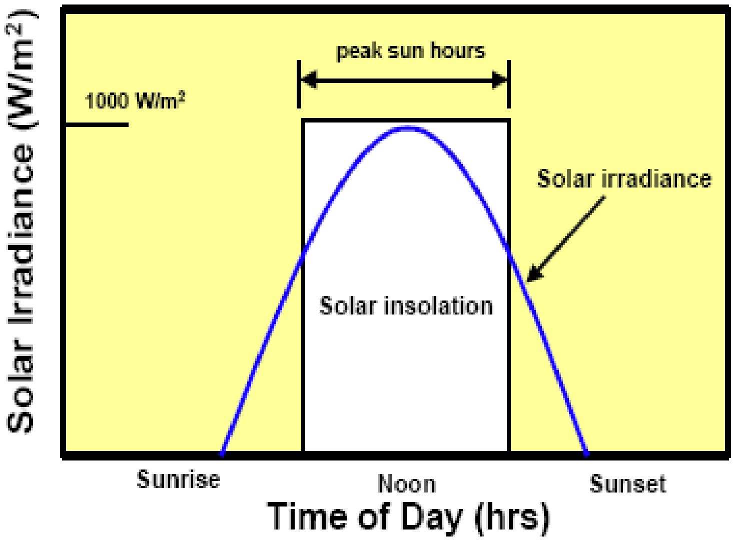

Figure 2.10: Relationship between solar irradiance and insolation.

2.6 Effects of temperature and solar radiation on the solar cells

It is useful to understand the effect of irradiance and temperature on the performance of a photovoltaic cell and module, in order to estimate their I-V curves under various climate conditions and to determine their power and energy ratings.

2.6.1 Effects of temperature

Temperature has an important effect on the power output of a PV cell. Most significant is the temperature dependence of the voltage, which decreases with increasing temperature. The voltage decrease of a silicon cell is typically 2.3 mV per °C. The changes in both the current and the fill factor as a result of temperature variations are minimal, and are usually neglected in PVs design (Markvart, 2000; Treble, 1991).

The important electrical specifications of a PV module are the short circuit current, the open circuit voltage, and the maximum power point as a function of temperature and irradiance. These specifications of a cell (or module or array) can be represented by current-voltage characteristic curves. For a particular solar cell the typical effect of the temperature and irradiance on the module I-V specification is depicted in Figure 2.11.

2.6.2 Effect of irradiance

The solar radiation of absorbed by PV cells depends critically on the spectral distribution of this radiation (Fahrenbruch, 2012). The process of emission of radiation from the Sun at about 5800 K, is closely approximated by the thermal emission from a blackbody. In general, the total power received from a radiant source and falling on a unit area is called irradiance (Markvart, 2000).

Important characteristics of a solar cell under different levels of illumination are shown in Figure 2.11. As discussed earlier, the current generated from sunlight, is proportional to the flux of photons with energy equal to or higher than the band-gap energy. Increasing the irradiance increases the photon flux in the same proportion, which in turn, generates a proportionately higher current. Therefore, the short-circuit current of a solar cell is directly proportional to the irradiance (Markvart, 2000).

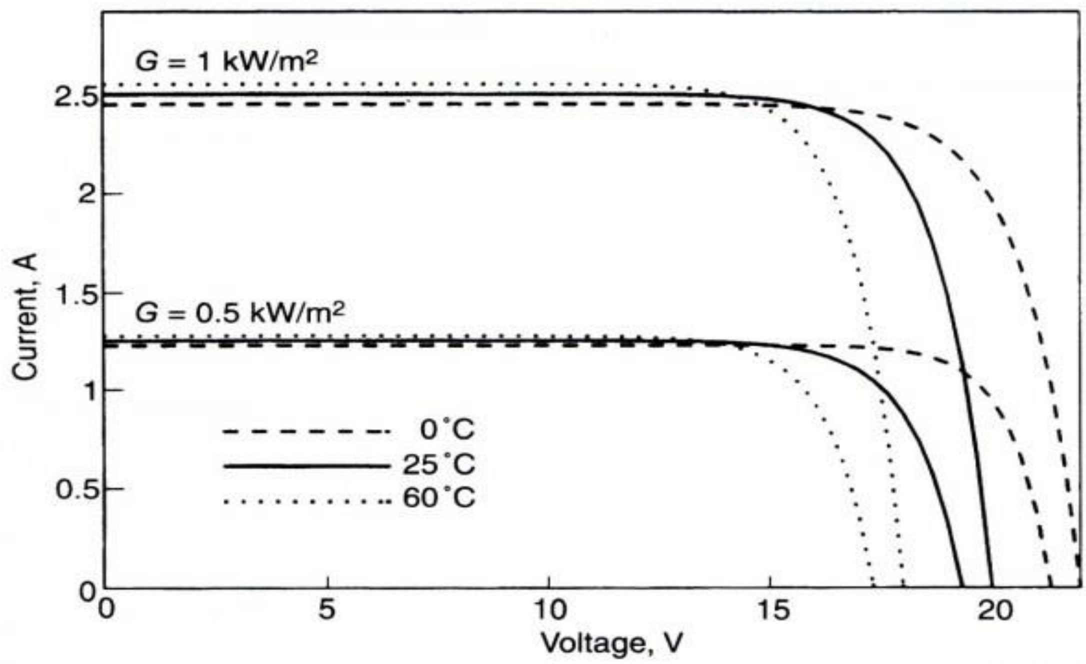

Figure 2.11: Temperature and irradiance dependence of the I-V specifications of a module

2.7 Types of PV systems

PV power systems are generally classified according to their functional and operational requirements, and according to how the equipment is connected to other power sources and electrical loads. The two principle classifications are either a stand-alone system, or grid-connected system (Markvart, 2000).

2.7.1 Stand-alone PV system

Stand-alone systems are designed to operate independently from an electrical utility grid. In its simple form a stand-alone system consists of a PV array supplying the load directly, as shown in Figure 2.12; such a system can be used for charging batteries via a charge controller, or used for pumping water , where the storage medium is a storage tank.

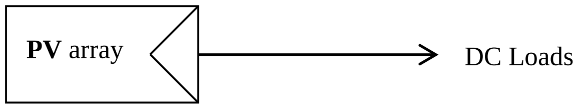

Figure 2.12: Stand-alone DC system without battery.

The addition of an inverter, as shown in Figure 2.13 makes the system suitable for power AC loads, such as an AC water pumps.

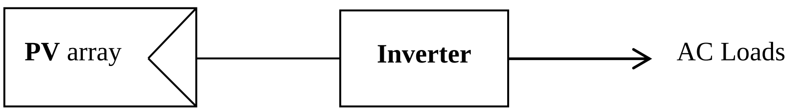

Figure 2.13: Stand-alone AC system without battery.

Systems such as Telecommunications equipment, cathodic protection, navigational aids, and traffic control warning signs, require a continuous DC supply. To overcome overcast days when irradiation is low, or at night when there is no irradiation at all, surplus electrical energy must preserved. Thus the DC basic system must be expanded to include storage batteries with a charge regulator; this is shown in Figure 2.14.

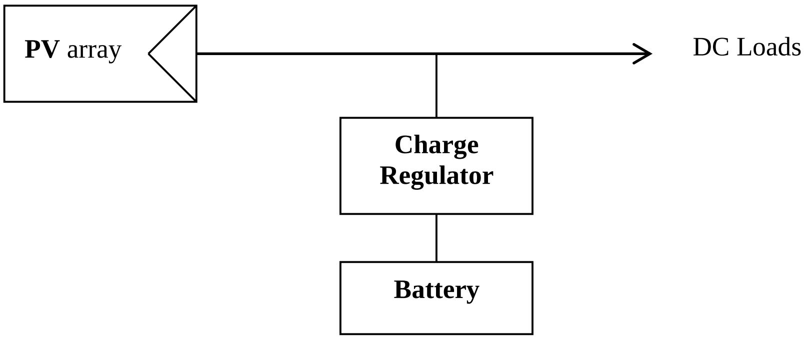

Figure 2.14: Stand-alone DC system with battery.

Combining systems of the types shown in Figures 2.13 and 2.14, gives a mixed AC/DC system with battery storage, as shown in Figure 2.15; this type of system is appropriate for domestic supplies in remote houses and villages.

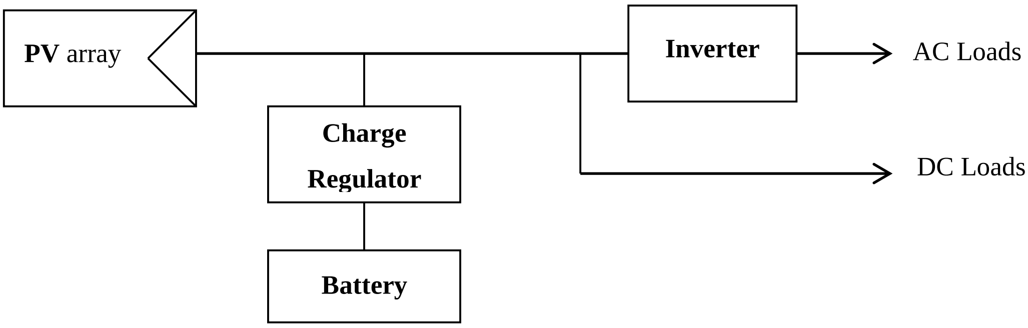

Figure 2.15: Stand-alone AC/DC system with battery storage

A back-up generator is commonly used to improve the security of supply; in a hybrid system an auxiliary source such as a wind turbine, a hydro electric generator or a diesel generator can be integrated with the PV system, to reduce the required storage capacity and lower the capital cost (Mohamed & Papadakis, 2004; Heavens, 1991). This is shown in Figure 2.16.

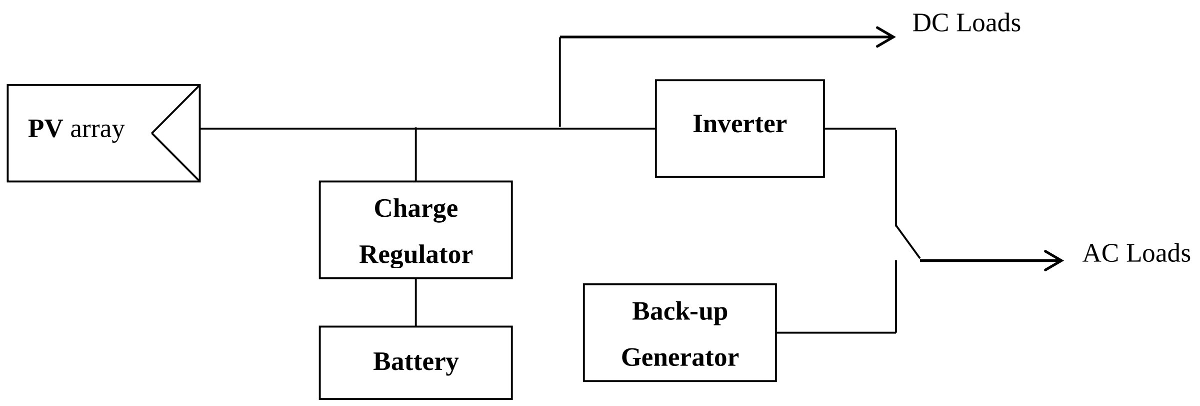

Figure 2.16: Stand-alone AC system with battery and back-up generator.

2.7.2 Grid-Connected PV system:

A grid-connected PV system as shown in Figure 2.17, is designed to operate in parallel with and interconnected to the electric utility grid. The primary component in grid-connected PV systems is the inverter. The inverter converts the DC power produced by the PV array, into AC power consistent with the voltage and power quality requirements of the utility grid, and automatically stops supplying power to the grid when the utility grid is not energized. A bi-directional interface is made between the AC output of the PV system and the electric utility network. This allows the AC power produced by the PV system to either supply on-site electrical loads, or to back-feed the grid when the output of the PV system is greater than the on-site load demand. At night and during other periods when the electrical loads are greater than the output of the PV system, the balance of power required by the loads is received from the electric utility.

The above schematics can be varied to suit a particular application. For example, the PV array may be divided into sub-arrays, each with its own inverter to improve the system performance.

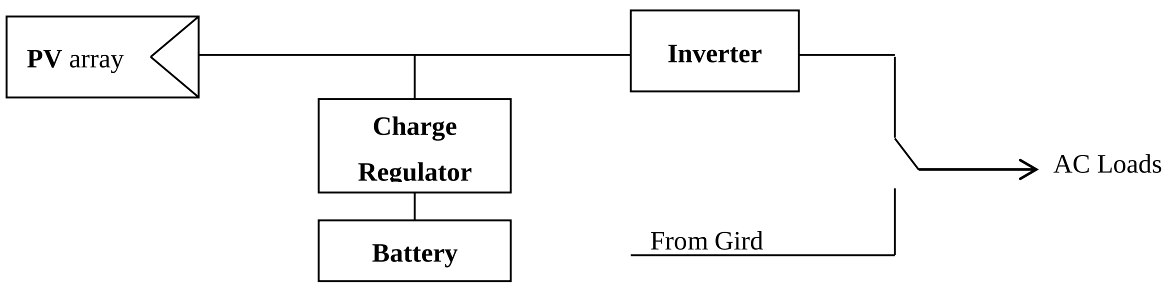

Figure 2.17: A grid-connected PV system.

2.8 Advantages and Disadvantages of PV systems

The advantages that photovoltaic systems have over competing power options are:

a) there is no fuel supply problem—the source is sunlight .

b) long lifespan—in excess of 20 years.

c) pollution free.

d) high reliability.

e) requires little maintenance.

f) easy to install.

g) easy to expand.

PV systems do however have few disadvantages, which are:

i. initial cost is high.

ii. conversion efficiency is low.

Recently, the importance of PV power systems for the generation of electricity has attracted the attention of researchers because solar energy is a free, efficient, clean, and an environmentally renewable and sustainable energy resource (Liu et al., 2016).

Some of the benefits of solar cells are:

1- they are environmentally friendly.

2- they emit no noise.

3- there are no moving elements.

4- there are no emissions.

5- they require no of fuels or water.

6- the maintenance requirements are minimal.

7- they have a long span (up to thirty years), and electricity is generated where it is required.

8- PV cells can even operate in cloudy conditions; modular, custom-made systems are often sized for specific applications, from a watch to a multi-megawatt power station.

Some of the disadvantages PV cells are:

1- they can not operate without light (no output at night).

2- a lower output in unfavourable weather.

3- the use of toxic materials in the manufacture of some photovoltaic cells.

4- a high initial cost that offsets the low maintenance costs.

5- the large area required for big-scale applications.

6- PV systems generate direct current and thus special DC appliances, or alternatively inverters are needed.

7- For off-grid applications energy storage is needed. (Dhankhar et al., 2014) .

2.9 PV Lighting Applications

PV lighting systems are used for a variety of applications, ranging from small consumer devices such as flashlights, portable lanterns and low-level walkway lights, to larger structurally-integrated independent power systems, designed to illuminate large surface areas or highway signs. Other PV lighting applications include flashing, signalling and warning devices where the primary function is the luminance, or brightness of the light. Perhaps the most significant application for PV lighting is for residential households and community centres in developing countries. Commonly called solar home systems (SHS), over one million such systems have been installed around the world, as part of rural electrification programs. Table 1 lists common PV lighting system applications and associated key user groups (Guide, 1998a)

2.10 Market Overview of Photovoltaics

The decreasing cost of PV systems and the increasing number of manufacturers and dealers for PV equipment have contributed to widespread use of this technology. In the early days of phovoltaics, do-it-yourselfers had to search for companies that manufactured PV modules, and often had to adapt or reconfigure components from other non-PV systems. Today, dealers offer ready-to-use systems and state-of-the-art equipment, designed specifically for PV systems (OFEN, 1997)

The year 2014 experienced a renewed growth of the PV market and confirmed the Asian leadership in the PV market and industry. PV system is rapidly entering into a new era where the PV market will be concentrated in countries with energy needs

Table 2.2: PV Lighting Application Matrix

Principal Function	**Lighting Application**	**User Groups**
Area Illumination		
	Parks and recreation areas	Federal, state and local government
	Parking lots	Public and private organizations
	Residential street lighting	Homeowners, developers and utilities
	Pedestrian and cycle paths	Municipalities
	Bus stops and shelters	Municipalities and transportation bodies
	Security lighting and remote illumination	Utilities, homeowners, public and private organizations
	Storage yards	Public and private organizations
	Portable lighting systems	Contractors, emergency lighting
Sign Illumination		
	Highway information signs	Transportation bodies
	Billboards	Advertisers and utilities
	Internally illuminated variable message boards.	Transportation bodies and contractors
Flashing and Signaling Devices		
	Navigational aids	Navigational authorities
	Highway warning signals	Transportation
	Traffic and railway signals	Transportation and railway
	Transmission and antenna tower warning lights	Electricity utilities, telecommunications and aviation authorities
	Work area protection devices including flashing arrow boards and barricades	Transportation officials, municipalities, and contractors
	Signaling systems for bridges and other general hazards	Maritime and transportation authorities, public and private organizations
Consumer Products		
	Low-level pathway and landscape lighting	Homeowners and builders
	Rechargeable flashlights	Vehicle owners and homeowners
	Portable lanterns	Emergency management, bodies development organizations, homeowners
Solar Home Systems		
	Rural residential lighting, remote cabins, restrooms	Development/conservation organizations, rural electrification authorities, homeowners

Two of the top three markets in 2015 were located in Asia (China and Japan), followed by Europe (mainly Germany and Italy), and the USA market; this is shown in Figure 2.18. This trend should be confirmed again in 2016, with Asia consolidating the core of the PV market, followed by the USA and Europe. With PV development occurring in Latin America, Africa and the Middle East, it becomes clear that in the short term all continents will experience substantial growth in the deployment of PV installations. It is important to note that new markets have opened up in many places around the world, like the Philippines, Dubai, Jordan, Panama and Honduras, confirming the globalisation trends. Besides China and Japan, there are several other Asian countries where the use of PV-generated electricity is burgeoning, like Thailand, Korea, Taiwan, the Philippines and many other countries which are either starting or continuing to develop. India will most probably become soon the fifth largest user of PV technology, if the plans to install 100 GW PV systems in the coming years come to fruition.

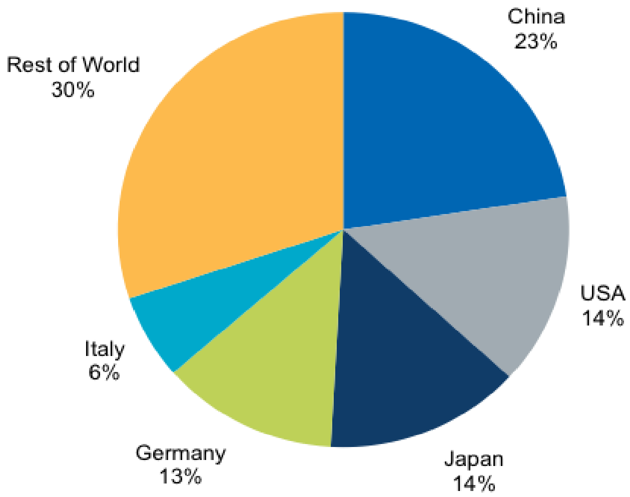

Figure 2.18: Installed PV capacity globally in 2015 — China, USA, Japan and Germany are the leading countries in terms of PV installations.

The price decrease of PV components that has been experienced over the last couple of years continued at a slower pace in 2015. This decrease in the price of PV technology has decreased the cost of electricity produced, to a level where it is competitive with electricity from the national grid; this is particularly true of Germany and Italy where the retail price of electricity from the national grid is now higher electricity produced by PV systems. This is also true in several other countries which have developed utility-scale PV systems, or hybrid systems. Competitive tenders have also paved the way for low PV electricity prices in several key markets. These declining prices are opening new business models for PV deployment. PV technology is seen increasingly as a way to produce electricity locally, rather than buying it from the grid. Self-consumption opens the door for the large deployment of PV installations on rooftops, and the transformation to decentralized electricity systems. The output of parallel, large-scale PV installations is currently well above 500 MW. This maximum output is on the increase; a 550 MW plant opened in the USA in 2014, This plant will be exceeded by a proposed 579 MW AC installation, also in the USA, scheduled for completion in 2016, making it the largest plant built to date. Each year, larger plants are connected to the grid and plans for even bigger plants are being disclosed. Sustainable PV installations are not only on the rise in developed countries, but the PV industry also offer adequate products to bring electricity in places where national grids have not yet developed. Figure 2.9 shows global installed capacity and average PV system installation costs for 2013 and 2014, and projected through to 2020. The decline of prices for off-grid systems offers new opportunities to electrify millions of people around the world who have never benefited from it before. The challenges are still numerous before PV can become a major source of electricity in the world. The way in which distribution grids could cope with high shares of PV electricity, generation adequacy and balancing challenges in systems with high shares of variable renewables, and the cost of transforming existing grids will from the cornerstone of PV deployment in the coming years. Moreover, the ability to successfully transform electricity markets to integrate PV electricity in a fair and sustainable way will have to be scrutinized NO (PVPS, 2015). The top PV system markets in the world in 2016 are depicted in Figure 2.20.

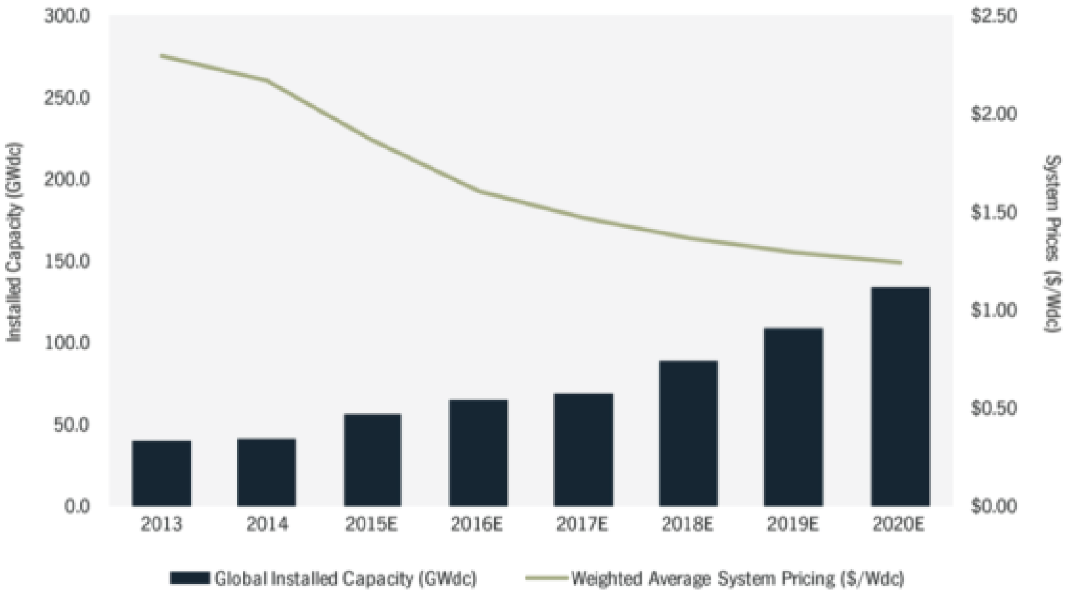

Figure 2.19: Projected global installed capacity and average cost of PV systems installed, 2013‒2020E

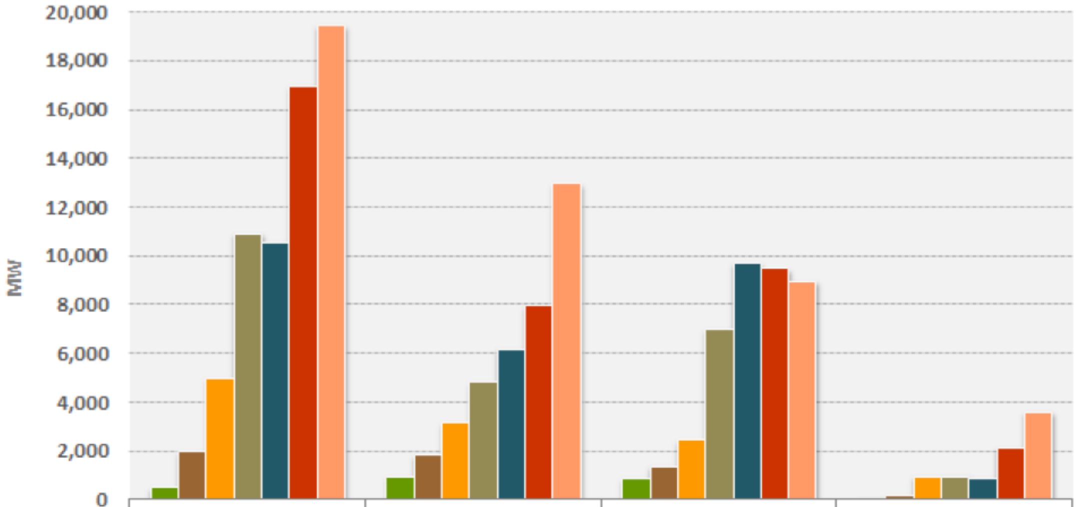

	China	US	Japan	India
2010	520	961	893	12
2011	2,000	1,855	1,404	172
2012	5,000	3,192	2,467	986
2013	10,950	4,840	7,042	1,004
2014	10,600	6,200	9,740	883
2015F	17,000	8,000	9,500	2,154
2016F	19,500	13,000	9,000	3,645

Figure 2.20: Top PV systems markets.

2.11 PV Lighting System Components

The principal components in any PV lighting system are an array of photovoltaic modules, a battery, a battery charger and light controller, and the lighting load. A stand-alone PV lighting system is depicted in Figure 2.21. The array charges the battery during the day, and the battery delivers energy to the lighting load at night. The control system manages the battery state-of charge and in automatic systems, controls operation of the light. In any system design, it is important that the individual components are compatible and interact properly with one another. The characteristics and functions of these major system components are described in the following sections.

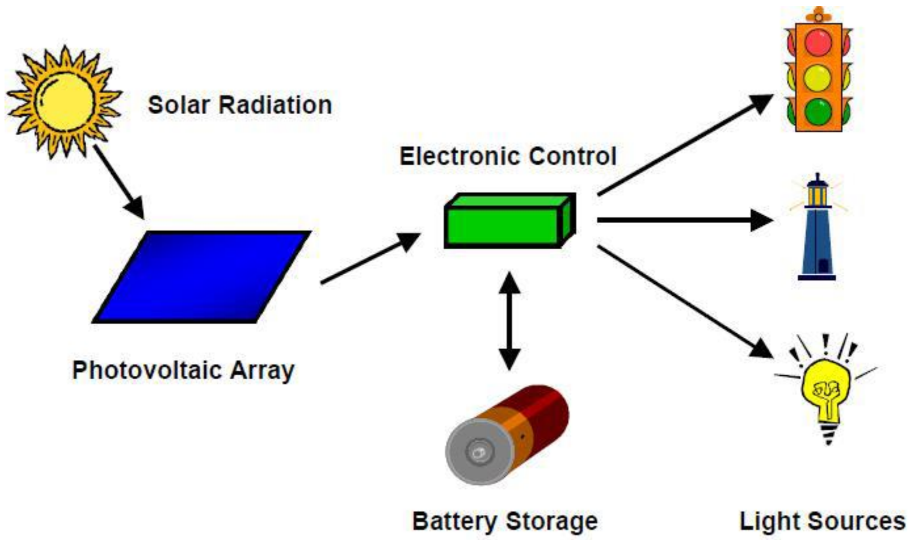

Figure 2.21: Stand-alone Photovoltaic Lighting Systems

2.11.1 Luminaires

A luminaire is a complete lighting unit, comprised of a light source (lamp or lamps), together with the parts that distribute the light, position and protect the lamps, and connect the lamps to the power supply. The function of a luminaire is to direct light to appropriate locations, without causing glare or discomfort. With thousands of different luminaires made by hundreds of manufacturers, there are more luminaires on the market than any other type of lighting equipment. Choosing luminaires that efficiently provide appropriate luminance patterns for the application is an important part of energy efficient lighting design (Sarkar, 2012). Luminaires generally consist of some or all of the following parts:

a) *Lamps* and lamp holders or sockets

b) *Ballasts* to start and operate the lamps

c) *Reflectors* to direct the light

d) *Shielding/diffusion components* (lens, diffuser, louvre) to shield the lamps at normal viewing angles, reduce discomfort and disable glare, and to distribute light evenly

e) *Housings* to contain the above elements as well as electrical components, such as wiring connections.

2.11.2 PV Cells, Modules and Arrays

Photovoltaic cells represent the smallest unit in a photovoltaic power producing device, and are typically available in 12.5 and 15 cm square sizes, although they are also available in several other shapes and sizes; the most common shapes are rectangles, circles, and squares. The size, form and the output range of PV cells needed to make up one PV module, depend on the material from which the PV cell was made (National Energy Education Project, 2015). Several shapes of PV cells are depicted in Figure 2.22.

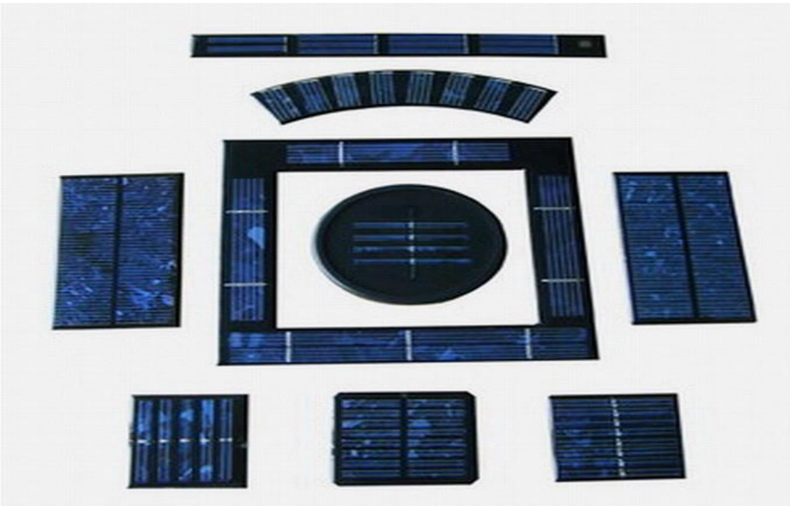

Figure 2.22: Types of PV cells

In general, cells can be classified as either wafer-based crystalline (single crystal silicon and multicrystalline silicon), compound semiconductor (thin-film), or organic. Currently, crystalline silicon technologies account for more than 80% of the overall cell production in the IEA PVPS countries. Single crystal silicon (sc-Si) PV cells are formed with the wafers manufactured using a single crystal growth method and have commercial efficiencies between 16% and 24%. Multicrystalline silicon (mc-Si) cells, usually formed with multicrystalline wafers manufactured from a cast solidification process, have remained popular as they are less expensive to produce; they are however, less efficient, with an average conversion efficiency of around 14–18%. A high efficiency is yielded by III-V compound semiconductor PV cells, formed using materials such as GaAs on the Ge substrates; these cells have high conversion efficiencies of 40% and more. Due to their high cost, they are typically used in concentrator PV (CPV) systems with tracking systems, or for space applications. Thin-film cells are formed by depositing extremely thin layers of photovoltaic semiconductor materials onto a backing material such as glass, stainless steel or plastic. Thin-film modules have lower conversion efficiencies but they are potentially less expensive to manufacture than crystalline cells. The disadvantage of low conversion efficiencies is that larger areas of photovoltaic arrays are required to produce the same amount of electricity. Thin-film materials commercially used, are amorphous and micromorph silicon (a-Si), cadmium telluride (CdTe), and copper-indium-gallium-diselenide (CIGS). Organic thin-film PV cells using dye or organic semiconductors, have created research interest, which will stimulate development and lead to the availability of prototypes in the foreseeable future. In recent years, perovskite solar cells have reached efficiencies higher than 20% in laboratories, but development has not yet resulted in related market products (PVPS, 2015).

Photovoltaic modules are typically rated between 50 W and 350 W, with specialized products for building integrated PV systems (BIPV) at even larger outputs. Wafer-based crystalline silicon modules have commercial efficiencies between 14 and 21.5%. Crystalline silicon modules consist of individual PV cells connected together and encapsulated between a transparent front, usually glass, and a backing material, usually plastic or glass. Thin-film modules encapsulate PV cells formed into a single substrate, in a flexible or fixed module, with transparent plastic or glass as the front material. Their efficiency ranges between 7% (a-Si) and 16.3% (CdTe). CPV modules now offer now efficiencies up to 36% (PVPS, 2015) Groups of cells are connected electrically in series or in parallel and sealed by environmentally protective laminates to construct PV modules; one or more modules comprising the complete PV generating unit for a system, is called a PV array—see Figure 2.23.

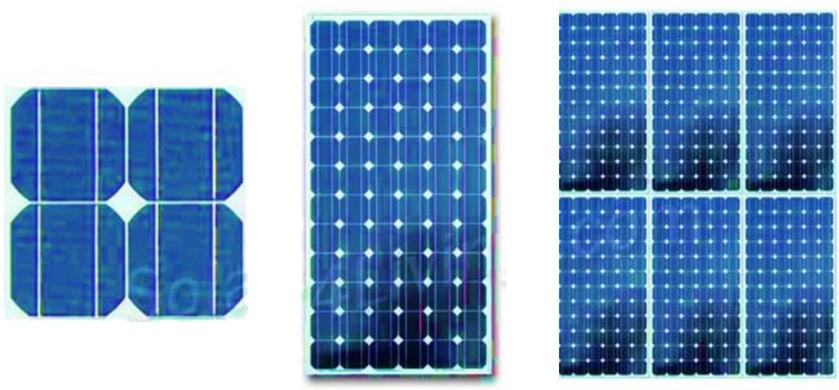

Figure 2.23: Examples of a PV cell, a module and an array

2.11.3 Balance of system equipment

Although a PV module produces power when exposed to sunlight, a number of other components are required before usable power is obtained; the harvested power must be conducted to a charge controller, a battery (where the energy can be stored), an inverter (for loads requiring alternating current), and finally distributed to the loads. Depending on the type of system, these systems may include some or all of the components discussed in the subsections which follow.

2.11.3.1 PV Lighting System Controllers

System controllers are required in PV lighting systems to regulate the battery charge and to control the operation of the lighting load. The function of a PV lighting system controller is to:

a) prevent the battery from being overcharged by the PV array (voltage regulation - temperature compensated)
b) prevent the battery from being overdischarged by the lighting load (low voltage load disconnect)
c) maintain the battery at its highest possible state-of-charge
d) control the timing and operation of the lighting load
e) serve as a terminal connection point between the array, battery and lighting load

Optional features of some PV lighting controllers include:

a) system status indicators, lights and meters
b) advanced load control
c) battery charge equalization
d) data monitoring and recording for system diagnostics

The following characteristics should also be considered before selecting a controller:

a) adjustable setpoints.
b) high voltage disconnect.
c) low voltage disconnect.
d) temperature compensation.
e) low voltage warning.
f) reverse current protection.
g) maximum power tracking.
h) on/off operation system.

Figures 2.24 and 2.25 show two typical system controllers used in PV lighting applications. These controllers use battery voltage sensing to regulate the state-of-charge of the battery and to disconnect the load if the battery becomes overdischarged. These controllers use the PV array to sense dusk conditions to activate a light, and can be set to operate the light until dawn, or for a fixed number of hours after dusk. In some cases, a separate lighting controller may be used independently of the battery charge controller. Two of these devices are shown in Figure

2.26 below. The controller on the left allows for time of day and weekly programming, and the unit on the right uses the PV array sensing and timing circuits to control the light.(Guide, 1998b)

Figure 2.24: PV lighting system controller (Trace Engineering).

Figure 2.25: PV lighting system controller (Morningstar).

Figure 2.26: PV lighting system controls (SEPCO, SCI).

Charge regulators are the link between the PV modules, the battery and the load. They protect the battery from overcharging or from excessive discharging. Charge and discharge voltage limits should be carefully selected to suit the battery type and the operating temperature. These settings can significantly affect maximum operational life of a battery. High temperatures tend to reduce battery life because they accelerate corrosion and self-discharge. High temperatures may also increase out-gassing during charging and should therefore be controlled. The resistance of lead-acid batteries to freezing is reduced when they are discharged, so these batteries should be kept charged when they are subjected to low temperature conditions during the winter (Zeman, 1998).

PV modules that are used to charge batteries usually operate at an approximately constant voltage, which is selected to suit the local temperature. However some PV systems regulators employ a maximum power point tracker (MPPT), which automatically permits the PV modules to operate at the voltage that produces maximum power output. Such regulators employ an electronic DC-DC converter to maintain their output at the required system voltage. The benefit of using an MPPT depends on the application and should be weighed against the additional cost and reliability risks. For many applications, it may be equally, or more cost effective to operate the system at a fixed voltage(Zeman, 1998). Figure 2.27 shows a typical system controller used in PV lighting applications.

Figure 2.27: PV lighting system controller (Morningstar)

2.11.3.2 Battery

Batteries are electrochemical cells that store energy in chemical bonds. This chemical energy is converted to electrical energy when a battery is connected to an electrical load and discharged. By reversing the flow of current, the chemical nature of the battery is restored to its charged condition. Because the time when electrical energy produced by the PV array does not always coincide with the time when the energy is needed, rechargeable batteries are commonly used in stand-alone PV lighting systems. The principal function of batteries in these systems is to:

a) store energy produced by the PV array during the day, and supply it to the lighting load at night and for use on days of below-average sunlight.

b) operate the lighting loads at stable voltages, and supply surge currents if needed.

c) establish a suitable operating voltage to maximise PV array output.

To provide electricity over long periods, PV systems require deep-cycle batteries. These batteries are designed to gradually discharge to 80% of their capacity and then to be recharges; a cycle that can be repeated hundreds of times. Automotive batteries are shallow-cycle batteries and should not be used in PV systems because they are designed to discharge only about 20% of their capacity. Factors that affect the choice of battery are: the climatic conditions in which it will operate; how frequently it will receive maintenance; and the types of chemicals it uses to store and release electricity. A PV system may have to be sized to store a sufficient amount of power in the batteries to meet power demand during several days of cloudy weather; this is known as days of autonomy (Grothoff, 2015).

The batteries are the central part of any stand-alone PV system, and must be designed for the service requirements of the application. Batteries in PV lighting systems sometimes experience deep discharge cycles; to maximize performance and cycle life they should be tolerant of this treatment. One of the single most important cost drivers for PV lighting systems is battery replacement. For this reason an optimal battery cycle life is desirable. For typical PV lighting applications, batteries may last anywhere from three to ten years. Factors that affect battery cycle life include:

- battery design and construction
- temperature
- frequency and depth of discharges
- average state-of-charge
- charging methods
- required maintenance.

Temperature is perhaps the most important operational variable affecting battery life. Higher temperatures accelerate battery grid corrosion and result in greater gassing and electrolyte loss. For all types of batteries, lifetime decreases by a factor of about two for every 10^{o}C increase in average operating temperature. On the other hand, low operating temperatures extend battery life, although available battery capacity is reduced. In any application, battery life can be optimized by proper charging (not overcharging or overdischarging), maintaining high a state-of-charge, limiting the frequency and depth of discharges, moderating the temperature and conducting regularly scheduled maintenance (Grothoff, 2015).

2.12 Summary

In this chapter state-of-the-art PV system technology and its applications, were expounded on. At the start of the chapter, a history of photovoltaics and the principles of solar PV cell operation, solar irradiation, the effects of temperature and solar radiation on solar cells, were discussed. Also deliberate were the different PV system, highlighting their advantages and disadvantages, and their applications, as well as an overview of commercially available PV systems. This followed by an explanation of PV lighting components. The objective of this chapter is to provide a general background of PV systems, PV system components, and their applications.

CHAPTER THREE

METHODOLOGY

"Component Selection Criteria, Sizing and Evaluation of SSP System"

3.1 Introduction

3.2 Component Selection Criteria for Standalone Solar Pathway System

3.2.1 Selection criteria for PV modules and arrays

3.2.2 Battery selection criteria

3.2.3 PV lighting system controllers selection criteria

3.2.4 Luminaires selection criteria

3.3 Sizing and Design of Stand-alone PV Pathway Systems for Public Park Lighting

3.3.1 Estimating the electrical load for lighting

3.3.2 PV array sizing to fully provide the energy requirements

3.3.2.1 Calculation of average power for one PV module

3.3.2.2 Number of PV panels and configuration of PV array

3.3.3 Battery capacity estimation and calculation

3.4 Performance analysis of an SSP system

3.4.1 Existing parameter values for system performance assessment and their limitations.

3.4.2 A new coefficient: the Production Factor (PF)

3.5 Summary

3.1 Introduction

Thousands of PV lighting systems are being installed annually throughout the world, including applications for park lighting, remote-area lighting, sign lighting, flashing and signalling systems, consumer devices and home lighting systems. PV lighting systems are simple, easy to install, and if properly designed and maintained, can provide years of maintenance-free service. When selecting the proper components for lighting applications, many different constraints are taken into account. By predetermining the number of components required and how the system will operate, cost and redesigning time can be minimized. This chapter provides an overview of PV lighting components, system design principles, existing benchmarks for system performance assessment, as well as the limitations of PV lighting systems. This information is intended for those individuals that specify PV lighting equipment and evaluate system designs, as well as those that design and integrate systems. In this chapter the fundamentals and selection criteria for the major PV lighting system components–the PV array, batteries, controls and luminaires are included. Furthermore this chapter discusses the procedures for sizing the system and provides justification for the selection of each component. The benchmarks used to evaluate SSP technology for pathway public lighting from the generation stage to the load are also discussed. This chapter also covers a detailed explanation of methodology which will be used to complete this project and ensure that it functions properly.

3.2 Component Selection Criteria for a Stand-alone Solar Pathway System

In designing and the proper selection of components for lighting applications in a solar pathway system, it is important to consider the system as a whole: how the components work together and how the PV system fits in with the selected site. An elementary PV system layout diagram is provided in Figure 3.1 below. It consists of the source of energy (sun), photovoltaic array, electronic controller, different loads and electrochemical storage system.

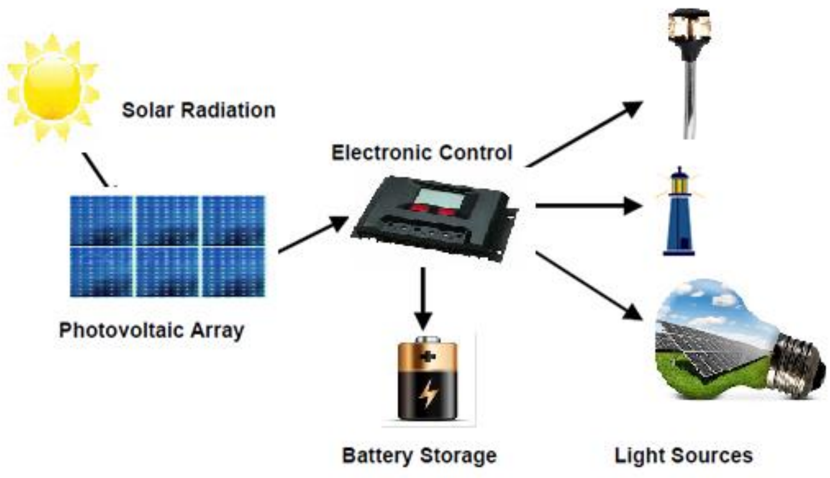

Figure 3.1: A typical stand-alone photovoltaic lighting system

3.2.1 Selection criteria for PV modules and arrays

A number of factors should be considered when selecting PV modules for a given lighting application. These criteria include:

a) electrical performance (rated output)

b) physical properties (for example size, weight)

c) mechanical properties (such as construction materials, mounting attachment)

d) reliability (qualification tests, Underwriter Laboratory (UL) listing)

e) efficiency and surface area requirements for the PV array

f) cost, lifespan and warranty of the PV array (Guide, 1998b)

3.2.2 Battery selection criteria

Certain battery designs are more suitable for the operating conditions found in PV lighting systems. However, the ultimate selection of a battery involves many trade-offs, including:

a) performance (capacity, voltage)

b) lifespan (cycles, years to certain average daily depth of discharge)

c) physical characteristics (size, weight, casing)

d) electrical configuration (series, parallel arrangement)

e) maintenance requirements (testing, cleaning, adding water)

f) warranty and cost (initial and replacement)

g) availability.

Both flooded and sealed valve-regulated lead-acid (VRLA) batteries are commonly used in PV lighting systems, the latter having lower maintenance requirements. Nickel-cadmium and nickel-metal hydride cells are sometimes used in small consumer products and also in extremely low-temperature and critical-power applications, such as navigational aids. Table 3.1 lists some advantages and disadvantages of various battery types used in PV lighting applications (Guide, 1998b; Le, 2011)

Table 3.1: Battery Comparison

Battery Type	Advantages	Disadvantages
Flooded Lead-Acid		
Lead-Antimony	Low cost, wide availability, good deep cycle and high temperature performance. Can replenish electrolyte. Good cycle life.	High water loss and maintenance. Need for periodic equalization.
Lead-Calcium Open Vent	Low cost, wide availability, low water loss. Can replenish electrolyte	Average to poor deep cycle performance, intolerant of high temperatures and overcharge. Need for periodic equalization
Lead-Calcium Sealed Vent	Low cost, wide availability, low water loss.	Average to poor deep cycle performance, intolerant to high temperatures and overcharge. Cannot replenish electrolyte.
Lead Antimony/Calcium Hybrid	Moderate cost, low water loss, good deep cycle performance. Good cycle life.	Limited availability, potential for stratification. Need for periodic equalization
Captive Electrolyte Lead-Acid		
Gelled	Moderate cost and cycle life, little or no maintenance. No liquid electrolyte, install in any orientation.	Fair deep cycle performance, intolerant of overcharge and high temperatures. Limited availability.
Absorbed Glass Mat	Moderate cost and cycle life, little maintenance. No liquid electrolyte, install in any orientation.	Fair deep cycle performance, intolerant to overcharge and high temperatures. Limited availability.
Nickel-Cadmium		
Sealed Sintered-Plate	Wide availability, excellent low and high temperature performance. Maintenance free and long life.	High cost, only available in low capacities. Suffer from ‘memory’ effect when partially discharged
Flooded Pocket-Plate	Excellent deep cycle and high/low temperature performance. Tolerant of overcharge.	High cost, limited availability. Water additions required.

3.2.3 PV Lighting system controller selection criteria

The controller in a PV lighting system plays a critical role in the operational performance of the system. The following criteria should be considered when specifying or selecting controllers for PV lighting applications:

a) nominal system operating voltage (12, 24 or 48 volt DC)

b) maximum PV array and lighting load currents

c) battery characteristics (charging requirements, allowable depth of discharge)

d) regulation and load disconnect set point requirements

e) charge algorithms and switching element

f) lighting load control strategies

g) battery charge voltage temperature compensation (on-board or external probe)

h) expected environmental operating conditions and appropriate mechanical packaging

i) availability of system status indicators

j) availability of battery overcurrent and disconnect provisions

k) overall compatibility with system functional requirements and other components

l) cost and warranty.

One of the most important features of a battery charge controller is the voltage settings at which it respectively controls the PV array and the load, to protect the battery from being overcharged or overdischarged. Table 3.2 provides the recommended set point values for PV array regulation and load disconnect for two controller classifications and for four battery technologies. Specific set point requirements may vary for particular designs and applications (Guide, 1998b)

Table 3.2: Suggested charge controller set point values.

Charge Controller		Suggested Regulation and Load Disconnect Voltages for a Nominal 12 V Battery			
Controller Design Type	**Controller Set Points at 25°C**	**Flooded Lead-Antimony**	**Flooded Lead-Calcium**	**Sealed, Valve Regulated Lead-Acid**	**Flooded Pocket Plate Nickel-Cadmium**
On-Off, Interrupting	**Charge Regulation Voltage**	14.6–14.8	14.4–15.0	14.2–14.4	14.5–15.0
	Array Reconnect Voltage	13.5–14.0	13.5–14.0	13.5–14.0	13.5–14.0
Constant-Voltage, PWM, Linear	**Charge Regulation Voltage at 25°C**	14.4–14.6	14.4–14.7	14.0–14.2	14.5–15.0
All Controllers	**Load Disconnect Voltage**	11.3–12.0	11.3–12.0	11.3–12.0	11.3–12.0
	Load Reconnect Voltage	12.5–13.5	12.5–13.5	12.5 –13.5	12.5–13.5

3.2.4 Luminaires selection criteria

Luminaires are the complete lighting unit consisting of lamp, socket, ballast, reflector, diffuser and fixture housing. Considerations in luminaire selection include (Guide, 1998b; Le, 2011).

1) proper candlepower distribution for the intended application
2) efficiency of converting electrical power to light output
3) equipment listing and outdoor rating
4) mechanical design, construction and use of materials
5) ease of lamp and ballast replacement
6) aesthetic appearance
7) cost and reliability.

3.3 Sizing and Design of Stand-alone PV Pathway Systems for Public Park Lighting

Stand-alone PV pathway systems are independent, fully-integrated power supplies with the primary function of operating lighting equipment. Depending on the given application, the PV power supply may be integrated with the lighting equipment in different ways, although the function, electrical design and component sizing considerations remain essentially the same.

The design of PV pathway systems involves a number of steps and possible iterations to select and size the individual components required for a functional system, Figure 3.2 presents an energy flow and sizing strategy for stand-alone PV lighting system. This section covers the basics of sizing and design for a stand-alone PV lighting system (Guide, 1998b)

The following steps outline the process for designing PV lighting systems:

1. Establish the ***quantity and quality of lighting*** required. Select luminaires based on the application requirements.
2. Determine the ***magnitude and duration of the electrical load for the lighting,*** on both an average daily basis and a seasonal basis.
3. Estimate the ***battery storage size,*** based on the desired autonomy period and maximum and average daily depth of discharge. Select a battery based on the application requirements.
4. Estimate the ***PV array size,*** based on the time of year with the highest average daily lighting load and minimum solar radiation. Select PV modules that will form an array which will meet the application requirements.
5. Determine the ***control strategy*** to be used for battery protection and lighting control and specify the control set points and conditions. Select system controls based on the application requirements.
6. Complete ***electrical design*** requirements.
7. Complete the ***mechanical design*** and system configuration.

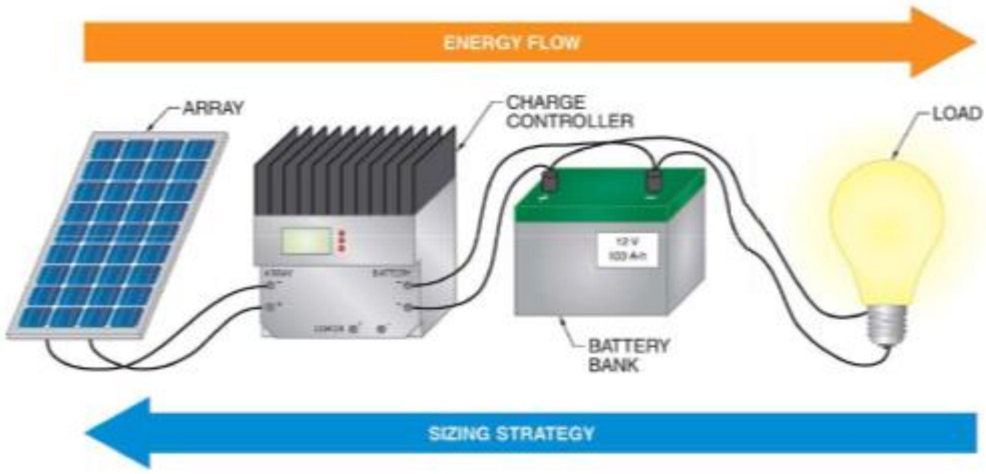

Figure 3.2: The direction of the energy flow and sizing strategy for a stand-alone PV lighting system.

3.3.1 Estimating the electrical load for lighting

The first step in the design process of a stand-alone solar pathway for public park lighting, is to estimate the electrical load required for lighting. It is the electrical load that determines the size and design of a PV-powered system; therefore the energy efficiency of the load is a critical concern. For this reason, steps are often taken to improve the efficiency of lighting design as part of any PV lighting application. This may involve several factors, including the selection of more efficient light sources and improved luminaire design, better orientation and distribution of the light, and special controls to limit the time of operation, or to reduce the level of lighting when artificial light is available. Adoption of any of these measures will result in a corresponding reduction in the both the size and the design requirements of an SSP system.The daily energy requirement for the lighting load is determined by the product of the current of the load and the operation time, and is expressed in ampere-hours (Ah). If the lighting is designed to operate from dusk to dawn throughout the year, then seasonal variations in the lighting load should also be considered (Guide, 1998b; Le, 2011).

Estimating the required load of the system is achieved by listing the power demand of all the loads, the number of hours that each load is active per day, and the corresponding operating voltage. The following equations can be used to calculate the night hours for any location as a function of the latitude and time of year.

$$D = \sin^{-1}[0.3975 \times \cos(0.98563(N-173))] \quad (3.1)$$

$$H = \cos^{-1}[-\tan(L) \times \tan(D)] \quad (3.2)$$

$$T = 2[12-(12H/180)] \quad (3.3)$$

where: D: solar declination (degrees)
N: Julian day number (1-365)
H: solar hour angle (degrees)
L: latitude (degrees)
T: night hours (sunset to sunrise)

From the load current in ampere-hours, and the given operating voltage for each load, the power demand is calculated. The recommended voltage for an SSP is determined by considering the information obtained by grouping the loads together by type with the corresponding operating voltage, and calculating the power demand for each group. When AC loads dominate, the DC system voltage should be selected for compatibility with the inverter input. If DC loads have the largest power demand, the voltage accompanying the largest load is selected.

3.3.2 PV array sizing to fully provide the energy requirements

Estimating the size of PV array required for stand-alone solar pathway is based on providing adequate energy to meet the highest average daily load during periods when solar insolation on the array surface is at its lowest. Figure 3.3 shows flowchart of a stand-alone solar pathway. Steps for determining the size of PV array required, are to:

1. obtain solar radiation data and determine the optimal array tilt angle required to maximise the minimum monthly ratio of solar insolation to electrical load.
2. estimate the average daily load requirement for each month of the year (in ampere-hour).
3. increase the system load requirement to compensate for system losses and inefficiencies in charging and discharging batteries (typically 110 to 120 per cent).
4. select a PV module and the module output for temperature and degradation (typically 85 to 90 percent of the rated output).
5. determine the number of parallel-connected modules required to satisfy the average daily system load demand for the design month solar insolation.
6. determine the number of series-connected PV modules required, based on the nominal system voltage and module peak power voltage.

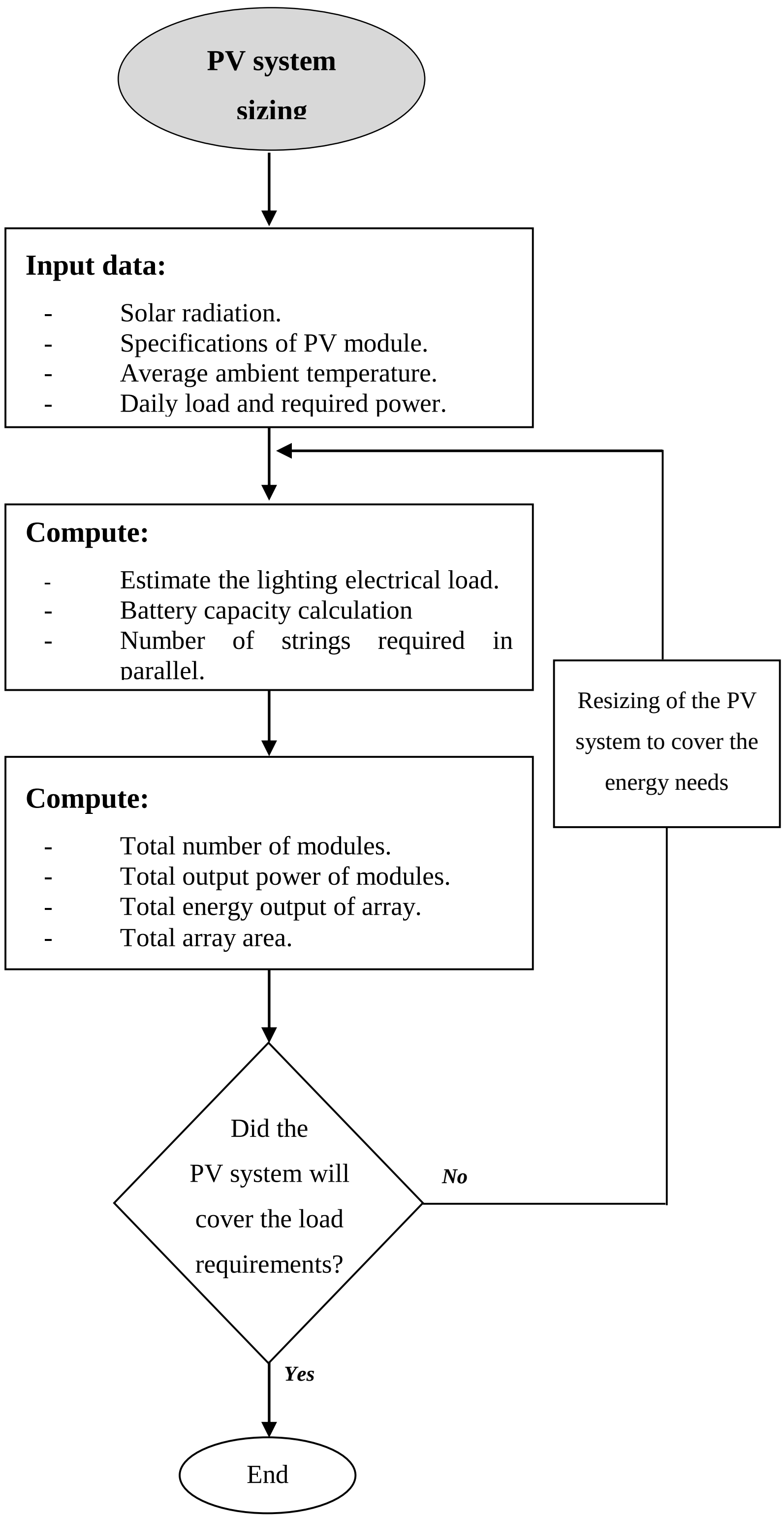

Figure 3.3: Flowchart of stand-alone solar pathway

Before the PV array can be sized, the designer must obtain solar radiation data for the application site. The optimal array tilt angle must also be determined to maximize the solar insolation to load ratio during the critical design month – thus minimizing the size of the PV array. Solar insolation data is usually given as the average daily insolation for each month; the units are kWh/m^2/day. This information can also be thought of as the equivalent number of hours per day that the irradiance on a surface is at a peak level of 1 kW/m^2 – the same standard as used for module peak output ratings. For this reason solar insolation data (in units of kWh/m^2/day) are often referred to as peak sun hours. The National Renewable Energy Laboratory (NREL) publishes this data in tabular and graphical form for the purpose of solar energy system design. (NREL website).

3.3.2.1 Calculation of average power for one PV module

The electrical power generated by a PV module depends on solar radiation and ambient temperature. To calculate the maximum output power from one PV module for every month of the year (Treble, 1991) Equation 3.4 is used.

$$P_{mx} = P_m \times (1.0 - \alpha \times (T_a - 25)) \qquad (3.4)$$

where:

P_{mx} : maximum output power from one PV module (watt)

P_m : maximum power under standard condition (watt) (at 25 ^oC)

α : temperature coefficient of power (per ^oC)

T_a : the average ambient temperature (^oC)

3.3.2.2 Number of PV panels and configuration of PV array

Calculation steps carried out to determine the system sizing are listed below:

1- Choose the type and specifications of the PV module.

2- Determine the number of modules to be connected in series (this is called a string) by using Equation 3.5.

$$n_s = \frac{V_{DC}}{V_m} \qquad (3.5)$$

where:

n_s : Number of modules connected in a string.

V_{DC} : The selected DC bus voltage (volt).

V_m : The module voltage corrected for operating conditions.

3- To calculate the number of strings required in parallel, divide the annual average daily load by the annual average daily output from a string, by using Equations 3.6 and 3.7.

$$n_p = \frac{E_L}{A_{om}} \tag{3.6}$$

$$A_{om} = n_s \times P_m \times t \tag{3.7}$$

4- The number of PV panels needs to cover 100% of power needs , and it is calculated By dividing the peak array power by the maximum power under standard conditions:

$$n_{pv} = \frac{P_{a,\max}}{P_m} \tag{3.8}$$

where:

n_{pv} : number of PV panels.

$P_{a, max}$: peak array power (kW).

P_m : maximum power under standard condition (watt).

5- Calculation of average daily energy output from PV array.

$$E_a = n \times P_{mx} \times (1.0 - TL) \times Gt \tag{3.9}$$

where:

E_a : array output energy (kWh/d).

n_{pv} : number of PV panels.

P_{mx}: maximum output power from one PV module (watt).

TL : total system losses (per unit).

Gt : average daily hours of sunshine (solar rad. / 1000 $W.m^{-2}$).

3.3.3 Battery capacity estimation and calculation

The battery should able to supply the load for a predefined number of days even when the average radiation on these days is low. Battery size is a design variable, and is generally based on the desired autonomy period, maximum allowable depth of discharge, and derating for low operating temperatures. Similar to load energy, the of battery storage capacity is expressed in ampere-hours.

Also referred to as the days of energy storage, autonomy is the time a fully charged battery can supply energy to the lighting load when there is no energy input from the PV array, for example, several consecutive days when heavily overcast skies could occur. Less critical PV lighting applications are typically designed for three to five days of autonomy, while more critical applications can be sized for ten or more days. Greater autonomy means that the battery will be cycled less deeply on an average daily basis; a much larger and more expensive battery is however required. It also means that while it takes a long time for the battery to become fully discharged, it takes equally long to recharge it. This could present a problem in systems with marginally sized PV arrays, increasing the potential for the battery to remain at damaging low levels of charge for extended periods.

The ***maximum allowable depth of discharge*** is the desired limit of battery discharge or usable capacity, and it is pre-determined by the low voltage load disconnect set point on the system controller, as well as the discharge rate of the lighting load. For deep-cycle battery designs, 80 percent maximum depth of discharge (DOD) is typically used. For the size range of most PV lighting system designs, this occurs at a battery voltage of between 11.3 and 11.7 volts for nominal 12-volt lead-acid batteries. For batteries designed for shallower cycle service, the maximum allowable DOD is typically limited to 40 to 60 percent to achieve the rated lifespan. Note that the allowable depth of discharge is a design limit, and is seldom reached in well-designed PV lighting systems.

To protect the battery from freezing, the maximum allowable depth of discharge must also be limited for batteries operating in cold climates. Although the freezing point of a typical fully charged lead-acid battery is between -50 and -70^{o}C, the freezing point of a battery at 50 percent state-of-charge is about -15^{o}C. As a lead-acid battery becomes more discharged, the concentration of the sulfuric acid electrolyte decreases to a point where it is essentially water. At this fully discharged condition, the freezing point of the battery is 0^{o}C. To prevent freezing in cases where low battery temperatures are expected, a higher low voltage load disconnect set point must be used to limit the maximum DOD.

Low temperatures also slow down the electrochemical process in a battery, reducing the available capacity. Lead-acid batteries are particularly affected, when operated at 0ºC and at the typical low discharge rates found in PV lighting systems (Guide, 1998b; Le, 2011). And can only deliver approximately 80 percent of their rated capacity at 25ºC, The following simple formula can be used to calculate battery storage capacity requirements in PV lighting systems.

$$Required\ Battery\ Capacity\ (rated\ at\ 25°C\ at\ load\ discharge\ rate) = \frac{[Days\ of\ Autonomy \text{ x } Average\ Daily\ Load]}{[Allowable\ DOD \text{ x } Low\ Temperature\ Capacity\ Factor]} \quad (3.10)$$

Often discharge rates are expressed by *C/t*, where *t* is the discharge time in hours and *C* is the rated battery capacity. Discharge hours are calculated by dividing the rated battery capacity by the load current. For example, a 100 Ah battery loaded at 5 amps would have a discharge rate of 20 hours, or C/20. Low discharge rates are common in stand-alone PV system designs, and result from the high autonomy requirements and allowable DOD limits.

In stand-alone PV systems with large autonomy, the average daily DOD is considerably less than the allowable DOD. The average daily DOD is calculated by dividing the average daily load by the total rated battery capacity. For example, a ten amp-hour average daily load results in ten percent average daily DOD for a 100 Ah battery.

The design flow chart of the battery capacity calculation is shown in Figure 3.4 (Ho & Hsu, 2010). when the relationship is given by Equation 3.11 :

$$C = \frac{D \times I_L}{U} \quad (3.11)$$

where:

$$I_L = I \times T \quad (3.12)$$

and:

C: The required capacity [Ah]

D: Longest days without sunlight

I_L: Daily required capacity (Ah)

I: Load Current (A)

T: Daily use time (hours)

U: Discharge depth, U is chosen as 0.8 for deep discharge type battery and 0.5 for others.

However, Equation 3.11 only gives a rough approach; for more accuracy, the influence of operating temperature and discharging rate on the capacity should be considered. Therefore Equation 8.11 is modified as Equation 3.13:

$$C = \frac{D \times I_L}{U \times \alpha \times R} \tag{3.13}$$

where:

R: Overall efficient circuit modification factor

α: Temperature modification factor and is less than 1.0 for temperatures lower than 25º C.

Once the capacity of battery and PV module have been calculated, there follows a checking requirement to ensure a good consideration of both designs.

Firstly, to prevent over-discharging, check the battery discharging depth as indicated by Equation 3.14:

$$Depth\ of\ discharging = \frac{daily\ total\ load\ (Ah)}{capacity\ of\ battery\ (Ah)} \tag{3.14}$$

If the results from Equation 3.14 are not acceptable, (based on the data sheet of battery) then the capacity of battery should be modified until it meets the requirements (Ho & Hsu, 2010).

3.4 Performance analysis of a stand-alone solar pathway (SSP)

A poor match between the production and the load will result in unsatisfactory performance of the system, even though the system does not encounter any technical problems. This thesis presents a performance evaluation of an SSP to power public park lighting through a case study. This evaluation provides an improved assessment of operational performance of an SSP, because not only are the commonly used factors viewed in terms of their limits, but some new coefficients are highlighted (Almaktoof et al., 2014; Almaktoof et al., 2015; Jahn et al., 2000; Mayer & Heidenreich, 2003).Various derived parameters related to the energy balance of the system and performance, can be calculated from the recorded data (Almaktoof et al., 2015; Mayer & Heidenreich, 2003)

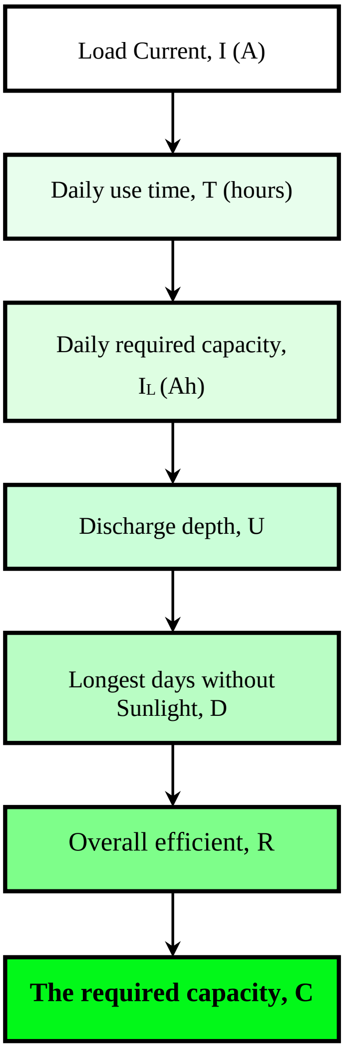

Figure 3.4: Flow chart of the capacity calculation for a battery

3.4.1 Existing parameter values for system performance assessment and their limitations

The quantities usually used to assess the performance of an SSP are shown in Table 3.3.

Table 3.3: Parameters of performance evaluation of stand-alone solar pathway.

Parameter	**Symbol**	**Equation**	**Unit**
Array Yield	Y_A	E_a/P_o	kWh/kWp
Final Yield	Y_f	E_{PV}/P_o	kWh/kWp
Reference Yield	Y_r	H_i/G_{STC}	kWh/kWp
Capture losses	L_c	Y_r-Y_A	kWh/kWp
System losses	L_s	Y_A-Y_f	kWh/kWp
Performance ratio	**PR**	$\mathbf{Y_f / Y_r}$	**--**

where:

P_o : Peak power (Wp)

H_i : Mean radiation in the plan of array (kWh/m^2.d)

G_{STC} : Reference irradiation at STC = 1 (kW/m^2)

E_a : Array output energy (kWh/d)

E_{PV} : PV energy consumed (kWh

Figure 3.5 relates the location of the various parameters used to evaluate the SSP technology for pathway public lighting, to a schematic layout of the system.

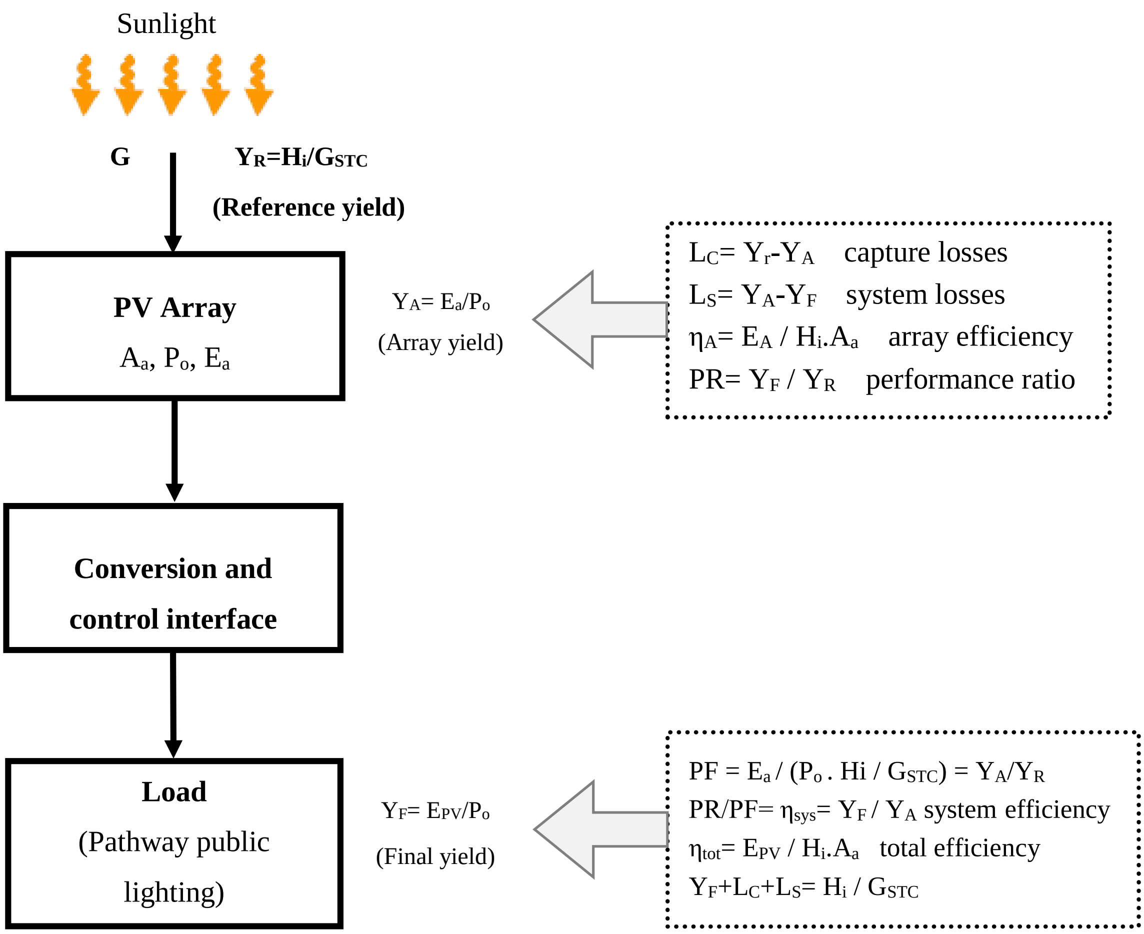

Figure 3.5: System performance analysis

The ***array yield,*** Y_A represents the number of hours per day that the array would need to operate at its peak power, P_o to contribute the same daily array energy to the system as was monitored.

The ***final PV system yield,*** Y_F is the portion of the daily energy of the entire PV plant which is delivered to the load per kilowatt peak of installed PV array.

The ***reference yield,*** Y_R represents the solar energy theoretically available per kilowatt peak of installed PV per day.

The normalized losses are calculated by subtracting the yields. Losses also have unit of h/d and indicate the amount of time during which the array would be required to operate at its peak power, $P_{o,}$ to provide for these losses.

Array capture losses, L_C are caused by thermal capture losses which occur when cell temperatures operate at a temperature higher than 25ºC (Almaktoof et al., 2015; Mayer & Heidenreich, 2003) as well as by miscellaneous causes such as:

a. low irradiance
b. wiring, string diodes
c. partial shading, contamination, snow covering, non-homogenous irradiance
d. maximum power point tracking errors
e. reduction of array power caused by inverter failure or by a fully-charged accumulatorSpectral losses, losses caused by glass reflections (use of pyranometers).

System losses, L_S are from inverter conversion and from accumulator storage losses in systems.

The performance ratio (PR) was introduced to characterize the system operation, regardless of the application under consideration. It indicates how the potential energy of a PV arrays is used. This potential energy is defined in the Standard Tests Conditions.

The higher the PR, the better the system uses its potential. A low PR value means production losses due to technical or design problems.

In an SSP, a high PR value does not always mean that the system is operating at optimum efficiency. If the system is underdesigned for the particular application, the PV cells will show a very high value of PR, but at the same time the user will not be supplied with electricity.

An oversized system will frequently incur partial or total disconnection of the array, directly affecting the PR value. The PR indicates the overall effect of losses on the nominal power of an array, due to array temperature, incomplete utilization of irradiation, and system component inefficiencies or failures (Jahn et al., 2000; Ma et al., 2013; Mayer & Heidenreich, 2003)

The ***mean array efficiency,*** $\eta_{A,mean}$ represents the mean energy conversion efficiency of the PV array, which is useful for comparison with the array efficiency, η_{Ao} at its peak power, P_o. The difference in efficiency values represents diode, wiring and mismatch losses, as well as energy wasted during plant operation.

3.4.2 A new coefficient: the Production Factor (PF):

An SSP which is not operating properly, will show a low PR. Hence a new coefficient is introduced below, by comparing the array production to the production specified at Standard Tests Conditions (STC) by the manufacturer of the system (Almaktoof et al., 2015; Ma et al., 2013; Mayer & Heidenreich, 2003). The production factor is defined as follows:

Production Factor: $PF = E_a / (P_o \cdot Hi / G_{STC}) = Y_A/Y_R$ (3.15)

System efficiency: $PR/PF = \eta_{sys} = Y_F/Y_A$ (3.16)

3.5 Summary

In this chapter an overview of PV lighting components, system design principles, and the values and limits of system parameters for assessing system performance, are provided. This information is intended for those individuals who specify PV lighting equipment and evaluate system designs, as well as those who design and integrate systems. All the components that have been used in the design of the SSP are fully described. Included in this chapter are the fundamentals of, and selection criteria for the major PV lighting system components — the PV array, batteries, controls and luminaires. Justification for the selection of each component, as well as the parameters used to evaluate the SSP technology for all stages pathway public lighting, were discussed. Additionally the procedures for determining component sizes, and the benchmarks used to evaluate SSP, were also considered. This chapter contains a detailed explanation of methodology that was implemented to make this project functional.

.

CHAPTER FOUR

Solar Pathway Operating Assessment for Public Park Lighting

4.1 Introduction

The development of solar roads to convert solar insolation on vast stretches of roadway in order to generate electricty, on surfaces otherwise dedicated solely transportation to electrical energy, is in its promising stage. Great potential is seen for PV application with the maturing of solar road technology. Apart from increasing the versatility by smart utilization of land resources, widening the covererage of renewable energy generation will lead to a sustainable, secure energy future.

The focus of this study is on gaining experience of the real- world operating characteristics of solar pathway systems. A variety of measurements were made to gather information on the solar insolation, and the operating temperature and energy yield. This chapter presents the modelling and simulation of a stand-alone solar pathway for public park lighting. The model is composed of a PV array, a DC-DC converter, charge controller, and batteries connected to the load.

The remaining part of this chapter is organised as follows: the selection of a case study to determine the sizing of components, and a performance analysis of the SSP technology chosen. The typical arrangement of an SSP system is described in Section 4.3. Next, the modelling of an SSP system was executed by computer program; the program software used was written by MALATB. The load requirements in terms of the quality, quantity and duration were determined, the load being the electrical lighting connected to the SSP system. The size of the storage batteries was estimated by taking account of the desired autonomy period and maximum and average daily depth of discharge. Based on the type and the specifications of available PV modules, the PV array was sized, by taking the time of year with the highest average daily lighting load and minimum solar radiation in-to consideration. A control strategy for battery protection, lighting control and the specification of set control points and conditions, was determined. In the penultimate section the operating efficiency of a solar pathway is presented. A conclusion is drawn in the last section.

4.2 Case study

A [65 m / sixty-five-metre] stretch of walkway, located next to the Electrical, Electronic and Computer Engineering Department Building was chosen to set up a case study. The case study presented a simplified method for sizing, performance evaluation and simulation of a stand-alone solar pathway to power public lighting on the Bellville Campus of the Cape Peninsula University of Technology. Figure 4.1 shows the characteristics of the selected site which has the following coordinates: -33.932677º N, 18.643299º E.

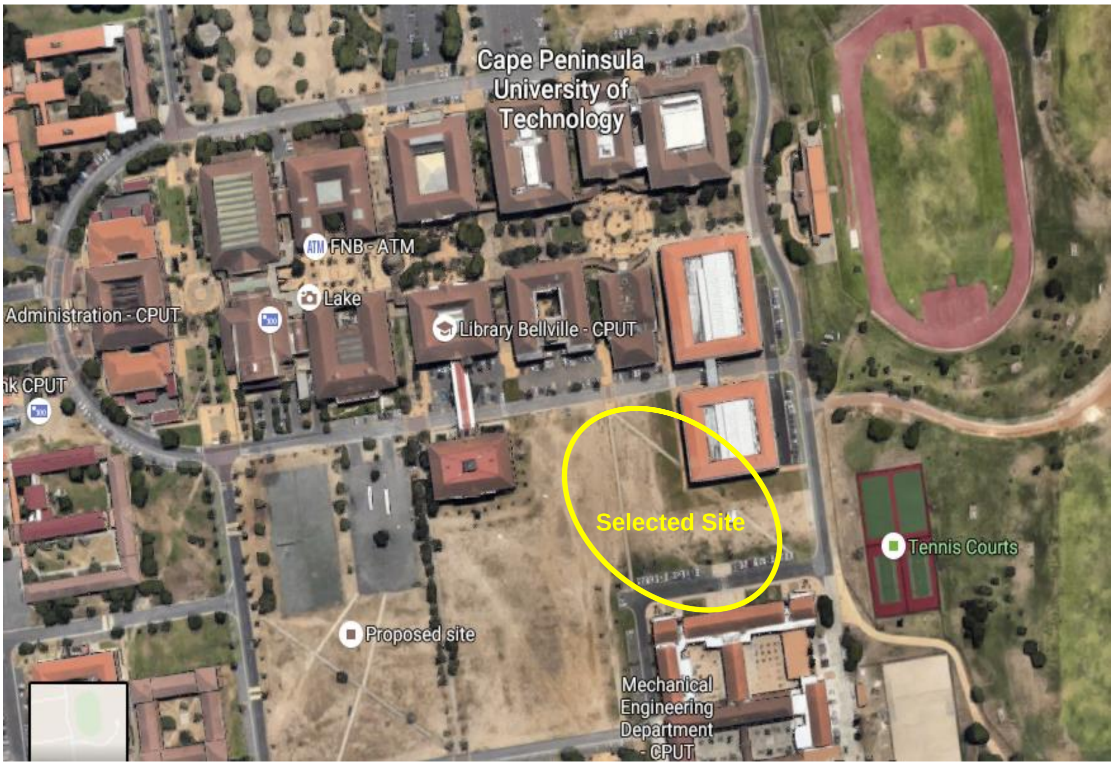

Figure 4.1: Aerial photograph showing the selected site

4.3 Steps of Sizing and Simulation of the System

The steps of sizing and performance evaluation of the SSP was executed by computer program called MATLAB software

Climate data at the selected site were sourced from Solargis, and NASA Surface meteorology and Solar Energy (SSE). These data (global solar radiation, annual mean temperature, average sunlight hours/day, average daylight hours/day, and percentage of sunny and cloudy daylight hours) were taken over 22-year period. Solargis data is the most reliable source of solar radiation data (Ineichen, 2013). Solargis data is not only useful for feasibility studies of new projects, but it is also for the performance assessment of operational projects. In addition to offering solar radiation data Solargis also provides tools for PV energy simulation, as well as expert consultancy support.

The NASA Surface meteorology and Solar Energy (SSE) data set is developing data sets from NASA Earth Science Enterprise (ESE) climate research to support renewable energy industries. The data sets contain solar parameters, principally derived from satellite observations and meteorology parameters from an atmospheric model constrained by satellite and sounding observations. These data sets cover a 22-year climatology history (July 1983-June 2005) on a grid of one-degree latitude by one-degree longitude. The global coverage of the NASA Earth Science data set fills the gap where remote locations lack ground measurement data. Most ground measurement stations are located near populated regions that may have an unnatural or an urban influence on the local climate. The Earth Science data set can augment ground-measured data affected by microclimates. The Earth Science data are considered accurate for preliminary feasibility studies of renewable energy projects.

The main components in an SSP system are array of PV modules, a battery, a charge controller and the DC lighting load. Figure 4.2 depicts the components and configuration of a stand-alone solar pathway system The steps for sizing and performance evaluation of the SSP are the following:

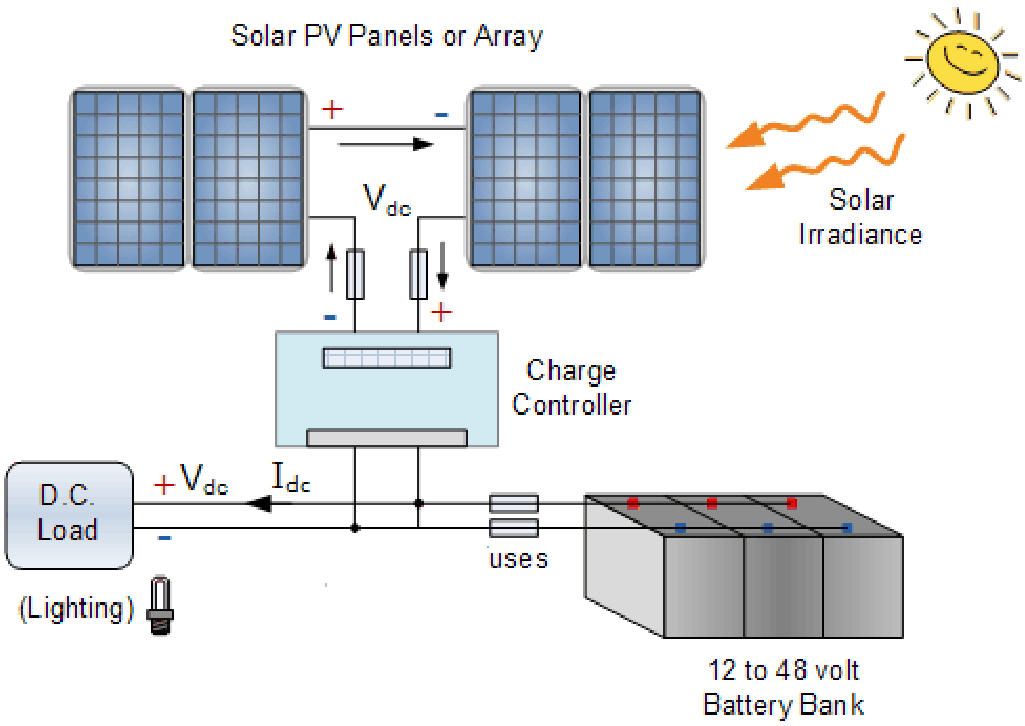

Figure 4.2: Stand-alone solar pathway system configuration

4.3.1 Evaluation of load needs—quantity and quality of lighting

To design an SSP the requirements of the load must be known; this means that the quantity and quality of the power required for lighting needs must be known. To determine this, one must firstly, select lighting fixtures based on application requirements, choosing the type and specifications of luminaire unit. The luminaire chosen was the GreenCobra™ Jr. LED Street Light GCJ; the technical specifications of this luminaire are given in Table 4.1. This luminaire has become the industry standard for many cities, utilities and transport departments throughout the world. Specification data sheets of the luminaire chosen can be observed in Appendix A.

Features of the Green Cobra Jr. include:

- An esthetically acceptable design.
- Options for warm white (3000 K), neutral white (4000 K), and cool white (5000 K) color temperatures.
- light trespass shielding.

Table 4.1: The technical specifications of GreenCobra™ Jr. GCJ: 4000K (NW), 5000K (CW) and 3000K (WW)

Product	Drive Current (mA)	System Wattage (W)	Delivered Lumens (lm)[1]	Efficacy (lm/W)	Type 2 BUG Rating	Type 3 BUG Rating
4000K (NW) and 5000K (CW)						
GCJ1	350	24	2400	100	B1 U0 G1	B1 U0 G1
	580	38	3700	97	B1 U0 G1	B1 U0 G1
	700	48	4400	92	B1 U0 G1	B1 U0 G1
GCJ2	700	48	4400	92	B1 U0 G1	B1 U0 G1
	1000	74	5900	80	B1 U0 G2	B2 U0 G2
3000K (WW)						
GCJ1	350	24	2400	100	B1 U0 G1	B1 U0 G1
	580	38	3650	96	B1 U0 G1	B1 U0 G1
	700	48	4300	90	B1 U0 G1	B1 U0 G1
GCJ2	700	48	4300	90	B1 U0 G1	B1 U0 G1
	1000	74	5700	77	B1 U0 G2	B2 U0 G2

Secondly, the number of hours between sunset and sunrise had to be established. The determination of monthly averaged daylight for each month was based on the monthly average day from the NASA Earth Science data base, which is the monthly average, averaged for a particular month over the 22-year span of the data base. Figure 4.3 presents the monthly averaged night hours (hours) between sunset till sunrise. Maximum of six-hour of operation has been selected per night for the SSP system.

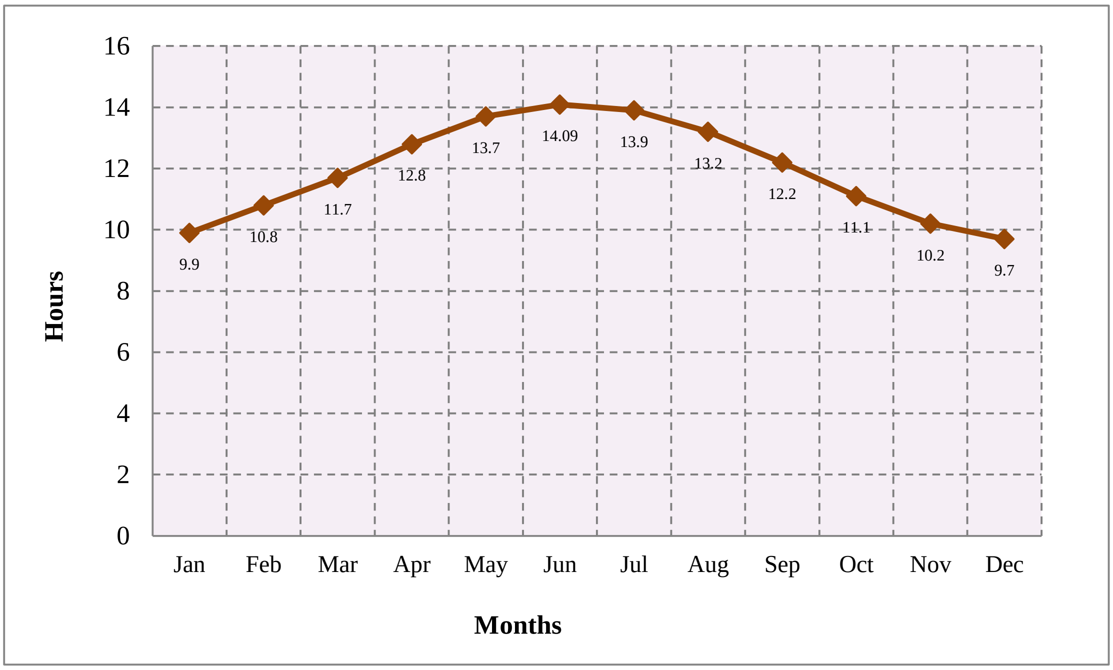

Figure 4.3: Monthly averaged night hours from sunset till sunrise in the selected site.

Finally, consider equivalent number of no-sun or black days for which a battery, or backup storage would be needed to supply power. The equivalent number of no-sun days over a number of consecutive days is depicted in Figure 4.4. Table 4.2 shows the equivalent number of no-sun. This parameter is very important for sizing the battery or any other energy- storage system.

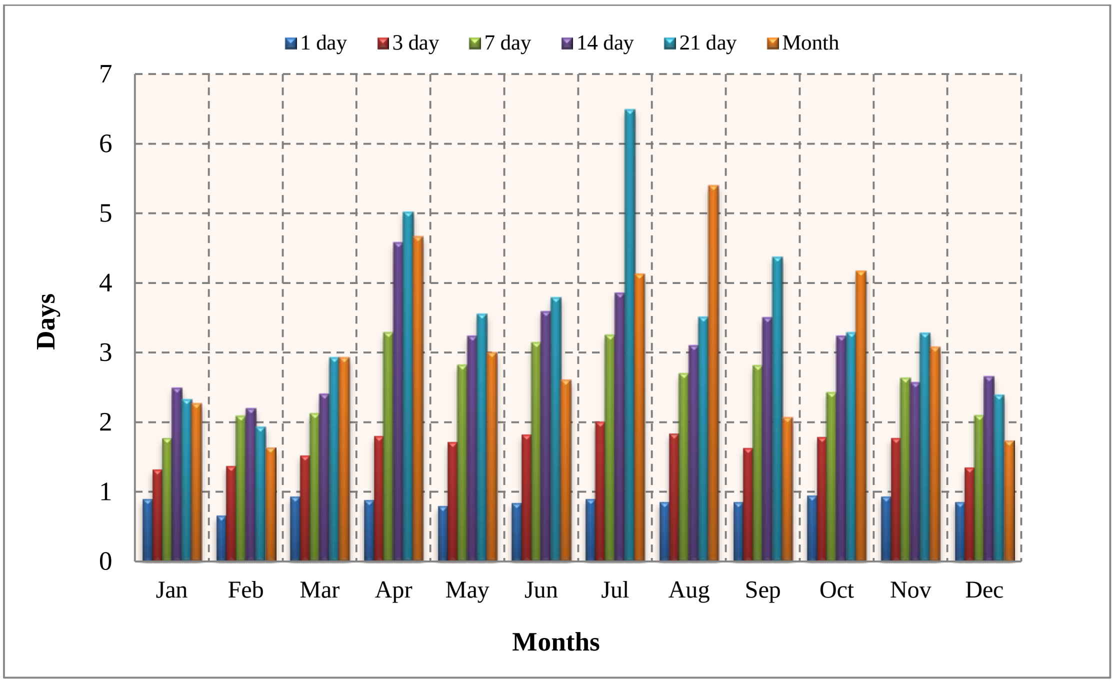

Figure 4.4: Equivalent number of no-sun.

Table 4.2: Equivalent number of no-sun.

S-33.933 E 18.643	Jan	Feb	Mar	Apr	May	Jun	Jul	Aug	Sep	Oct	Nov	Dec
1 day	0.90	0.66	0.93	0.88	0.79	0.84	0.90	0.85	0.85	0.95	0.93	0.85
3 day	1.32	1.37	1.52	1.80	1.71	1.82	2.00	1.84	1.63	1.79	1.77	1.35
7 day	1.77	2.09	2.12	3.29	2.82	3.14	3.25	2.70	2.81	2.43	2.63	2.10
14 day	2.49	2.20	2.40	4.58	3.24	3.59	3.86	3.10	3.50	3.24	2.57	2.66
21 day	2.33	1.93	2.93	5.02	3.55	3.79	6.49	3.51	4.37	3.29	3.28	2.39
Month	2.27	1.64	2.93	4.67	3.00	2.61	4.13	5.40	2.07	4.17	3.08	1.74

4.3.2 Calculation of the energy needs of lighting load

In this section a generalized form of energy is determined. An estimate of the required load of is achieved by listing the power demand of all loads, together with the number of hours of use per day and operating voltage of each of these loads. The number of hours of use per day between sunset and sunrise for the lighting load was determinedand and is depicted in Figure 4.3. The determination of monthly averaged night hours for each month is based on the "monthly average day" (SSE Methodology).

A 65 m stretch of walkway at the selected site needs twelve GreenCobra™ Jr. LED Street Light GCJ units, evenly distributed along the length of the pathway distributed; in total 288 W is needed for lighting load. The total daily power and energy requirements for the luminaires unit (lighting load) have been determined as shown in Table 4.3.

Table 4.3: The power and energy needs of the system.

Type of load	**Max. power & energy needs**
Total number of solar lights	12
One LED frame load	24 W
Lighting load (DC load)	0.288 kW
Load including charge controller losses (10 %)	(0.0288 kW) 0.317 kW
lighting hours of operation (average, per day)	Max. 6 at night (till midnight)
Total lighting load energy reqs/day	**0.317x 6 = 1.92 kWh**
Auxiliary loads (Wires, …)	0.0144 kW
Total auxiliary energy reqs/day	**0.0144 x 6 = 0.864 kWh**
Total power needs	0.3314 kW
Total system energy reqs/day	**2 kWh**

4.3.3 PV system sizing to cover 100% of energy needs

The following design methodology was applied for PV system to cover 100% of energy needs with energy recovery. Calculation steps carried out to determine the system sizing are presente in the subsections which follow.

4.3.3.1 Standalone PV module tilt angle

Since the pathway cannot be adjusted to the position of the sun, the panels will generate approximately 30% less energy than those placed at suitable angles on roofs (Hruska, 2014; Shekhar et al. 2015). However, the road is tilted slightly to aid water run-off and achieve a better angle to the sun and its creators expect to generate more energy.

4.3.3.2 Energy needs from the PV arrays

An initial sizing for the PV array is shown in Table 4.4.

Table 4.4: The power and energy needs of the PV array.

Type of load	Max. power & energy needs
Daily total system energy requirements/day	2 kWh
System losses (controller, …) 5 %	0.1 kWh
Total energy requirements from PV array	**2.1 kWh**
Hours of PV array operation	6 h
Daily total PV power needs	**0.35 kW**

4.3.4 Sizing the battery storage system

The batteries are the main components in the SSP system after the PV arrays; they store energy which are generated by the solar array during daytime, and meet the power consumption of lighting at night and lighting needs following consecutive rainy days. It is not possible to meet the needs of night lighting if the battery capacity is too small. Conversely, if the battery capacity is too large, a large solar array is needed to ensure that the batteries are fully charged during the limited time of the shorter days. The over size array and battery capacity will result in increased and unnecessary costs. If the solar array is not large enough, the battery cannot be fully charged in limited period of time during the shorter days, it will always be in a state of power deficit which will adversely affects the battery life.

The battery type selected for the system is the Aspen 24S-83 manufactured by Aquion Energy. Operation and performance of the Aspen 24S-83 Battery is depicted in Table 4.5; the product specification sheet is shown in Appendix B. This battery is a clean, 24V, saltwater battery that outperforms and outlasts traditional lead acid batteries. (Wholesale Solar, website).

Aquion's proprietary Aqueous Hybrid Ion (AHI) technology uses no heavy metals or toxic chemicals and is non-flammable and non-explosive. Also, these batteries are robust in partial state-of-charge cycling and over a wide range of ambient temperatures. It is important to choose a quality battery rated at a minimum of 12000 amp-hour storage capacity.

Table 4.5: Operation and performance of the Aspen 24S-83 Battery.

Parameter	Specifications Value
nominal capacity (10-hour charge/20-hour discharge)	83 Ah
nominal voltage	24 V
life cycles	3,000 cycles (to 70% retained capacity)
ambient operating temperature	-5°C to 40°C
voltage range	20.0 to 29.7 V
peak power	750 W
continuous current	30 A
usable depth of discharge	100%

Firstly, calculate the daily amp-hour requirement (Ah/day): 24V battery system, 12pcs lamp, power needed including the system losses 350W, $350\text{W} \div 24\text{V} = 14.6\ \text{Ah/day}$

Secondly, calculate the battery capacity needed. Number of the cloudy day (3 days)

Battery capacity = $14.6A \times 6\text{h} \times (3 + 1) = 350.4\ \text{Ah}$

Thirdly, calculate the depth of discharge for the battery you have chosen as follows:

a 50% safety factor is chosen to avoid over-discharging battery bank.

$350.4/0.5 = 700.8\ \text{Ah}$

Then, select the ambient temperature multiplier that battery bank will experience

Ambient temperature multiplier is 1.4.

Next, calculate the amp-hour that battery bank is having enough capacity to overcome cold weather affects (Ah).

$700.8 \times 1.4 = 981.12$Ah, this number represents the total battery capacity.

After that, take the amp-hour rating for the battery that has been chosen, the amp-hour rating of the Aspen 24S-83 battery that is selected is 83Ah

Then, divide the total battery capacity by the battery amp-hour rating to find the number of the batteries wired in parallel required: $981.12/83 = 12$ batteries.

And to find the required number of the batteries wired in series, divide the nominal system voltage (24V) by the battery voltage (24V) as follows: $24/24 = 1$ battery.

Finally, calculate the total number of batteries required: $12\text{x}1 = 12$ batteries.

4.3.5 Number of PV panels and arrangement of PV array

a) Choose the type and specifications of the PV module.

The chosen PV module is an STPS040-12 manufactured by Suntech Power Company. Table 4.6 shows the technical specifications of mono-crystalline silicon PV module. The STPS040-12 is a 40 watt, 12 volt solar panel, and will provide enough power to the deep cycle battery.

Table 4.6: The technical specifications of the mono-crystalline silicon solar PV module (STPS040-12)

Parameter	Specifications Value
STC: 1000 W/m^2, 25 °C, AM 1.5	
Electrical and Physical Characteristics	
Peak Power (Pmax)	40 Wp
Optimum operating voltage - Vmp	17.2 V
Optimum operating current - Imp	2.32 A
Open circuit voltage – Voc	21.6 V
Short circuit current – Isc	2.62 A
Operating temperature	-40 °C to +85 °C
Maximum system voltage	1000 V DC
Length & width	1.619 m x 0.814 m
Thickness,	0.039 m
Weight	12 kg

The STPS040-12 modules are composed of 36 monocrystalline silicon solar cells of similar performance, interconnected in series to obtain the 12 volt output. A solar road consists of 40 Wp Soltech PV modules. The specifications of the STPS040-12 module that used for the solar pathway are listed in Table 4.6.

b) Calculate the number of modules connected in series Modules connected in series are also referred to as string.

The number of modules to be connected in series is derived from Equation 3.5:

$$n_s = \frac{V_{DC}}{V_m} = \frac{24}{17.2} \cong 2$$

c) Calculate the number of strings required in parallel

By using Equation 3.6 and 3.7:

$$n_p = \frac{E_L}{A_{om}}$$

$$A_{om} = n_s \times P_m \times t$$

$$A_{om} = 2 \times 0.04 \times 6 = 0.48$$

$$n_p = \frac{E_L}{A_{om}} = \frac{2.1}{0.48} \cong 5$$

d) The number of PV panels needs to cover 100% of power needs

This is calculated by using Equation 3.8:

$$n_{pv} = \frac{P_{arry,\max}}{P_m} = \frac{0.35}{0.04} \cong 10 \ \ panels$$

$\therefore$ Number of PV panels and arrangement of PV array are:

Number of PV panels $\cong$ 10

Number of PV modules connected in series = 2

Number of PV modules connected in parallel = 5

e) Calculate the average daily energy output from PV array

Use Equation 3.9:

$$E_a = n_{pv} \times P_{mx} \times (1.0 - TL) \times Gt$$

where; P_{mx} can be calculated by using equation 3.10:

$$P_{mx} = P_m \times \left(1.0 - \alpha \times \left(T^*{}_a - 25\right)\right)$$

To calculate the average daily energy output from a PV array, the monthly global radiation in array panels and average monthly temperature at the selected site must be known.

Figure 4.5 depicts the monthly global radiation on array panels at the selected site versus Cape Town City (Cape Town Data was from NASA as per record of weather satellite), this global radiation was calculated in the selected site, the average monthly data are taken over the 22-year period (Jul 1983 Jun 2005), as shown in Appendix C. Global irradiation of South Africa is presented in Appendix D.

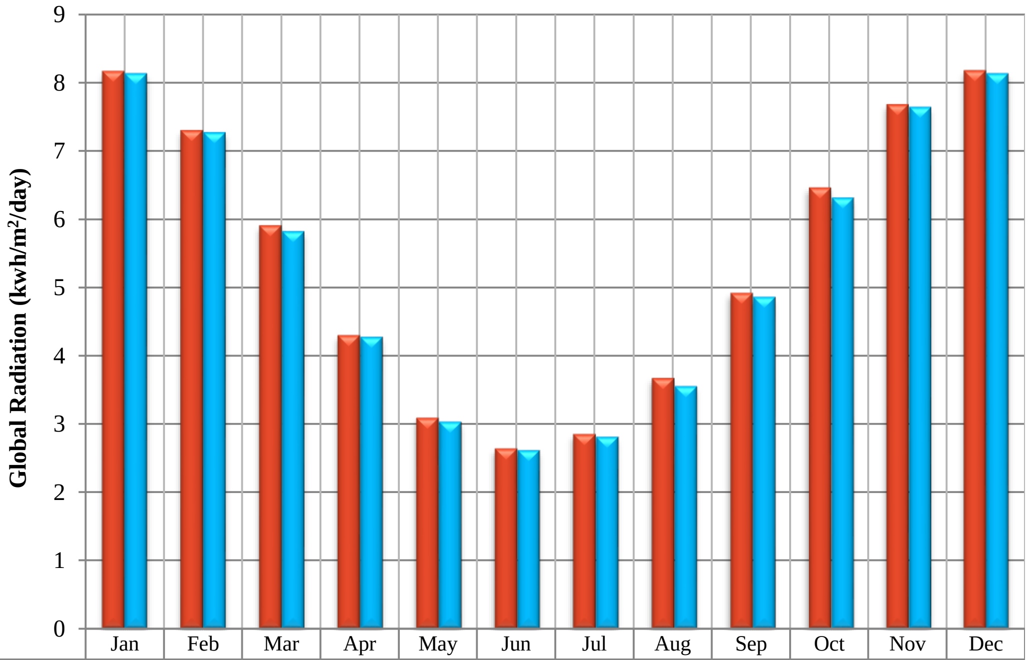

	Jan	Feb	Mar	Apr	May	Jun	Jul	Aug	Sep	Oct	Nov	Dec
Selected Site	8.17	7.3	5.91	4.3	3.09	2.64	2.85	3.67	4.92	6.46	7.68	8.18
Cape Town	8.13	7.27	5.82	4.27	3.03	2.61	2.81	3.55	4.86	6.31	7.64	8.13

Months

Figure 4.5: Comparing the average monthly irradiation on array panels at the selected site, with the City of Cape Town obtained from a global satellite (NASA) database.

Figure 4.6 shows the daily average minimum (blue graph) and maximum (red graph) temperatures at the selected site, with percentile bands (inner band from 25th to 75th percentile, outer band from 10th to 90th percentile). Over the course of a year, the temperature typically varies from 7°C to 27°C and is rarely below 4°C or above 31°C. The *warm season* lasts from December 9 to March 27 with an average daily high temperature above 25°C. The hottest day of the year is February 15, with an average high of 27°C and low of 17°C. The *cold season* lasts from May 26 to September 14 with an average daily high temperature below 19°C. The coldest average day of the year is July 5, with an average low of 7°C and high of 18°C.

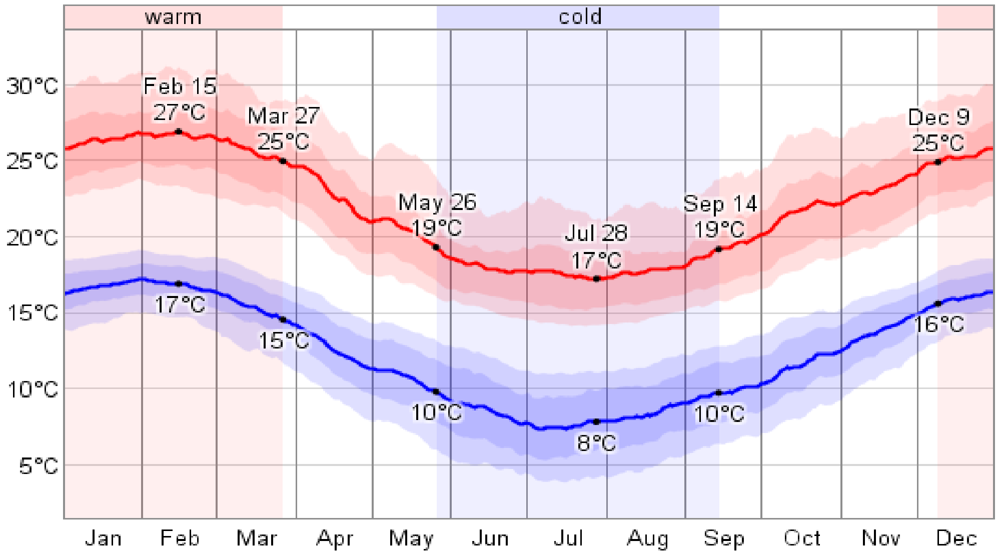

Figure 4.6: The daily average temperature at the site selected: minimum (blue) and maximum (red) temperature with percentile bands.

Figure 4.7 shows the average number of hours of monthly sunshine duration according to data from nearest weather station: Cape Town City, South Africa and NASA Surface meteorology and Solar Energy (SSE) sources; the average monthly data are taking over the 22-year period (Jul 1983 Jun 2005), (See Appendix C). As depicted in Figure 4.7, on average, January is the most sunny and June has the lowest amount of sunshine. The determination of monthly average daylight for each month, is based on the ‘monthly average day’ (SSE Methodology).

Therefore, July and December have been chosen to represent winter and summer weather respectively at the selected site as follows:

Firstly, in December

- The average temperature in the location in December is somewhat warm at 19.5 °C
- Afternoons can be fairly hot with average high temperatures reaching 25 °C.
- Overnight temperatures are generally mild with an average low of 14 °C.
- The mean daily temperature rangeis 11 °C.
- The heavens above location site are beaming having an average of a hefty 11:05 of glaring solar irradiation daily.
- The shortest day is 14:15 hours and the longest day is 14:24 hours with an average length of 14:21 hours.
- On average there are approximately 3:07 hours per day when it is hazy, or cloudy, or when the sun is being too low on the horizon to register.
- On average it is sunny for approximately 78% of daylight hours and cloudy 22% of daylight hours.

Secondly, in June

- The average temperature at the selected site in June is mild at 13 °C.
- Afternoons can be somewhat warm with average high temperatures reaching 18 °C.
- In June there is a range/variation of mean diurnal temperatures of 10 °C.
- In June the blue above location site is fair having on average a moderate 5:48 of radiant sunlight daily.
- The shortest day is 9 hours 52 minutes long and the longest day is 10 hours 2 minutes long with an average length of 9 hours 55 minutes.

- There are approximately 3 hours 58 minutes per day when bright sunshine is absent due to cloud, haze or the sun being too low on the horizon to register.
- It is sunny for approximately 59.4% of daylight hours and cloudy 40.6% of daylight hours.

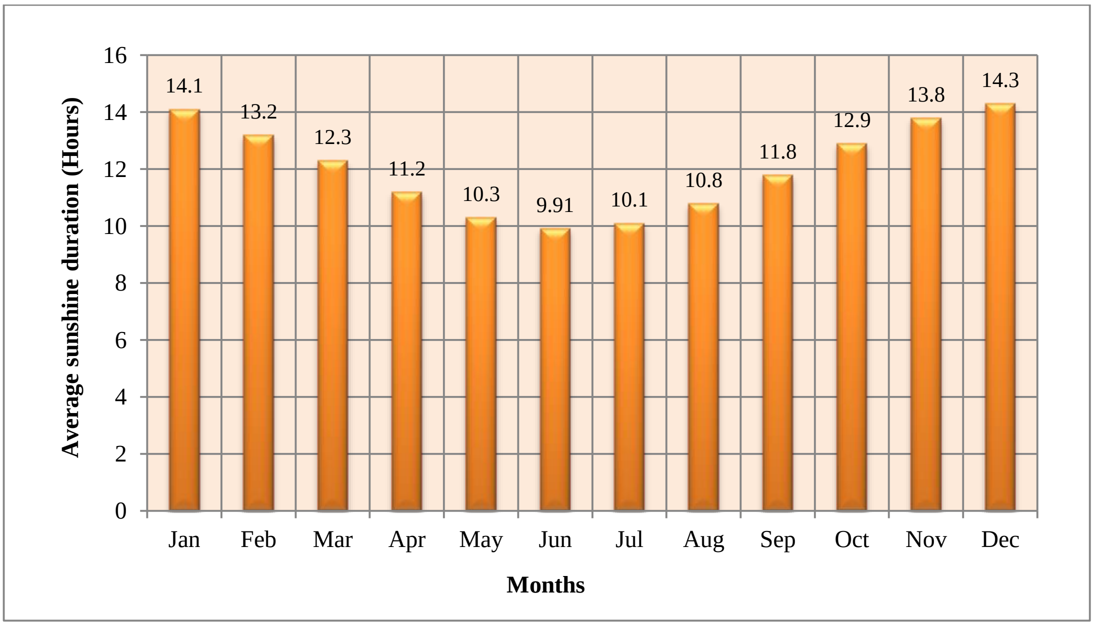

Figure 4.7: The average monthly total of sunshine (hour) over the year.

The determination of average monthly energy output from PV array (Ea) and energy load (EL) for each month are depicted in Figure 4.8.

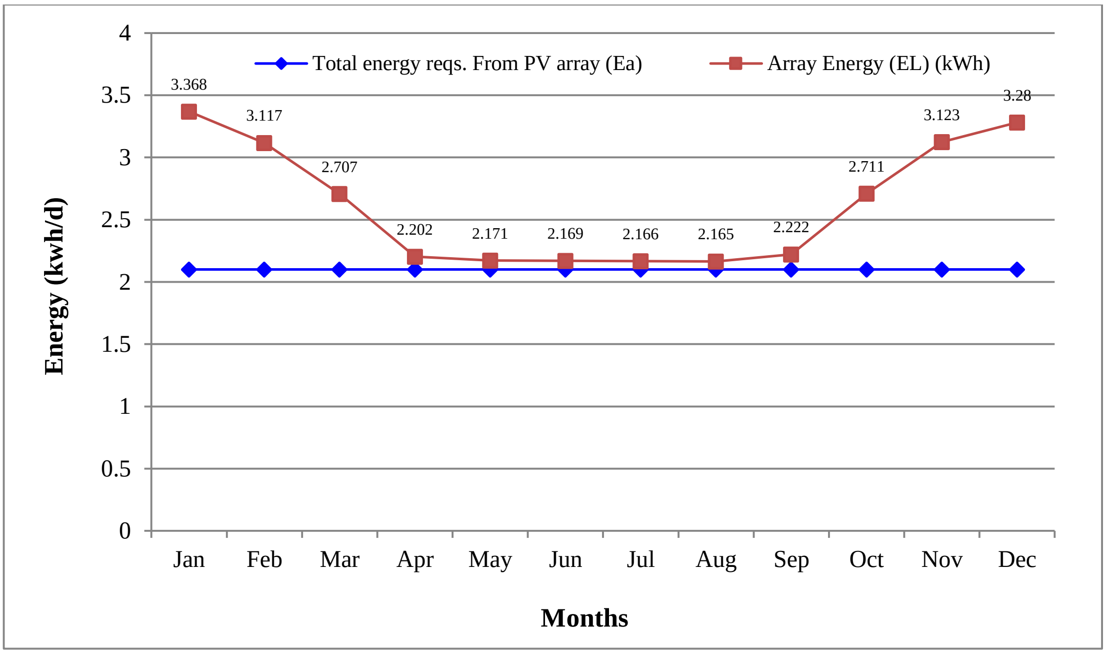

Figure 4.8: The average monthly energy output from PV array (Ea) and energy load (EL).

4.4 Performance Analysis of an SSP System.

A stand-alone solar pathway system has been programmed with MATLAB, in order to size and evaluate the performance of the system. The quantities used to assess the performance of an SSP system are shown in Table 4.7. The computer program can be applied to any site with different weather conditions. Figure 3.5 is repeated here as Figure 4.9 for easy of reference.

Table 4.7: Overview of derived parameters for performance evaluation.

Parameter	Symbol	Equation	Unit
Array Yield	Y_A	E_a/P_o & $Y_f + L_S$	kWh/kWp.d
Final Yield	Y_F	E_{PV}/P_o	kWh/kWp.d
Reference Yield	Y_C	Hi/G_{STC} & $Y_f + L_S + L_C$	kWh/kWp.d
Capture losses	L_C	Yr-YA	kWh/kWp.d
System losses	L_S	Y_A-Y_f	kWh/kWp.d
Performance ratio	**PR**	Y_f/Y_r	--
Production factor	**PF**	$E_a/(P_o.Hi/G_{STC}) = Y_A/Y_R$	--
System efficiency	η_{sys}	PR/PF = Y_F/Y_A.100%	%
Mean array efficiency	$\eta_{A,\ mean}$	$E_a/H_i.A_a$.100%	%
Total efficiency	η_{tot}	$E_{PV}/H_i.A_a$.100%	%

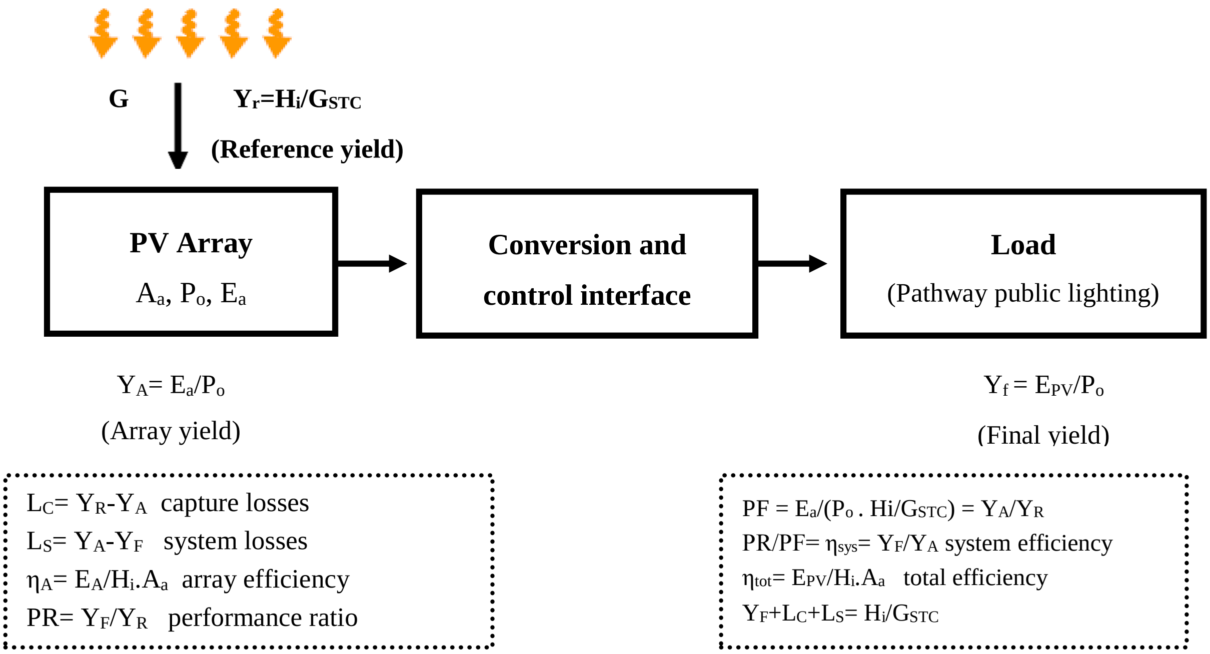

Figure 4.9: System performance analysis of an SSP system.

The performance ratio (PR), being the ratio of the final yield to the performance yield, PR is the most useful normalized performance indicator. It indicates the overall effect of losses on the nominal energy output of the array, due to array temperature, incomplete utilization of irradiation, and system component inefficiencies or failures. The PR is widely used because it is independent of the system size and the location of the plant.

The higher PR value, the better the system uses its potential. A low PR value means production losses due to technical or design problem.

A bar graph in Figure 4.10 shows the monthly PRs of the SSP system over a year; it can be seen that the monthly mean values of the PR can directly be compared for each month per year. The annual mean value of the monthly PR is 0.853.

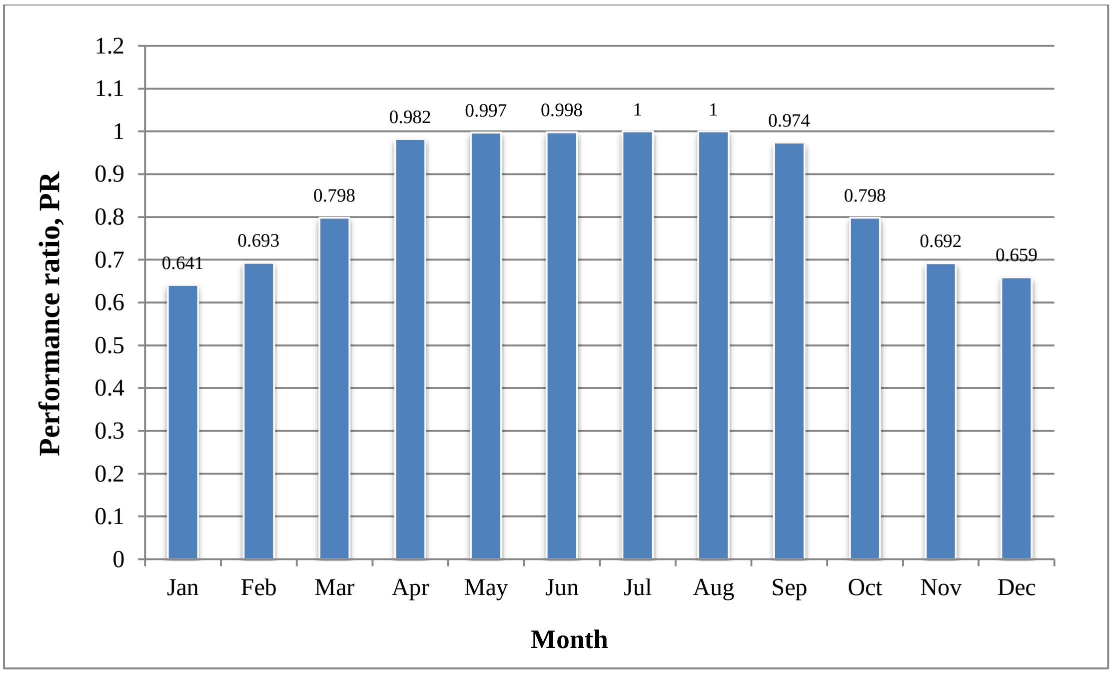

Figure 4.10: Monthly PR per year for SSP system.

The performance results from software program are given in Figure 4.11. The bar graph shows monthly final yields (Y_F) and system losses (L_S) stacked for each month and expressed in kWh/(kWp.d) or h/d. The annual yields and losses are calculated and displayed in Figure 4.11 expressed in kWh/kWp.d or h/y. The annual yields and losses are calculated as Y_F is 72 h/y and L_S is 17.720 h/y.

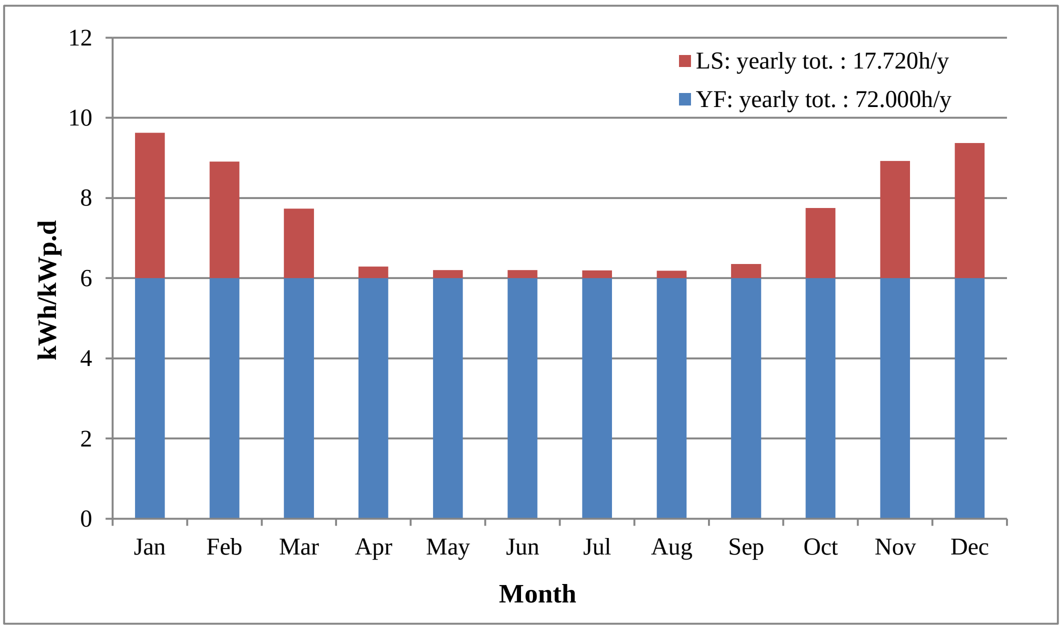

Figure 4.11: Indicators of performance for SSP system.

Figure 4.12 shows the annual values of the reference yield and the final yield for the SSP system. The mean value of the reference yield is 6 h/day and for the final yield of 7.26 h/day giving an average PR of 0.853 (sees Figure 4.9).

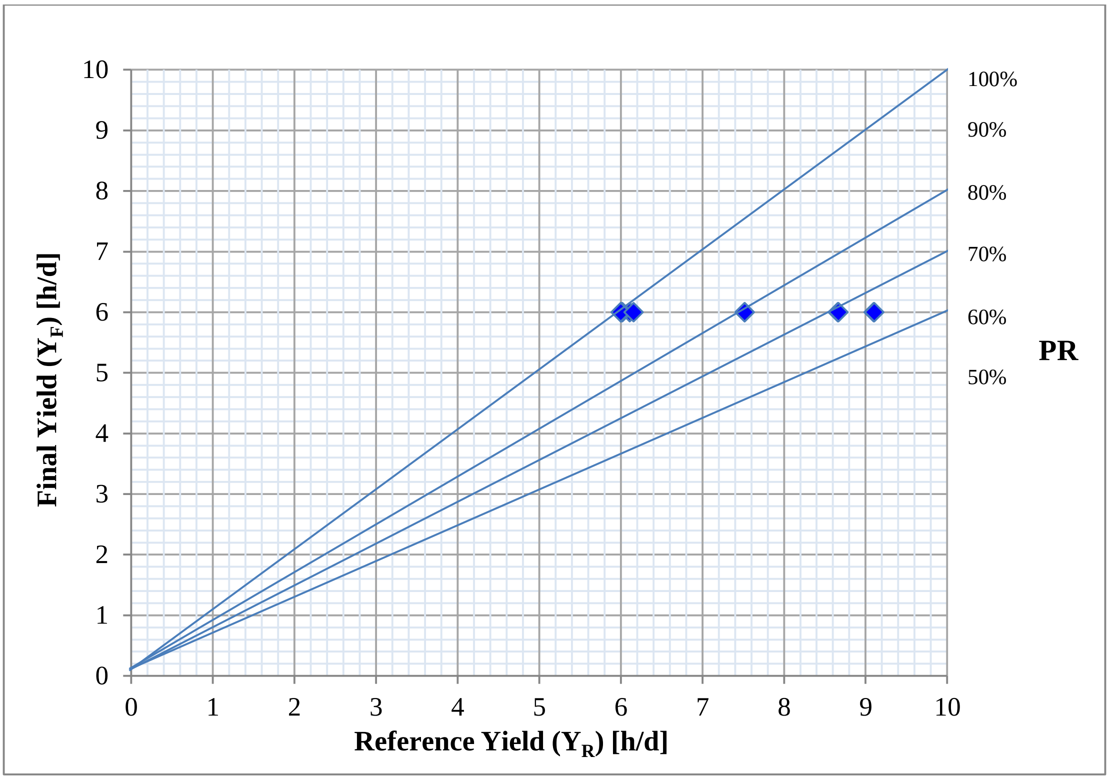

Figure 4.12: Y_R versus Y_F for the SSP system.

To calculate the system efficiency, a new performance coefficient, the production factor (PF) is introduced. System efficiency (η_{sys}) can be calculated as presented in Table 4.7 by using the following equation:

$$\eta_{sys} = PR/PF.100 \quad (4.1)$$

where:

$$PR = Y_F/Y_R \quad (4.2)$$

and

$$PF = Ea/(P_O \times H_i/GSTC) = YA/YR \quad (4.3)$$

Substituting Equations 4.2 and 4.3 into Equation 4.1 and multiplying the result by 100 yields the system efficiency (η_{sys}) as percentage:

$$\eta_{sys} = Y_F/Y_A.100 \quad (4.4)$$

The array yield (Y_A) represents the number of hours per day that the array would need to operate at its peak power, Po to contribute the same daily array energy of the system as was monitored, and the final PV system yield (Y_F) is the portion of the daily energy of the entcen PV plant which is delivered to the load per kilowatt peak of installed PV array.

Figure 4.13 depicts the average array yield (Y_A), final yield (Y_F) and the efficiency of the system (η_{sys}). Analysis of the system efficiency as presented in Figure 4.13, leads to the following results:

i. Array yield (Y_A) and final yield (Y_F) (PR and PF) are indications on the system operation.

ii. The system efficiency of SSP systems is in the range 62.3% to 96%.

iii. The system which is indicated by the red diamonds, has high Y_A values, and low efficiencies. Efficiencies lower than 70%, are caused by technical problems.

iv. The system identified by the green and blue diamonds has low Y_A values, but has high efficiency (η_{sys}).

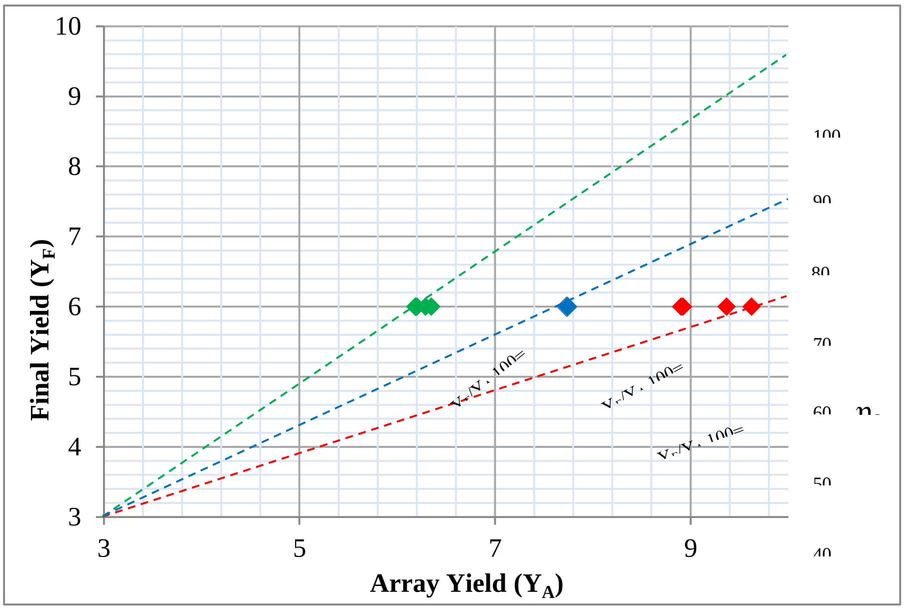

Figure 4.13: Y_R versus Y_F for the SSP system.

The most important quantities used to assess the performance of an SSP system are given in Figure 4.14. The bar graph shows the monthly performance ratio, production factor and system efficiency. The annual average value of the monthly performance ratio is 0.853, the production factor is 1.030 and the system efficiency is 0.828.

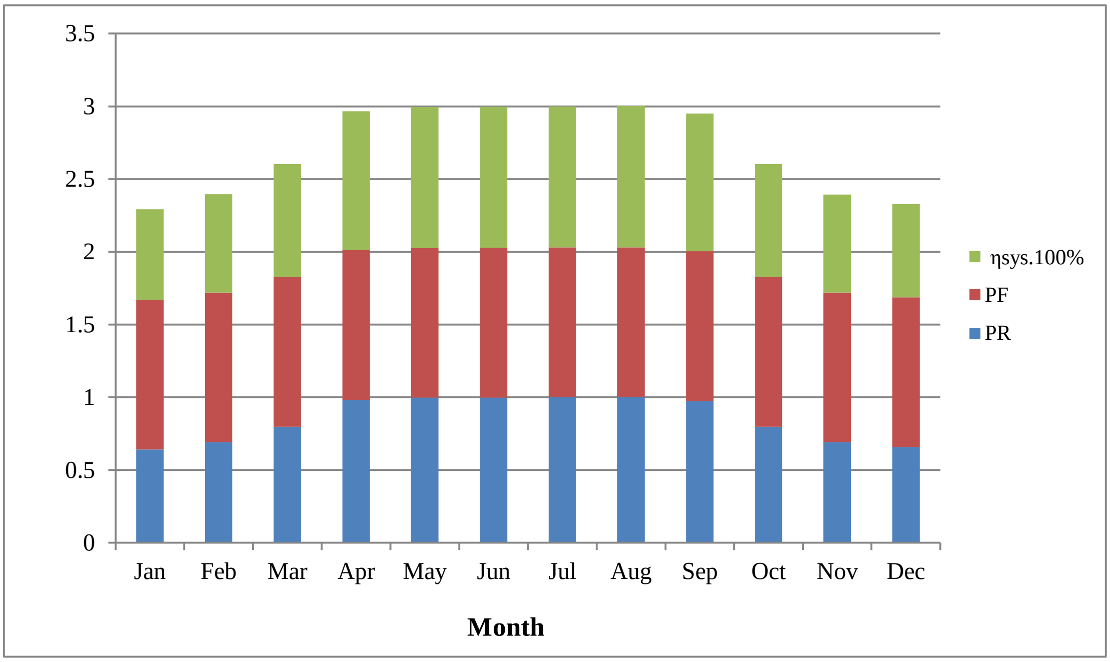

Figure 4.14: The most quantities used to assess the performance of an SSP system.

4.5 Summary

The focus of this study was to improve the operating characteristics of a solar pathway system. In this respect, a variety of measurements were made to gather information on the insolation, operating temperature and energy yield. This chapter presented the modelling and simulation of a stand-alone solar pathway for public park lighting. The model is composed of a PV array, charge controller, and batteries connected to the load power. A case study was chosen to study the sizing, and performance analysis of an SSP technology to power public park lighting was chosen and illustrated. Subsequently, the modelling of selected SSP system at the site chosen, was executed by computer program.

The load was calculated in terms of quantity and quality of lighting needed, as well as the duration of the lighting electrical load required. Battery storage capacity based on the desired autonomy period and maximum and average daily depth of discharge, was sized. The PV array size, based on the type and specifications of a commercially available PV module, the time of year with the highest average daily lighting load and minimum solar radiation, was determined. The control strategy for battery protection and lighting control and specify the control set points and conditions, was determined. The operating efficiency of solar pathway was evaluated and showed excellent performance, with an annual average value of the monthly performance ratio of 0.853, and system efficiency is 0.828.

CHAPTER FIVE

Conclusion and recommendations

5.1 Conclusion

5.2 Recommendations for future work

5.1 Conclusion

The use of PV power systems is becoming increasingly attractive because of their high reliability, low maintenance requirements (as they do not have moving parts when generating electricity), low running costs, suitability at most locations and the long life expectancy of the main components. From this study it was evident that solar energy is an impractical source of power for year-long usage for a stand-alone system to operate public lighting. The SSP system to supply public lighting on the Bellville Campus of the Cape Peninsula University of Technology was executed by computer program; this program was written using MATLAB software.

In CHAPTER ONE an introduction to the control of power converters in general with specific reference to the state-of-the-art as published in the literature was presented. This chapter further describes the scope of this thesis and formulates the problems that were discussed in the manuscript.

In CHAPTER TWO of this thesis, the state-of-the-art of PV system technology and its applications were expounded on. The chapter begins with a history of photovoltaics and the principles of solar PV cell operation, solar irradiation, and in addition the effects of temperature and solar radiation on solar cells were discussed. Also presented are the types of PV systems, highlighting their advantages and disadvantages, photovoltaic applications, and an overview of commercially available PV systems. PV lighting components were explained, and the characteristics and functions of these major system components were described. The objective of this chapter was to provide interested readers with a general background of PV systems, and PV system components and their applications.

In CHAPTER THREE, an overview of PV lighting components, system design principles and existing quantities for system performance assessment and their limitations, was provided. This information was intended for those individuals who specify PV lighting equipment and evaluate system designs, as well as those who design and integrate systems. All the components that were used in the design of the SSP, are fully described. Included in this chapter are the fundamentals and selection criteria for the major PV lighting system components — the PV array, batteries, controllers and luminaires. The procedures for determining product sizing and justification for the selection of each component is provided. Also, the parameters that were used to evaluate the SSP technology for public lighting, from the generation stage to the load, were discussed. The benchmarks used to evaluate SSP technology for public lighting, from the generation stage to the load, are also discussed. This chapter contains a detailed explanation of methodology that was implemented to make this project functional.

In CHAPTER FOUR of this thesis, the focus of this study was to gain experience on the real-world operating characteristics of the stand-alone solar pathway system. In this respect, a variety of measurements were made to gather information on the insolation, operating temperature and energy yield. CHAPTER FOUR presented the modelling and simulation of a stand-alone solar pathway for public lighting. The model was composed of a PV array designed for public lighting, a charge controller, and batteries connected to the load.

In this study, a 65 m stretch of walkway, located next to the building housing the Electrical, Electronic and Computer Engineering Department on the Bellville Campus of the Cape Peninsula University of Technology, Cape Town, South Africa was selected as a case study . The selected case study to study sizing, and performance analysis of a stand-alone solar pathway system to power public lighting, was chosen and illustrated. Then, the modelling of SSP system to supply public lighting for the selected site, was executed by computer program. The quantity and quality of lighting, and the required duration of the electrical load needed for lighting, were calculated. Battery storage capacity based on the desired autonomy period and maximum and average daily depth of discharge, was sized. The PV array size, based on the type and specifications of PV module, the time of year with the highest average daily lighting load and minimum solar radiation, were selected and measured. A control strategy for battery protection and lighting control was determined, and the control set points and conditions were specified. The operating efficiency of a solar pathway was evaluated and the following concluding remarks can be made:

1. The study indicated that the model was able to supply adequately the power needs of the public lighting on a 65m standalone pathway network.

2. This study presented a simplified method for sizing and simulating a stand-alone solar pathway system to power public lighting at the Bellville Campus of the Cape Peninsula University of Technology, Cape Town.

3. Ambient temperature and solar radiation are the most important external factors which influence such a system.

4. SSP system technology represents a good alternative for public lighting and energy savings for municipalities.

5. The best performance of the system depends on the technology selected for its components and this can affect costing.

6. Array yield (Y_A) and final yield (Y_F) are system performance indicators of the system operation.
7. The system efficiency of SSP systems is in the range 62% to 96%.
8. The system, identified by the red graph in Figure 4.12, has high Y_A values, and a low efficiency. Efficiencies lower than 70% are caused by technical problems.
9. The system, identified by the green graph in Figure 4.12, has low Y_A values but a high efficiency (η_{sys}).
10. The annual average value of the monthly performance ratio is 0.853 (with 85.3%), (Figure 4.9). The production factor is 1.030 and system efficiency is 0.828 (with 82.8%) (Figure 4.14)

5.2 Recommendations for future work:

The results of this thesis have the potential to be extended in several directions. The following are some recommendations for future work:

1. Review and evaluate solar energy projects implemented in southern Africa and explore their advantages and disadvantages in public lighting.

2. For roads and pathways that do not have enough shadow free areas, stand-alone solar street lighting system is not recommended. Instead a centralized solar PV system should be considered.

3. For stand-alone street lighting schemes, a detailed site-specific technical survey and design has to be carried out to compare it with the current design.

4. Solar PV modules must be cleaned at two to three weeks intervals, depending upon the local weather and environmental conditions.

5. Battery maintenance should be looked at such as the impact of cleaning and greasing the battery terminals quarterly.

6. Adopt renewable energy resources for appropriate coupling with the various desalination technologies to cover needs of fresh water and decrease the water production cost.

7. Advance the development solar roads that are capable of generating energy and storing it.

REFERENCES

Almaktoof, A.M., Raji, A.K., Kahn, M.T.E. & Ekhlat, M.A. 2015. Batteryless PV desalination system for rural areas: A case study. *Journal of Energy in Southern Africa*, 26(4): 29–37.

Almaktoof A. M., Raji A. K., Kahn M. T. E. and Ekhlat M. Ali, 2014. "Sizing and Evaluation of A Battery-less PV System-Driven Desalination with RO for Rural Areas-Case Study" 2014 Proceeding of the 22nd Domestic Use of Energy, 31 March–2 April 2014 in Cape Town, South Africa. pp. 173–180.

Aquion Energy Aspen 24S-83 Sodium-Ion 83Ah 24V Battery - Wholesale Solar. [online]. Available: http://www.wholesalesolar.com/9949502/aquion-energy/batteries/aquion-energy-aspen-24s-83-sodium-ion-83ah-24v-battery. [3 June 2016}.

Fahrenbruch, A. & Bube, R. 2012. *Fundamentals of Solar Cells: Photovoltaic Solar Energy Conversion.* New York, London: Academic Press

Center, F.S.E. 1999. Installing Photovoltaic Systems. *A question and answer guide for solar electric systems* [online]. Available: http://www.firemarshalsarchives.org/pdf/PVPrimer. [14 December 2015].

Dhankhar, M., Pal Singh, O. & Singh, V.N. 2014. Physical principles of losses in thin film solar cells and efficiency enhancement methods. *Renewable and Sustainable Energy Reviews*, 40: 214–223.

Energy.gov. 2013. *Photovoltaic Technology Basics* [online]. Available: http://energy.gov/eere/energybasics/articles/photovoltaic-technology-basics. [14 March 2016].

Energyinformative.org. 2013. Solar Cell Comparison Chart – Mono-, Polycrystalline and Thin Film. *Energy Informative* [online]. Available: http://energyinformative.org/solar-cell-comparison-chart-mono-polycrystalline-thin-film/. [14 April 2016].

Goswami, D.Y. & Kreith, F. 2007. *Handbook of Energy Efficiency and Renewable Energy*. in: Messenger, R., Goswami, D.Y., Upadhyaya, H.M., Razykov, T.M., Tiwari, A.N., Winston, R. and McConnell, R. (eds). *Photovoltaics Fundamentals, Technology and Application.* London- New York: Taylor & Francis Group.Chapter 23 (1-58).

Grothoff, J.M. 2015. *Battery storage for renewables: market status and technology outlook*. Technical Report January, International Renewable Energy Agency (IRENA) [online] . Available: http://www.primeinvestgreenpower.com/app/download/18319597/IRENA_Battery_Storage_report_2015+-+Johannes+Michael+Grothoff. [13 December 2016].

Guide, A.D.-M. 1998a. Stand-Alone Photovoltaic Lighting Systems A Decision-Maker's Guide Volume 1: Photovoltaic Lighting Applications [online] . Available: http://www.fsec.ucf.edu/en/publications/pdf/FSEC-RR-54-98. [12 May 2016].

Guide, A.D.-M. 1998b. Stand-Alone Photovoltaic Lighting Systems. Volume 2: PV Lighting Components and System Design. http://www.fsec.ucf.edu/en/publications/pdf/fsec-rr-54-98-2.pdf 12 December 2016.

Heavens, O.S. 1991. *Optical Properties of Thin Solid Films*. USA, New York Courier Corporation.

Ho, J.-M. & Hsu, J.-L. 2010. Design and implementation of a stand-alone photovoltaic road lighting system. In *Proceedings of the 9th WSEAS international conference on Circuits, systems, electronics, control & signal processing*. World Scientific and Engineering Academy and Society (WSEAS): 60–65.

Holding. 2011. *World solar irradiation map - Google Search* [online]. Available: https://www.google.com/search?q=World+solar+irradiation+map&tbm=isch&tbo=u&source=univ&sa=X&ved=0ahUKEwia8eaKw-7QAhUrJMAKHcpXB14QsAQIIA&biw=1366&bih=633. [8 December 2015].

Hruska. 2014a. *The Netherlands has laid the world's first solar road. almere 2022* [online] . Available: http://www.2022almere.nl/floriade-2022/the-netherlands-has-laid-the-worlds-first-solar-road/. [6 December 2015].

Hruska. 2014b. *The Netherlands has laid the world's first solar road – we go eyes-on to investigate*. *ExtremeTech* [online]. Available: http://www.extremetech.com/extreme/194313-the-netherlands-has-laid-the-worlds-first-solar-road-we-go-eyes-on-to-investigate [24 March 2016].

Jahn, U., Grimmig, B., Nasse, W. & Ohrberg, A. 2000. *Analysis of photovoltaic Systems* [online] . Available: http://www. iea-pvps-task2. org/public/download/Report IEA PVPS, 2: 01. [10 July 2016].

Khare, V., Nema, S. & Baredar, P. 2016. Solar–wind hybrid renewable energy system: A review. *Renewable and Sustainable Energy Reviews*, 58: 23–33.

Le, Q. 2011. Off-Grid Public Lighting System - Design and Characterization of an LED Luminaire. Master's Theses and Project Reports. the Faculty of California Polytechnic State University, USA.

Liu, L., Meng, X. & Liu, C. 2016. A review of maximum power point tracking methods of PV power system at uniform and partial shading. *Renewable and Sustainable Energy Reviews*, 53: 1500–1507.

Luque, A. & Hegedus, S. 2011. *Handbook of Photovoltaic Science and Engineering*. 2nd edition.USA: John Wiley & Sons.

Markvart, T. 2000. *Solar Electricity*. 2nd edition. UK: John Wiley & Sons.

Ma, T., Yang, H. & Lu, L. 2013. Performance evaluation of a stand-alone photovoltaic system on an isolated island in Hong Kong. *Applied Energy*, 112: 663–672.

Mayer, D. & Heidenreich, M. 2003. Performance analysis of stand alone PV systems from a rational use of energy point of view. In *Proceedings of 3rd World Conference onPhotovoltaic Energy Conversion, 2003*. Proceedings of 3rd World Conference onPhotovoltaic Energy Conversion, 2003. 2155–2158 Vol.3.

Mohamed, E.S. & Papadakis, G. 2004. Design, simulation and economic analysis of a stand-alone reverse osmosis desalination unit powered by wind turbines and photovoltaics. *Desalination*, 164(1): 87–97.

NanoShell. 2016. *Self-Cleaning Solar Panel Coating | Protective Coatings | nanoShell Solar PV* [online]. Available: http://www.nanoshell.co.uk/protective-coatings/solar-panel-pv [30 August 2016].

National Energy Education Project. 2015. *Photovoltaics Student Guide* [online]. Available: http://www.need.org/files/curriculum/guides/Photovoltaics%20Student%20Guide.pdf [29 January 2016].

National Renewable Energy Laboratory (NREL) Home Page. [online]. Available http://www.nrel.gov/ [9 March 2016].

Ineichen P., 2013. "Long term satellite global, beam and diffuse irradiance validation". In Proceedings of the 2nd International Conference on Solar Heating and Cooling for Buildings and Industry, Freiburg, 2013.

OFEN, T. 1997. *CLEARINGHOUSEENERGY* [online]. Available: http://www.oregon.gov/energy/P-I/Solar/docs/pvbasics. [1 March 2016].

Patel, A., Patel, A., Patel, M.. & Vyas, D. 2011. *Microsoft Word - v3-1-1.doc - modeling-and-simulation-of-photovoltaic-based-led-lighting-system* [online]. Available: http://waset.org/publications/13125/modeling-and-simulation-of-photovoltaic-based-led-lighting-system [6 September 2016].

PVPS, I. 2015. *Trends 2015 in Photovoltaic Applications. Report No. IEA-PVPS T1-27* [online]. Available: http://www.iea-pvps.org/fileadmin/dam/public/report/national/IEA-PVPS_-_Trends_2015_-_MedRes. [17 April 2016].

Sarkar, S. 2012. *Energy Efficient Lighting Design and Electrical Installation of a Hospital Building. JADAVPUR UNIVERSITY KOLKATA* [online]. Available: http://dspace.jdvu.ac.in/handle/123456789/26347 [10 May 2016].

Schmidt, W. 2014. *The Netherlands Builds World's First Solar-Paneled Road* [online]. Available: http://tech.co/solaroad-netherlands-2014-11 [28 April 2016].

Shekhar, A., Klerks, S., Bauer, P. & Prasanth, V. 2015. *Solar Road Operating Efficiency and Energy Yield – an Integrated Approach towards Inductive Power Transfer* [online]. Available: https://www.researchgate.net/publication/283579396_Solar_Road_Operating_Efficiency_and_Energy_Yield_-_an_Integrated_Approach_towards_Inductive_Power_Transfer. [8 September 2016].

Treble, F.C. 1991. *Generating Electricity from the Sun*. 1st edition. New York: Pergamon Press.

United Nations, Department of Economic and Social Affairs. 2013. *World population projected to reach 9.6 billion by 2050* [Online]. Available: http://www.un.org/en/development/desa/news/population/un-report-world-population-projected-to-reach-9-6-billion-by-2050.html. [10 November 2016].

VASSILI GROUP. 2016. *Solar Roads - VASSILI GROUP* [Online]. Available: http://www.vassili-group.com/solar-roads.html. [12 November 2015].

Zeman, M. 2003. Introduction to photovoltaic solar energy. *Delft University of Technology*, 2(6).

Zeman, M. 1998. *Photovoltaic systems*. Delft University of Technology [Online]. Available: http://theopenacademy.com/sites/default/files/oadb/Engineering/Microelectronics/Solar%20Cells%20-%20TU%20Delft%20-%20Miro%20Zeman%20-%20BYNCSA/Notes/Course%20Notes/Photovoltaic%20Systems. [12 November 2015].

APPENDICES

Appendix A: Specification data sheets luminaire chosen

LEOTEK
LITE-ON GROUP

Project
Type
Catalog No.

GreenCobra™ Jr. LED Street Light
GCJ

Luminaire Data

Weight 7 lbs [3.2 kg]
EPA 0.39 ft^2

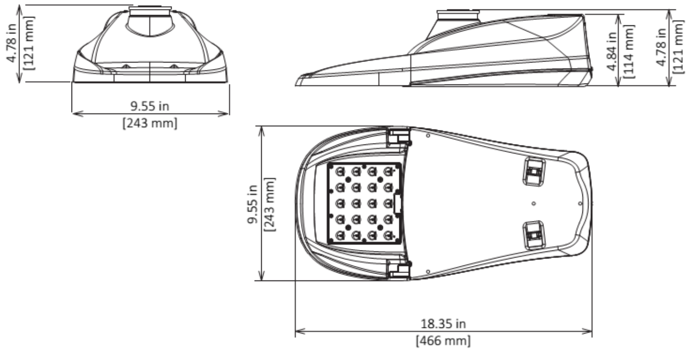

Ordering Information

Sample Catalog No. GCJ1 20G MV NW 2 GY 580

Product	LED No. & Type	Voltage	Color Temperature	Distribution	Finish	Drive Current[1]	Options
GCJ1 350mA to 700mA	**20G**	**MV** 120-277V	**WW** 3000K	**2** Type 2	**GY** Gray	**350**[2] 350mA	**FDC**[4] Fixed Drive Current
			NW 4000K	**3** Type 3	**DB** Dark Bronze	**580**[2] 580mA	**LPCR** Less Photocontrol Receptacle
			CW 5000K		**BK** Black	**700** 700mA	**PCR5**[5] ANSI 5-wire Photo-control Receptacle
GCJ2 700mA to 1A						**1A**[3] 1A	**PCR7**[5] ANSI 7-wire Photo-control Receptacle
							PCR5-CR[6] Control Ready 5-wire PC Receptacle
							PCR7-CR[6] Control Ready 7-wire PC Receptacle
							WL Utility Wattage Label
							4B 4-Bolt Mounting Bracket
							DSC Door Safety Cable
							RWG Rubber Wildlife Guard

Notes:
1 Factory set drive current, field adjustable standard. Refer to Performance Data Table. Consult factory if wattage limits require a special drive current.
2 350mA and 580mA drive current available with GCJ1 only.
3 1A drive current available with GCJ2 only.
4 Non-field adjustable, fixed drive current. Specify required drive current. Not available with PCR5-CR or PCR7-CR options.
5 Field adjustable current selector included. Wireless node dimming is disabled, field changeable connectors included to enable dimming with PCR5/7.
6 Control-ready wiring at factory for wireless node dimming. Default maximum drive current (700mA or 1A) must be specified.
7 Flush mounted house side shield. Shield cuts light off at 1/2 mounting height behind luminaire.
8 Flush mounted cul-de-sac shield. Shield cuts light off at 1/2 mounting height behind luminaire and 1-1/2 mounting height on either side of luminaire.
9 Specify Color (GY, DB, BK)

Accessories*	
HSS[7]	House Side Shield, Snap-On*
CSS[8]	Cul-De-Sac Side Shield, Snap-On*
SPB[9]	Square Pole Horizontal Arm Bracket
RPB[9]	Round Pole Horizontal Arm Bracket
PTB[9]	Pole Top Tenon Horizontal Arm Bracket
WB[9]	Wall Horizontal Arm Bracket
BSK	Bird Deterrent Spider Kit
PC	Twist Lock Photocontrol
LLPC	Long-Life Twist Lock Photocontrol
SC	Twist Lock Shorting Cap

*Accessories are ordered separately and not to be included in the catalog number. For factory installed HSS, CSS specify as option in luminaire catalog number.

GreenCobra™ Jr. LED Street Light
GCJ

LEOTEK LITE-ON GROUP

Luminaire Specifications

Housing
Die cast aluminum housing with universal two-bolt slip fitter mounts to 1-1/4" to 2" (1-5/8" to 2-3/8" O.D.) diameter mast arm. One-piece aluminum housing provides passive heat-sinking of the LEDs and has upper surfaces that shed precipitation. Four-bolt mounting bracket is available. Mounting provisions meet 3G vibration per ANSI C136.31-2001 Normal Application, Bridge & Overpass. Mounting has leveling adjustment from ± 5° in 2.5° steps. Electrical components are accessed without tools via a high-strength, non-conductive polycarbonate door with quick-release latches. Polycarbonate material meets UL 746C for outdoor usage. Available rubber wildlife guard (RWG option) conforms to mast arm with no gaps.

Light Emitting Diodes
Hi-flux/Hi-power white LEDs produce a minimum of 90% of initial intensity at 100,000 hours of life based on IES TM-21. LEDs are tested in accordance with IES LM-80 testing procedures. LEDS have correlated color temperature of 3000K (WW), 4000K (NW), or 5000K (CW) and 70 CRI minimum. LEDs are 100% mercury and lead free.

Optical Systems
Micro-lens optical systems produce IESNA Type 2 or Type 3 distributions and are fully sealed to maintain an IP66 rating. Luminaire produces 0% total lumens above 90° (BUG Rating, U=0). Optional house side shield cuts light off at 1/2 mounting height behind luminaire. Cul-de-sac shield provides back and side light control for end of cul-de-sac applications. Both shields are field installable without tools.

Electrical
Rated life of electrical components is 100,000 hours. Uses isolated power supply that is 1-10V dimmable. Power supply is wired with quick-disconnect terminals. LED drive current can be changed in the field to adjust light output for local conditions (not available with PCR5-CR or PCR7-CR options). Power supply features a minimum power factor of .90 and <20% Total Harmonic Distortion (THD). EMC meets or exceeds FCC CFR Part 15. Terminal block accommodates 6 to 14 gauge wire. Surge protection complies with IEEE/ANSI C62.41 Category C High, 20kV/10kA.

Controls
3-Wire photocontrol receptacle is standard. ANSI C136.41 5-wire (PCR5) or 7-wire (PCR7) photocontrol receptacles are available. All photocontrol receptacles have tool-less rotatable bases. Wireless control module is provided by others.

Finish
Housing receives a durable, fade-resistant polyester powder coat finish. Finish tested to withstand 3000 hours in salt spray exposure per ASTM B117. Finish tested 500 hours in UV exposure per ASTM G154 and meets ASTM D523 gloss retention.

Listings/Ratings/Labels
Luminaires are UL listed for use in wet locations in the United States and Canada. DesignLights Consortium™ qualified 120-277V product.2 International Dark Sky Association listed. Luminaire is qualified to operate at ambient temperatures of -40°C to 40°C. Assembled in the U.S.A.

Photometry
Luminaires photometrics are tested by certified independent testing laboratories in accordance with IES LM-79 testing procedures. IES files for all CCTs are available at leotek.com.

Warranty
10-year limited warranty is standard on luminaire and components.

Performance Data: 4000K (NW) and 5000K (CW)
All data nominal. IES files for all CCTs are available at leotek.com.

Product	Drive Current (mA)	System Wattage (W)	Delivered Lumens (Lm)[1]	Efficacy (Lm/W)	Type 2 BUG Rating	Type 3 BUG Rating
GCJ1	350	24	2400	100	B1 U0 G1	B1 U0 G1
	580	38	3700	97	B1 U0 G1	B1 U0 G1
	700	48	4400	92	B1 U0 G1	B1 U0 G1
GCJ2	700	48	4400	92	B1 U0 G1	B1 U0 G1
	1000	74	5900	80	B1 U0 G2	B2 U0 G2

Performance Data: 3000K (WW)
All data nominal. IES files for all CCTs are available at leotek.com.

Product	Drive Current (mA)	System Wattage (W)	Delivered Lumens (Lm)[1]	Efficacy (Lm/W)	Type 2 BUG Rating	Type 3 BUG Rating
GCJ1	350	24	2400	100	B1 U0 G1	B1 U0 G1
	580	38	3650	96	B1 U0 G1	B1 U0 G1
	700	48	4300	90	B1 U0 G1	B1 U0 G1
GCJ2	700	48	4300	90	B1 U0 G1	B1 U0 G1
	1000	74	5700	77	B1 U0 G1	B2 U0 G2

Notes:
1 Nominal lumens. Normal tolerance ± 10% due to factors including distribution type, LED bin variance, and ambient temperatures.
2 Not all versions DLC qualified. Consult qualified product list at www.designlights.org for latest product listing.

Appendix B: Product specification sheet of Aspen 24S-83 battery

Aspen 24S-83 Battery

AQUION ENERGY

PRODUCT SPECIFICATION SHEET

The Aspen 24S-83 is a clean, 24 V, saltwater battery that outperforms and outlasts traditional lead acid batteries. Aquion's proprietary Aqueous Hybrid Ion (AHI™) technology uses no heavy metals or toxic chemicals and is non-flammable and non-explosive, making Aspen batteries the safest and most sustainable in the world. They are also robust in partial state-of-charge cycling and a wide range of ambient temperatures. Aspen batteries are ideal for applications that limit the life, performance, or safety of traditional battery technologies.

PRODUCT PERFORMANCE

Testing performed at 30°C

Embodied Energy (Wh)		Charge Current (A)				
		4	8	12	16	20
Discharge Current (A)	4	2,323	2,171	1,933	1,699	1,456
	8	2,176	1,963	1,812	1,593	1,366
	12	2,050	1,851	1,649	1,469	1,275
	16	1,932	1,761	1,576	1,409	1,227
	20	1,830	1,670	1,502	1,348	1,179

Embodied Capacity (Ah)		Charge Current (A)				
		4	8	12	16	20
Discharge Current (A)	4	94.2	86.7	77.7	69.7	61.0
	8	90.2	82.6	73.9	66.3	58.1
	12	88.0	80.2	71.7	64.4	56.3
	16	84.8	77.8	69.6	62.4	54.6
	20	81.4	75.3	67.3	60.4	52.8

OPERATION & PERFORMANCE

Nominal Capacity (10-hour charge/20-hour discharge)	83 Ah
Nominal Voltage	24 V
Cycle Life	3,000 cycles (to 70% retained capacity)
Ambient Operating Temperature	-5°C to 40°C
Voltage Range	20.0 to 29.7 V
Peak Power	750 W
Continuous Current	30 A
Usable Depth of Discharge	100%

WARRANTY

Limited Warranty	8 years: 5 years full + 3 years prorated

PHYSICAL CHARACTERISTICS

Height	935 mm (36.8")
Width	330 mm (13.0")
Depth	310 mm (12.2")
Weight	118 kg (260 lbs)

CERTIFICATIONS

Sustainability	Cradle to Cradle Certified™ Bronze product
UL Recognition	In process
CE	CE marked
Shipping Testing	Modified ISTA 3H
IP Rating	IP22

Performance characteristics based on testing conducted by Aquion Energy. Performance may vary depending on use, conditions, and application. For the most up-to-date specification, visit http://aquionenergy.com.

Aspen 24S-83 Battery

AQUION ENERGY

PERFORMANCE AT CONSTANT CURRENT DISCHARGE

Nominal Energy & Capacity by Charge and Discharge Duration

Wh & Ah		10-hour Charge	
		Wh	Ah
Discharge Duration (hr)	4	1,576	73.3
	8	1,753	77.6
	10	1,812	78.8
	12	1,872	80.0
	20	2,167	83.3

Round Trip Energy Efficiency

RTE (%)		Charge Current (A)				
		4	8	12	16	20
Discharge Current (A)	4	90	90	89	88	87
	8	88	88	87	86	85
	12	87	87	86	85	84
	16	85	85	84	83	82
	20	83	83	82	81	80

Voltage vs. Charge Energy

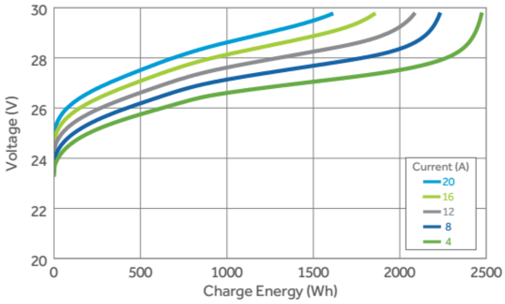

Voltage vs. Discharge Energy (from 10-hour charge)

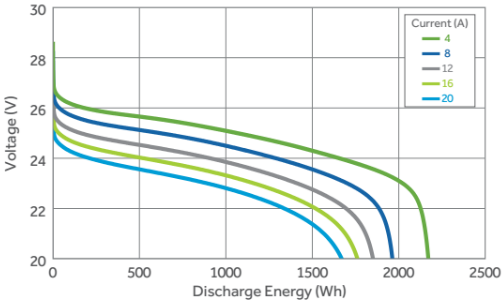

5-Minute Peak Power

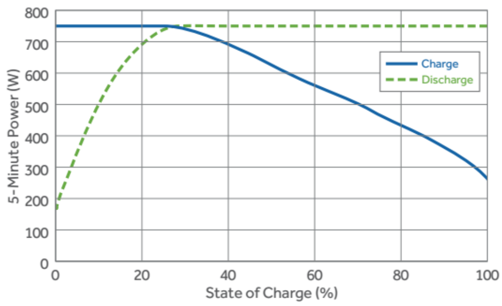

CRADLE TO CRADLE CERTIFIED™ BRONZE

Aquion batteries are the first and only batteries in the world to be Cradle to Cradle Certified™, an esteemed quality mark for products made from sustainable materials and manufacturing processes. Cradle to Cradle Certified™ is a certification mark licensed by the Cradle to Cradle Products Innovation Institute. Visit www.c2ccertified.org for more details.

Performance characteristics based on testing conducted by Aquion Energy. Performance may vary depending on use, conditions, and application. For the most up-to-date specification, visit http://aquionenergy.com.

Appendix C: NASA Surface meteorology and Solar Energy

C1: Available Tables for the selected site.

ATMOSPHERIC SCIENCE DATA CENTER

NASA Surface meteorology and Solar Energy - Available Tables

Latitude -33.933 / Longitude 18.643 was chosen.

Geometry Information

Elevation: **239** meters
taken from the NASA GEOS-4 model elevation

Northern boundary **-33**

Western boundary **18**

Center Latitude **-33.5** Longitude **18.5**

Eastern boundary **19**

Southern boundary **-34**

Parameters for Solar Cooking:

Monthly Averaged Insolation Incident On A Horizontal Surface ($kWh/m^2/day$)

Lat -33.933 Lon 18.643	Jan	Feb	Mar	Apr	May	Jun	Jul	Aug	Sep	Oct	Nov	Dec
22-year Average	8.17	7.30	5.91	4.30	3.09	2.64	2.85	3.67	4.92	6.46	7.68	8.18

Parameter Definition

Monthly Averaged Midday Insolation Incident On A Horizontal Surface (kW/m^2)

Lat -33.933 Lon 18.643	Jan	Feb	Mar	Apr	May	Jun	Jul	Aug	Sep	Oct	Nov	Dec
22-year Average	0.92	0.87	0.74	0.56	0.43	0.38	0.41	0.50	0.62	0.72	0.85	0.90

Parameter Definition

Monthly Averaged Clear Sky Insolation Incident On A Horizontal Surface ($kWh/m^2/day$)

Lat -33.933 Lon 18.643	Jan	Feb	Mar	Apr	May	Jun	Jul	Aug	Sep	Oct	Nov	Dec
22-year Average	8.96	7.96	6.64	5.07	3.80	3.26	3.53	4.56	6.05	7.58	8.73	9.11

Parameter Definition

Monthly Averaged Clear Sky Days (days)

Lat -33.933 Lon 18.643	Jan	Feb	Mar	Apr	May	Jun	Jul	Aug	Sep	Oct	Nov	Dec
22-year Average	7	7	6	6	5	7	8	6	6	5	5	7

Parameter Definition

Parameters for Sizing and Pointing of Solar Panels and for Solar Thermal Applications:

Monthly Averaged Insolation Incident On A Horizontal Surface ($kWh/m^2/day$)

Lat -33.933 Lon 18.643	Jan	Feb	Mar	Apr	May	Jun	Jul	Aug	Sep	Oct	Nov	Dec	Annual Average
22-year Average	8.17	7.30	5.91	4.30	3.09	2.64	2.85	3.67	4.92	6.46	7.68	8.18	5.42

Minimum And Maximum Difference From Monthly Averaged Insolation (%)

Lat -33.933 Lon 18.643	Jan	Feb	Mar	Apr	May	Jun	Jul	Aug	Sep	Oct	Nov	Dec
Minimum	-7	-6	-9	-16	-10	-9	-13	-17	-7	-13	-10	-6
Maximum	4	8	7	8	8	14	12	11	11	7	8	8

Parameter Definition

Monthly Averaged Clear Sky Insolation Incident On A Horizontal Surface (kWh/m^2/day)

Lat -33.933 Lon 18.643	Jan	Feb	Mar	Apr	May	Jun	Jul	Aug	Sep	Oct	Nov	Dec	Annual Average
22-year Average	8.96	7.96	6.64	5.07	3.80	3.26	3.53	4.56	6.05	7.58	8.73	9.11	6.26

Parameter Definition

Solar Geometry:

Monthly Averaged Solar Noon (GMT time)

Lat -33.933 Lon 18.643	Jan	Feb	Mar	Apr	May	Jun	Jul	Aug	Sep	Oct	Nov	Dec
Average	1056	1100	1055	1046	1042	1045	1052	1050	1041	1032	1030	1039

Parameter Definition

Monthly Averaged Daylight Hours (hours)

Lat -33.933 Lon 18.643	Jan	Feb	Mar	Apr	May	Jun	Jul	Aug	Sep	Oct	Nov	Dec
Average	14.1	13.2	12.3	11.2	10.3	9.91	10.1	10.8	11.8	12.9	13.8	14.3

Parameter Definition

Monthly Averaged Daylight Average Of Hourly Cosine Solar Zenith Angles (dimensionless)

Lat -33.933 Lon 18.643	Jan	Feb	Mar	Apr	May	Jun	Jul	Aug	Sep	Oct	Nov	Dec
Average	0.60	0.59	0.54	0.46	0.40	0.34	0.36	0.42	0.49	0.60	0.59	0.62

Parameter Definition

Monthly Averaged Declination (degrees)

Lat -33.933 Lon 18.643	Jan	Feb	Mar	Apr	May	Jun	Jul	Aug	Sep	Oct	Nov	Dec
Average	-20.7	-12.3	-1.8	9.71	18.8	23.0	21.2	13.7	3.08	-8.45	-18.1	-22.8

Parameter Definition

Monthly Averaged Maximum Solar Angle Relative To The Horizon (degrees)

Lat -33.933 Lon 18.643	Jan	Feb	Mar	Apr	May	Jun	Jul	Aug	Sep	Oct	Nov	Dec
Average	76.8	68.4	57.8	46.3	37.2	32.9	34.8	42.2	52.9	64.5	74.2	78.9

Parameter Definition

Monthly Averaged Hourly Solar Angles Relative To The Horizon (degrees)

Lat -33.933 Lon 18.643	Jan	Feb	Mar	Apr	May	Jun	Jul	Aug	Sep	Oct	Nov	Dec
0000 GMT	n/a	n/a	n/a	n/a	n/a	n/a	n/a	n/a	n/a	n/a	n/a	n/a
0100 GMT	n/a	n/a	n/a	n/a	n/a	n/a	n/a	n/a	n/a	n/a	n/a	n/a
0200 GMT	n/a	n/a	n/a	n/a	n/a	n/a	n/a	n/a	n/a	n/a	n/a	n/a
0300 GMT	n/a	n/a	n/a	n/a	n/a	n/a	n/a	n/a	n/a	n/a	n/a	n/a
0400 GMT	0.74	n/a	n/a	n/a	n/a	n/a	n/a	n/a	n/a	n/a	4.09	5.22
0500 GMT	12.3	7.01	2.24	n/a	n/a	n/a	n/a	n/a	2.18	10.5	16.0	16.8
0600 GMT	24.4	19.3	14.6	9.63	4.77	1.54	1.44	6.27	14.4	23.0	28.4	29.0
0700 GMT	36.8	31.7	26.7	21.0	15.4	11.8	12.0	17.4	26.2	35.2	40.8	41.3
0800 GMT	49.2	43.9	38.2	31.3	24.7	20.8	21.3	27.4	37.0	46.8	53.1	53.7
0900 GMT	61.3	55.3	48.2	39.6	31.9	27.7	28.7	35.5	45.9	56.9	64.5	65.8
1000 GMT	72.0	64.5	55.4	45.0	36.3	32.0	33.4	40.8	51.7	63.5	72.8	76.1
1100 GMT	76.7	68.4	57.8	46.2	37.0	32.8	34.8	42.2	52.7	63.6	72.8	77.9
1200 GMT	70.5	64.4	54.3	42.8	34.0	30.2	32.4	39.4	48.5	57.3	64.4	68.9
1300 GMT	59.5	55.1	46.4	35.9	27.7	24.5	26.9	33.1	40.5	47.4	53.0	57.1
1400 GMT	47.3	43.7	36.0	26.4	19.1	16.5	18.9	24.2	30.3	35.8	40.8	44.7
1500 GMT	34.9	31.5	24.3	15.5	9.01	6.81	9.20	13.8	18.8	23.6	28.4	32.3
1600 GMT	22.5	19.0	12.1	3.80	n/a	n/a	n/a	2.35	6.72	11.2	16.0	20.1
1700 GMT	10.5	6.73	n/a	n/a	n/a	n/a	n/a	n/a	n/a	n/a	4.09	8.32
1800 GMT	n/a	n/a	n/a	n/a	n/a	n/a	n/a	n/a	n/a	n/a	n/a	n/a
1900 GMT	n/a	n/a	n/a	n/a	n/a	n/a	n/a	n/a	n/a	n/a	n/a	n/a
2000 GMT	n/a	n/a	n/a	n/a	n/a	n/a	n/a	n/a	n/a	n/a	n/a	n/a
2100 GMT	n/a	n/a	n/a	n/a	n/a	n/a	n/a	n/a	n/a	n/a	n/a	n/a
2200 GMT	n/a	n/a	n/a	n/a	n/a	n/a	n/a	n/a	n/a	n/a	n/a	n/a
2300 GMT	n/a	n/a	n/a	n/a	n/a	n/a	n/a	n/a	n/a	n/a	n/a	n/a

Parameter Definition

Monthly Averaged Hourly Solar Azimuth Angles (degrees)

Lat -33.933 Lon 18.643	Jan	Feb	Mar	Apr	May	Jun	Jul	Aug	Sep	Oct	Nov	Dec
0000 GMT	n/a	n/a	n/a	n/a	n/a	n/a	n/a	n/a	n/a	n/a	n/a	n/a
0100 GMT	n/a	n/a	n/a	n/a	n/a	n/a	n/a	n/a	n/a	n/a	n/a	n/a
0200 GMT	n/a	n/a	n/a	n/a	n/a	n/a	n/a	n/a	n/a	n/a	n/a	n/a
0300 GMT	n/a	n/a	n/a	n/a	n/a	n/a	n/a	n/a	n/a	n/a	n/a	n/a
0400 GMT	114	n/a	n/a	n/a	n/a	n/a	n/a	n/a	n/a	n/a	109	114
0500 GMT	106	100	90.7	n/a	n/a	n/a	n/a	n/a	84.6	93.0	101	106
0600 GMT	99.4	92.2	82.2	71.4	63.5	60.6	62.9	68.6	75.9	84.5	93.5	99.3
0700 GMT	91.7	83.6	72.8	61.6	53.9	51.4	53.8	59.0	66.0	74.9	85.0	91.8
0800 GMT	82.8	73.2	61.2	49.7	42.5	40.4	42.9	47.6	53.8	62.5	74.2	82.7
0900 GMT	70.1	58.8	45.8	34.7	28.6	27.3	29.8	33.3	37.7	44.7	57.4	69.1
1000 GMT	46.5	35.7	24.4	15.9	12.2	12.2	14.4	16.0	16.5	17.5	24.7	39.5
1100 GMT	355	359	357	354	354	355	357	356	352	343	334	335
1200 GMT	308	323	330	334	337	339	341	337	329	316	302	296
1300 GMT	287	300	310	317	322	325	326	321	311	297	285	280

1400 GMT	275	286	296	304	310	313	313	308	297	285	274	270
1500 GMT	267	276	285	293	300	303	303	297	287	275	266	262
1600 GMT	259	267	276	284	n/a	n/a	n/a	288	278	267	258	255
1700 GMT	252	259	n/a	n/a	n/a	n/a	n/a	n/a	n/a	n/a	250	247
1800 GMT	n/a	n/a	n/a	n/a	n/a	n/a	n/a	n/a	n/a	n/a	n/a	n/a
1900 GMT	n/a	n/a	n/a	n/a	n/a	n/a	n/a	n/a	n/a	n/a	n/a	n/a
2000 GMT	n/a	n/a	n/a	n/a	n/a	n/a	n/a	n/a	n/a	n/a	n/a	n/a
2100 GMT	n/a	n/a	n/a	n/a	n/a	n/a	n/a	n/a	n/a	n/a	n/a	n/a
2200 GMT	n/a	n/a	n/a	n/a	n/a	n/a	n/a	n/a	n/a	n/a	n/a	n/a
2300 GMT	n/a	n/a	n/a	n/a	n/a	n/a	n/a	n/a	n/a	n/a	n/a	n/a

Parameter Definition

Parameters for Tilted Solar Panels:

Monthly Averaged Radiation Incident On An Equator-Pointed Tilted Surface ($kWh/m^2/day$)

Lat -33.933 Lon 18.643	Jan	Feb	Mar	Apr	May	Jun	Jul	Aug	Sep	Oct	Nov	Dec	Annual Average
SSE HRZ	8.17	7.30	5.91	4.30	3.09	2.64	2.85	3.67	4.92	6.46	7.68	8.18	5.42
K	0.68	0.67	0.65	0.61	0.57	0.56	0.57	0.58	0.60	0.63	0.66	0.66	0.62
Diffuse	1.88	1.66	1.38	1.12	0.90	0.76	0.82	1.05	1.38	1.66	1.88	2.02	1.37
Direct	9.36	8.66	7.52	6.11	5.02	4.76	4.91	5.38	6.16	7.52	8.67	9.11	6.92
Tilt 0	8.13	7.27	5.82	4.27	3.03	2.61	2.81	3.55	4.86	6.31	7.64	8.13	5.36
Tilt 18	7.92	7.43	6.41	5.13	3.93	3.57	3.75	4.37	5.49	6.62	7.53	7.83	5.82
Tilt 33	7.28	7.12	6.52	5.54	4.44	4.16	4.31	4.78	5.70	6.49	7.00	7.12	5.87
Tilt 48	6.27	6.44	6.27	5.65	4.70	4.50	4.62	4.93	5.59	6.02	6.11	6.06	5.59
Tilt 90	2.62	3.21	3.90	4.31	4.00	4.06	4.07	3.92	3.79	3.22	2.69	2.47	3.52
OPT	8.13	7.44	6.53	5.65	4.73	4.59	4.68	4.94	5.70	6.63	7.67	8.13	6.23
OPT ANG	3.00	14.0	30.0	45.0	55.0	60.0	58.0	49.0	35.0	20.0	6.00	0.00	31.3

NOTE:	*Diffuse radiation, direct normal radiation and tilted surface radiation are not calculated when the clearness index (K) is below 0.3 or above 0.8.*

Parameter Definition

Minimum Radiation Incident On An Equator-pointed Tilted Surface ($kWh/m^2/day$)

Lat -33.933 Lon 18.643	Jan	Feb	Mar	Apr	May	Jun	Jul	Aug	Sep	Oct	Nov	Dec	Annual Average
SSE MIN	7.57	6.87	5.35	3.63	2.79	2.41	2.46	3.03	4.58	5.59	6.89	7.72	4.89
K	0.63	0.63	0.59	0.51	0.51	0.51	0.49	0.48	0.55	0.55	0.59	0.63	0.56
Diffuse	2.13	1.84	1.60	1.33	0.98	0.83	0.92	1.21	1.50	1.95	2.18	2.21	1.56
Direct	8.70	8.42	6.90	5.11	4.56	4.55	4.31	4.41	5.98	6.48	7.93	8.89	6.34
Tilt 0	7.53	6.84	5.27	3.60	2.73	2.38	2.43	2.93	4.53	5.46	6.86	7.67	4.84
Tilt 18	7.34	6.98	5.75	4.21	3.47	3.19	3.14	3.48	5.07	5.68	6.76	7.40	5.20
Tilt 33	6.77	6.69	5.82	4.48	3.87	3.67	3.55	3.75	5.23	5.56	6.31	6.75	5.20
Tilt 48	5.86	6.06	5.58	4.52	4.07	3.94	3.76	3.82	5.12	5.16	5.54	5.77	4.93
Tilt 90	2.57	3.08	3.50	3.41	3.43	3.52	3.26	2.99	3.48	2.86	2.58	2.45	3.09
OPT	7.54	6.99	5.83	4.53	4.09	4.00	3.79	3.82	5.23	5.68	6.88	7.67	5.50

OPT ANG	3.00	14.0	29.0	43.0	54.0	59.0	56.0	46.0	34.0	19.0	6.00	0.00	30.3

NOTE:	*Diffuse radiation, direct normal radiation and tilted surface radiation are not calculated when the clearness index (K) is below 0.3 or above 0.8.*

Parameter Definition

Maximum Radiation Incident On An Equator-pointed Tilted Surface (kWh/m^2/day)

Lat -33.933 Lon 18.643	Jan	Feb	Mar	Apr	May	Jun	Jul	Aug	Sep	Oct	Nov	Dec	Annual Average
SSE MAX	8.50	7.85	6.30	4.65	3.35	3.01	3.18	4.09	5.48	6.93	8.30	8.83	5.86
K	0.70	0.72	0.69	0.66	0.62	0.64	0.63	0.64	0.66	0.68	0.71	0.72	0.67
Diffuse	1.72	1.38	1.19	0.97	0.80	0.61	0.68	0.88	1.15	1.45	1.58	1.71	1.18
Direct	9.47	9.22	7.80	6.39	5.42	5.53	5.47	5.91	6.95	7.79	9.15	9.80	7.40
Tilt 0	8.45	7.81	6.20	4.61	3.28	2.98	3.13	3.96	5.42	6.77	8.26	8.77	5.79
Tilt 18	8.23	8.01	6.88	5.63	4.33	4.22	4.30	4.97	6.20	7.13	8.14	8.43	6.36
Tilt 33	7.55	7.68	7.02	6.12	4.94	4.99	5.00	5.50	6.48	7.01	7.55	7.64	6.45
Tilt 48	6.50	6.94	6.76	6.26	5.26	5.45	5.41	5.71	6.38	6.50	6.58	6.48	6.18
Tilt 90	2.64	3.36	4.18	4.80	4.52	4.99	4.82	4.58	4.33	3.42	2.76	2.47	3.91
OPT	8.46	8.02	7.02	6.27	5.31	5.59	5.50	5.71	6.49	7.14	8.29	8.77	6.87
OPT ANG	3.00	14.0	31.0	46.0	56.0	62.0	59.0	50.0	37.0	21.0	6.00	0.00	32.1

NOTE:	*Diffuse radiation, direct normal radiation and tilted surface radiation are not calculated when the clearness index (K) is below 0.3 or above 0.8.*

Parameter Definition

Parameters for Sizing Battery or other Energy-storage Systems:

Minimum Available Insolation Over A Consecutive-day Period (%)

Lat -33.933 Lon 18.643	Jan	Feb	Mar	Apr	May	Jun	Jul	Aug	Sep	Oct	Nov	Dec
Min/1 day	9.91	33.5	6.09	11.3	20.7	15.5	9.47	14.4	14.8	4.02	6.51	14.4
Min/3 day	55.9	54.1	49.1	39.6	42.9	39.0	33.0	38.5	45.5	40.1	40.8	54.8
Min/7 day	74.6	70.0	69.7	52.9	59.6	55.1	53.4	61.3	59.7	65.1	62.3	69.9
Min/14 day	82.1	84.2	82.8	67.2	76.8	74.3	72.4	77.8	74.9	76.7	81.6	80.9
Min/21 day	88.8	90.7	86.0	76.0	83.0	81.9	69.0	83.2	79.1	84.2	84.3	88.5
Min/Month	92.6	94.1	90.5	84.4	90.2	91.2	86.6	82.5	93.0	86.5	89.7	94.3

Parameter Definition

Solar Radiation Deficits Below Expected Values Incident On A Horizontal Surface Over A Consecutive-day Period (kWh/m^2)

Lat -33.933 Lon 18.643	Jan	Feb	Mar	Apr	May	Jun	Jul	Aug	Sep	Oct	Nov	Dec
1 day	7.36	4.84	5.55	3.81	2.45	2.23	2.58	3.14	4.19	6.20	7.18	7.00
3 day	10.8	10.0	9.02	7.77	5.29	4.83	5.72	6.77	8.04	11.6	13.6	11.0
7 day	14.5	15.2	12.5	14.1	8.71	8.29	9.27	9.93	13.8	15.7	20.2	17.1
14 day	20.3	16.1	14.2	19.7	10.0	9.48	11.0	11.4	17.2	20.9	19.7	21.8
21 day	19.0	14.1	17.3	21.5	10.9	10.0	18.5	12.9	21.5	21.3	25.2	19.5
Month	18.6	12.0	17.3	20.1	9.30	6.89	11.7	19.8	10.2	26.9	23.6	14.2

Parameter Definition

Equivalent Number Of NO-SUN Or BLACK Days (days)

Lat -33.933 Lon 18.643	Jan	Feb	Mar	Apr	May	Jun	Jul	Aug	Sep	Oct	Nov	Dec
1 day	0.90	0.66	0.93	0.88	0.79	0.84	0.90	0.85	0.85	0.95	0.93	0.85
3 day	1.32	1.37	1.52	1.80	1.71	1.82	2.00	1.84	1.63	1.79	1.77	1.35
7 day	1.77	2.09	2.12	3.29	2.82	3.14	3.25	2.70	2.81	2.43	2.63	2.10
14 day	2.49	2.20	2.40	4.58	3.24	3.59	3.86	3.10	3.50	3.24	2.57	2.66
21 day	2.33	1.93	2.93	5.02	3.55	3.79	6.49	3.51	4.37	3.29	3.28	2.39
Month	2.27	1.64	2.93	4.67	3.00	2.61	4.13	5.40	2.07	4.17	3.08	1.74

Parameter Definition

Meteorology (Temperature):

Monthly Averaged Air Temperature At 10 m Above The Surface Of The Earth (°C)

Lat -33.933 Lon 18.643	Jan	Feb	Mar	Apr	May	Jun	Jul	Aug	Sep	Oct	Nov	Dec	Annual Average
22-year Average	21.9	22.4	21.0	18.5	15.9	13.3	12.6	13.1	14.7	17.1	19.1	20.7	17.5
Minimum	17.9	18.4	17.2	14.9	12.4	9.97	8.99	9.24	10.7	12.9	14.9	16.7	13.6
Maximum	26.1	26.6	25.1	22.6	20.0	17.2	16.6	17.6	19.4	21.4	23.3	24.6	21.7

Parameter Definition

Average Daily Temperature Range (°C)

Lat -33.933 Lon 18.643	Jan	Feb	Mar	Apr	May	Jun	Jul	Aug	Sep	Oct	Nov	Dec
22-year Average	8.16	8.21 *	7.85	7.78	7.65	7.28	7.69	8.44	8.69	8.53	8.35	7.92

*** Warmest month**

Parameter Definition

Average Minimum, Maximum and Amplitude Of The Daily Mean Earth Temperature (°C)

Lat -33.933 Lon 18.643	Jan	Feb	Mar	Apr	May	Jun	Jul	Aug	Sep	Oct	Nov	Dec	Annual Amplitude
Minimum	17.9	18.2	16.8	14.1	11.4	8.77	7.71	8.17	10.0	12.4	14.7	16.7	
Maximum	37.5	36.6	33.6	28.8	24.2	19.9	19.3	21.9	25.6	30.0	34.3	36.3	
Amplitude	9.81	9.21	8.36	7.34	6.43	5.59	5.79	6.87	7.80	8.80	9.78	9.78	14.9

Parameter Definition

Monthly Averaged Frost Days (days)

Lat -33.933 Lon 18.643	Jan	Feb	Mar	Apr	May	Jun	Jul	Aug	Sep	Oct	Nov	Dec	Annual Sum
22-year Average	0	0	0	0	0	0	0	0	0	0	0	0	0

Parameter Definition

Supporting Information:

Monthly Averaged Top-of-atmosphere Insolation ($kWh/m^2/day$)

Lat -33.933 Lon 18.643	Jan	Feb	Mar	Apr	May	Jun	Jul	Aug	Sep	Oct	Nov	Dec	Annual Average

22-year Average	11.9	10.8	9.05	7.03	5.39	4.63	4.97	6.30	8.18	10.1	11.5	12.2	8.51

Parameter Definition

Monthly Averaged Surface Albedo (0 to 1.0)

Lat -33.933 Lon 18.643	Jan	Feb	Mar	Apr	May	Jun	Jul	Aug	Sep	Oct	Nov	Dec	Annual Average
22-year Average	0.12	0.12	0.11	0.11	0.11	0.10	0.11	0.11	0.12	0.11	0.13	0.13	0.11

Parameter Definition

Back to SSE Data Set Home Page

Responsible > Data: Paul W. Stackhouse, Jr., Ph.D.
Officials > Archive: John M. Kusterer
Site Administration/Help: NASA Langley ASDC User Services (Contact Us)
[Privacy Policy and Important Notices]
Document generated on Sat Sep 10 06:54:16 EDT 2016

C2: Parameters Definitions

NASA Surface meteorology and Solar Energy - Definitions

Parameters for Solar Cooking:

Monthly Averaged Insolation Incident On A Horizontal Surface

22-year Average
The monthly average amount of the total solar radiation incident on a horizontal surface at the surface of the earth for a given month, averaged for that month over the 22-year period (Jul 1983 - Jun 2005). Each monthly averaged value is evaluated as the numerical average of 3-hourly values for the given month.

Units
$kWh/m^2/day$

Note
also referred to as global horizontal radiation

Reference
SSE Methodology for detailed discussion of the methodology for deriving the SSE horizontal surface insolation from satellite observations.

Monthly Averaged Midday Insolation Incident On A Horizontal Surface

22-year Average
The monthly average amount of the total solar radiation incident on a horizontal surface at the surface of the earth for a given month, averaged for that month over the 22-year period (Jul 1983 - Jun 2005). Each monthly averaged value is evaluated as the numerical average of the 3-hourly values, one per day, at the time (GMT) closest to local solar noon. The time (GMT) used is within 1.5 hours of local solar noon.

Units
kW/m^2

Reference
SSE Methodology for detailed discussion of the methodology for deriving the SSE horizontal surface insolation from satellite observations.

Monthly Averaged Clear Sky Insolation Incident On A Horizontal Surface

22-year Average
The monthly average amount of the total solar radiation incident on a horizontal surface at the surface of the earth when the cloud cover is less than 10%, averaged for that month over the 22-year period (Jul 1983 - Jun 2005).

Units
$kWh/m^2/day$

Reference
SSE Methodology for detailed discussion of the methodology for deriving horizontal surface insolation from satellite observations.

Monthly Averaged Clear Sky Days

22-year Average
The monthly average of the number of days having an average cloud cover less than 10% during a given month, averaged for that month over the 22-year period (Jul 1983 - Jun 2005).

Units
days

Parameters for Sizing and Pointing of Solar Panels and for Solar Thermal Applications:

Monthly Averaged Insolation Incident On A Horizontal Surface

22-year Average
The monthly average amount of the total solar radiation incident on a horizontal surface at the surface of the earth for a given month, averaged for that month over the 22-year period (Jul 1983 - Jun 2005). Each monthly averaged value is evaluated as the numerical average of 3-hourly values for the given month.

Minimum And Maximum Difference From Monthly Averaged Insolation
The minimum and maximum values for a given month indicate the percent difference between the year that has the least (minimum) or most (maximum) monthly averaged insolation and the 22-year monthly averaged insolation.

Units

- Monthly averaged insolation incident on horizontal surface in $kWh/m^2/day$
- Minimum and maximum values in percent

Note
also referred to as global horizontal radiation

Reference
SSE Methodology for detailed discussion of the methodology for deriving surface insolation from satellite observations.

Monthly Averaged Diffuse Radiation Incident On A Horizontal Surface

22-year Average
The monthly average amount of solar radiation incident on a horizontal surface at the surface of the earth under all-sky conditions with the direct radiation from the sun's beam blocked by a shadow band or tracking disk for a given month, averaged for that month over the 22-year period (Jul 1983 - Jun 2005). The horizontal diffuse radiation was evaluated using the method described in SSE Methodology.

Minimum and Maximum Diffuse Radiation

The minimum and maximum values for a given month indicate the least (minimum) and most (maximum) monthly average diffuse radiation for any one year in the 22-year period.

Average Clearness Index (K)
The monthly average amount of the total solar radiation incident on a horizontal surface at the surface of the earth divided by the monthly average incoming top-of-atmosphere insolation for a given month, averaged for that month over the 22-year period (Jul 1983 - Jun 2005); (i.e. clearness index is the fraction of insolation at the top of the atmosphere which reaches the surface of the earth).

Minimum and Maximum Clearness Index (K)
The minimum and maximum values for a given month indicate the least (minimum) and most (maximum) monthly average clearness index for any one year in the 22-year period.

Units

- 22-year Average, minimum and maximum diffuse radiation values in $kWh/m^2/day$
- K values are dimensionless

Note
no data is available when the clearness index is < 0.3 or > 0.8

Reference
SSE Methodology

Monthly Averaged Direct Normal Radiation

22-year Average
The monthly average amount of solar radiation incident on a surface oriented normal to the solar radiation for a given month, averaged for that month over the 22-year period (Jul 1983 - Jun 2005). The direct normal radiation is evaluated using the RETScreen method discussed in SSE Methodology.

Minimum And Maximum Difference From Monthly Averaged Direct Normal Radiation
The minimum and maximum values for a given month indicate the percent difference between the year that has the least (minimum) or most (maximum) monthly averaged direct normal radiation and the 22-year monthly averaged value.

Units

- Monthly averaged direct normal radiation in $kWh/m^2/day$
- Minimum and maximum in percent

Reference
SSE Methodology

Monthly Averaged Insolation Incident On A Horizontal Surface At Indicated GMT Times

Average@GMT
The monthly average amount of the total solar radiation incident on a horizontal surface at the surface of the earth for 3-hour intervals of GMT during the given month, averaged for that month over the 22-year period (Jul 1983 - Jun 2005).

Units
kW/m^2

Reference
SSE Methodology for detailed discussion of the methodology for deriving the SSE horizontal surface insolation from satellite observations.

Monthly Averaged Insolation Clearness Index (0 to 1.0)

22-year Average
The monthly average amount of the total solar radiation incident on a horizontal surface at the surface of the earth divided by the monthly average incoming top-of-atmosphere insolation for a given month, averaged for that month over the 22-year period (Jul 1983 - Jun 2005); (i.e. clearness index is the fraction of insolation at the top of the atmosphere which reaches the surface of the earth).

Minimum and Maximum
The minimum and maximum values for a given month indicate the least (minimum) and most (maximum) monthly average clearness index for any one year in the 22-year period.

Units
dimensionless

Monthly Averaged Insolation Normalized Clearness Index (0 to 1.0)

22-year Average
The monthly average zenith angle-independent expression of the insolation clearness index for a given month, averaged for that month over the 22-year period (Jul 1983 - Jun 2005); (i.e. clearness index is the fraction of insolation at the top of the atmosphere which reaches the surface of the earth).

$$K' = K / (1.031 * \exp(-1.4 / (0.9 + 9.4 / m)) + 0.1)$$

where:
K' = normalized clearness index
K = clearness index
m = air mass from Kasten's pyrheliometric formula

Units
dimensionless

Monthly Averaged Clear Sky Insolation Incident On A Horizontal Surface

22-year Average

The monthly average amount of the total solar radiation incident on a horizontal surface at the surface of the earth when the cloud cover is less than 10%, averaged for that month over the 22-year period (Jul 1983 - Jun 2005).

Units

kWh/m^2/day

Monthly Averaged Clear Sky Insolation Clearness Index (0 to 1.0)

22-year Average

The monthly average amount of the total solar radiation incident on a horizontal surface at the surface of the earth when the cloud cover is less than 10% divided by the monthly average incoming top-of-atmosphere insolation for a given month, averaged for that month over the 22-year period (Jul 1983 - Jun 2005); (i.e. clearness index is the fraction of insolation at the top of the atmosphere which reaches the surface of the earth).

Units

dimensionless

Monthly Averaged Clear Sky Insolation Normalized Clearness Index (0 to 1.0)

22-year Average

The monthly averaged zenith angle-independent expression of the clear sky insolation clearness index for a given month, averaged for that month over the 22-year period (Jul 1983 - Jun 2005); (i.e. clearness index is the fraction of insolation at the top of the atmosphere which reaches the surface of the earth).

Units

dimensionless

Monthly Averaged Downward Longwave Radiative Flux

22-year Average

The monthly average amount of the downward longwave radiative flux, averaged for that month over the 22-year period (Jul 1983 - Jun 2005).

Units

kWh/m^2/day

Solar Geometry:

Monthly Averaged Solar Noon

Average

The time when the sun is due south in the northern hemisphere or due north in the southern hemisphere. The determination of monthly averaged solar noon for each month is based on the "monthly average day" (SSE Methodology).

Units

GMT time

Note

during polar winter the sun may be below the horizon at solar noon

---

Monthly Averaged Daylight Hours

Average

The number of hours between sunrise and sunset. The determination of monthly averaged daylight for each month is based on the "monthly average day" (SSE Methodology).

Units

hours

Note

polar daylight is 0 in winter and 24 in summer

Monthly Averaged Daylight Average Of Hourly Cosine Solar Zenith Angles

Average

The average cosine of the angle between the sun and directly overhead during daylight hours. The determination of monthly averaged daylight average of hourly cosine solar zenith angles for each month is based on the "monthly average day" (SSE Methodology).

Average $\cos(\Theta_Z) = \{f \cos^{-1}(-f/g) + g[1 - (f/g)^2]^{½}\} / \cos^{-1}(-f/g)$

where:

f = sin(latitude) * sin(solar declination)
g = cos(latitude) * cos(solar declination)

Units

dimensionless

Reference

SSE Methodology, Reference: Gupta et al., 2001, *The Langley Parameterized Shortwave Algorithm (LPSA) for Surface Radiation Budget Studies*

Monthly Averaged Cosine Solar Zenith Angle At Mid-Time Between Sunrise And Solar Noon

Average

Approximate monthy average ratio of horizontal surface solar beam radiation to direct normal radiation. The determination of monthly averaged cosine solar zenith angle at mid-time between sunrise and solar noon for each month is based on the "monthly average day" (SSE Methodology).

$\cos(\Theta_{ZMT}) = f + g[(g - f) / 2g]^{½}$

where:

f = sin(latitude) * sin(solar declination)
g = cos(latitude) * cos(solar declination)

Units
dimensionless

Reference
SSE Methodology

Monthly Averaged Declination

Average
The angular distance of the sun north (positive) or south (negative) of the equator. Declination varies through the year from 23.45° north to 23.45° south and reaches the minimum/maximum at the southern/northern summer solstices. The determination of monthly averaged declination for each month is based on the "monthly average day" (SSE Methodology).

Units
degrees

Monthly Averaged Sunset Hour Angle

Average
The angle that the earth has rotated between the time of solar noon and sunset. Note that the earth rotates 15° with respect to the sun each hour. The determination of monthly averaged sunset hour angle for each month is based on the "monthly average day" (SSE Methodology).

Units
degrees

Monthly Averaged Maximum Solar Angle Relative To The Horizon

Average
The maximum vertical angle of the sun above the horizon. The determination of monthly averaged maximum solar angle relative to the horizon for each month is based on the "monthly average day" (SSE Methodology).

Units
degrees

Monthly Averaged Hourly Solar Angles Relative To The Horizon

Average
The vertical angle of the sun above the horizon. The determination of monthly averaged hourly solar angles relative to the horizon for each month is based on the "monthly average day" (SSE Methodology).

Units
degrees

Note
This information is provided to assist the user in interpreting diurnal variations in both insolation and clouds.

Monthly Averaged Hourly Solar Azimuth Angles

Average
The arc of the horizon measured clockwise from True North, to the point where a vertical circle through the sun intersects the horizon. The determination of monthly averaged hourly solar azimuth angles for each month is based on the "monthly average day" (SSE Methodology).

Units
degrees

Note
These angles are provided as a function of GMT to assist the user in interpreting diurnal variations of insolation and clouds in this data set. If either mornings or afternoons are habitually cloudy, it may be useful to point the solar panels slightly to the east or west instead of directly south.

Parameters for Tilted Solar Panels:

Monthly Averaged Radiation Incident On An Equator-Pointed Tilted Surface

SSE HRZ
The monthly average amount of the total solar radiation incident on a horizontal surface at the surface of the earth for a given month, averaged for that month over the 22-year period (Jul 1983 - Jun 2005).

Clearness Index (K)
The monthly average amount of the total solar radiation incident on a horizontal surface at the surface of the earth divided by the monthly average incoming top-of-atmosphere insolation for a given month, averaged for that month over the 22-year period.

Diffuse
The monthly average amount of solar radiation for a given month incident on a horizontal surface at the surface of the earth under all-sky conditions with the direct radiation from the sun's beam blocked by a shadow band or tracking disk, averaged for that month over the 22-year period.

Direct Normal
The monthly average amount of direct normal radiation incident on a surface oriented normal to the solar radiation for a given month, averaged for that month over the 22-year period.

Tilt 0, Latitude-15, Latitude, Latitude+15, 90
The monthly average amount of the total solar radiation incident on a surface tilted relative to the horizontal and pointed toward the equator for a given month, averaged for that month over the 22-year period (Jul 1983 - Jun 2005). Note that the differences between the Tilt 0 values and the SSE HRZ values are due to

approximations in the inputs and time integration inaccuracies when processing the equations and integrating over the "monthly average day" (SSE Methodology). Total solar radiation for each tilt angle was determined using the RETScreen Isotopic Diffuse Method discussed in SSE Methodology.

OPT
The monthly average amount of total solar radiation incident on a surface tilted at the optimum angle relative to the horizontal and pointed toward the equator.

OPT ANG
The angle relative to the horizontal for which the monthly averaged total solar radiation is a maximum.

Units

- SSE HRZ, Diffuse, Direct Normal, and OPT in $kWh/m^2/day$
- Tilt angles and OPT ANG in degrees
- K is dimensionless

Reference
SSE Methodology

Monthly Averaged Minimum Radiation Incident On An Equator-pointed Tilted Surface

SSE MIN
The monthly average amount of the total solar radiation incident on a horizontal surface at the surface of the earth for the year that has the least, or minimum, monthly averaged value in the 22-year period (Jul 1983 - Jun 2005).

Clearness Index (K)
The monthly average amount of the total solar radiation incident on a horizontal surface at the surface of the earth for the year that has the least, or minimum, monthly averaged value over the 22-year period divided by the monthly average incoming top-of-atmosphere insolation for that month.

Diffuse
The monthly average amount of solar radiation for a given month incident on a horizontal surface at the surface of the earth under all-sky conditions with the direct radiation from the sun's beam blocked by a shadow band or tracking disk for the year that has the most, or maximum, monthly averaged value over the 22-year period.

Direct Normal
The monthly average amount of direct normal radiation incident on a surface oriented normal to the solar radiation for the year that has the least, or minimum, monthly averaged value in the 22-year period.

Tilt 0, Latitude-15, Latitude, Latitude+15, 90
The monthly average amount of the total solar radiation incident on a surface tilted relative to the horizontal and pointed toward the equator for the year that has the least, or minimum, monthly averaged value in the 22-year period. Note that the differences between the Tilt 0 values and the SSE MIN values are due to approximations in the inputs and time integration inaccuracies when processing the equations and integrating over the "monthly average day" (SSE Methodology). Total solar radiation for each tilt angle was determined using SSE MIN in the RETScreen Isotopic Diffuse Method discussed in SSE Methodology.

OPT
The monthly average amount of total solar radiation incident on a surface tilted at the optimum angle relative to the horizontal and pointed toward the equator.

OPT ANG
The angle relative to the horizontal for which the monthly averaged total solar radiation is a maximum.

Units

- SSE MIN, Diffuse, Direct Normal, and OPT in $kWh/m^2/day$
- Tilt angles and OPT ANG in degrees
- K is dimensionless

Monthly Averaged Maximum Radiation Incident On An Equator-pointed Tilted Surface

SSE MAX
The monthly average amount of the total solar radiation incident on a horizontal surface at the surface of the earth for the year that has the most, or maximum, monthly averaged value in the 22-year period (Jul 1983 - Jun 2005).

Clearness Index (K)
The monthly average amount of the total solar radiation incident on a horizontal surface at the surface of the earth for the year that has the most, or maximum, monthly averaged value in the 22-year period divided by the monthly average incoming top-of-atmosphere insolation for that month.

Diffuse
The monthly average amount of solar radiation for a given month incident on a horizontal surface at the surface of the earth under all-sky conditions with the direct radiation from the sun's beam blocked by a shadow band or tracking disk for the year that has the least, or minimum, monthly averaged value in the 22-year period.

Direct Normal
The monthly average amount of direct normal radiation incident on a surface oriented normal to the solar radiation for the year that has the most, or maximum, monthly averaged value in the 22-year period.

Tilt 0, Latitude-15, Latitude, Latitude+15, 90
The monthly average amount of the total solar radiation incident on a surface tilted relative to the horizontal and pointed toward the equator for the year that has the most, or maximum, monthly averaged value in the 22-year period. Note that the differences between the Tilt 0 values and the SSE MAX values are due to approximations in the inputs and time integration inaccuracies when processing the equations and integrating over the "monthly average day" (SSE Methodology). Total solar radiation for each tilt angle was determined using SSE MAX in the RETScreen Isotopic Diffuse Method discussed in SSE Methodology.

OPT
The monthly average amount of total solar radiation incident on a surface tilted at the optimum angle relative to the horizontal and pointed toward the equator.

OPT ANG
The angle relative to the horizontal for which the monthly averaged total solar radiation is a maximum.

Units

- SSE MAX, Diffuse, Direct Normal, and OPT in $kWh/m^2/day$
- Tilt angles and OPT ANG in degrees
- K is dimensionless

Parameters for Sizing Battery or other Energy-storage Systems:

Various industry organizations use different methods to size either battery or other types of backup systems. One international organization has required that all stand-alone medical equipment that it purchases must operate for 6 BLACK or NO-SUN days in parts of the tropics. The methods used require different solar insolation parameters. Three types of parameters are provided in the SSE data set. They are:

1. **Minimum available insolation over a consecutive-day period** (1, 3, 7, 14, or 21 days) within a particular month over the 22-year period (Jul 1983 - Jun 2005) as a % of the expected average kWh/m^2 value over the same consecutive-day period (%)
2. **Solar radiation deficits below expected values incident on a horizontal surface over a consecutive-day period** (kWh/m^2)
3. **Equivalent number of NO-SUN or BLACK days** that must be supplied by the storage backup system (days)

Parameters for Sizing Surplus-product Storage Systems:

Available Surplus Insolation Over A Consecutive-day Period

Available surplus insolation over a consecutive-day period (1, 3, 7, 14, or 21 days) within a particular month over the 22-year period (Jul 1983 - Jun 2005) as a % of the expected average kWh/m^2 value over the same consecutive-day period (%)

Cloud Information:

Monthly Averaged Daylight Cloud Amount

22-year Average
Percent of cloud amount during daylight for a given month, averaged for that month over the 22-year period (Jul 1983 - Jun 2005).

Units
percent

Note
a value of zero indicates clear skies and a value of 100 indicates overcast skies

---

Monthly Averaged Cloud Amount At Indicated GMT Times

Average@GMT
Percent of cloud amount during daylight at 3-hour intervals of GMT for a given month, averaged for that month over the 22-year period (Jul 1983 - Jun 2005).

Units
percent

Note
a value of zero indicates clear skies and a value of 100 indicates overcast skies

---

Monthly Averaged Frequency Of Cloud Amount At Indicated GMT Times

< 10% @GMT
Percent of time the cloud amount is less than 10% (clear skies) at 3-hour intervals of GMT during daylight for a given month, averaged for that month over the 22-year period (Jul 1983 - Jun 2005).

10 - 70% @GMT
Percent of time the cloud amount is between 10 - 70% (broken-cloud skies) at 3-hour intervals of GMT during daylight for a given month, averaged for that month over the 22-year period (Jul 1983 - Jun 2005).

>= 70% @GMT
Percent of time the cloud amount is greater than or equal to 70% (near-overcast skies) at 3-hour intervals of GMT during daylight for a given month, averaged for that month over the 22-year period (Jul 1983 - Jun 2005).

Units
percent

Meteorology (Temperature):

Monthly Averaged Air Temperature at 10 m Above The Surface Of The Earth

22-year Average
The monthly average air temperature for a given month, averaged for that month over the 22-year period (Jan 1983 - Dec 2004). Temperature values are for 10 meters above the surface of the earth. Each monthly averaged value is evaluated as the numerical average of 3-hourly values for the given month.

Units
degrees Celsius

Reference
SSE Methodology

Average Daily Temperature Range

22-year Average
The average difference between the average daily minimum and average daily maximum for a given month, averaged for that month over the 22-year period (Jan 1983 - Dec 2004). Temperature values are for 10 meters above the surface of the earth.

Units
degrees Celsius

Note
the warmest month is marked with an asterisk (*)

Reference
SSE Methodology

Monthly Averaged Cooling Degree Days Above 18° C

22-year Average
The monthly average of the accumulation of degrees when the daily mean temperature is above 18 degrees Celsius over the 22-year period (Jan 1983 - Dec 2004). Temperature values are for 10 meters above the surface of the earth.

Monthly Cooling Degree Days
For the days of a given month,
sum the quantity [((Tmin + Tmax) / 2) - 18]
when (Tmin + Tmax) / 2 > 18.

Units
degree days

Monthly Averaged Heating Degree Days Below 18° C

22-year Average
The monthly average of the accumulation of degrees when the daily mean temperature is below 18 degrees Celsius over the 22-year period (Jan 1983 - Dec 2004). Temperature values are for 10 meters above the surface of the earth.

Monthly Heating Degree Days
For the days of a given month,
sum the quantity [18 - (Tmin + Tmax) / 2]
when (Tmin + Tmax) / 2 < 18.

Units
degree days

Reference
SSE Methodology

Monthly Averaged Arctic Heating Degree Days Below 10° C

22-year Average
The monthly average of the accumulation of degrees when the daily mean temperature is below 10 degrees Celsius over the 22-year period (Jan 1983 - Dec 2004). Temperature values are for 10 meters above the surface of the earth.

Monthly Heating Degree Days
For the days of a given month,
sum the quantity [10 - (Tmin + Tmax) / 2]
when (Tmin + Tmax) / 2 < 10.

Units
degree days

Monthly Averaged Arctic Heating Degree Days Below 0° C

22-year Average
The monthly average of the accumulation of degrees when the daily mean temperature is below 0 degrees Celsius over the 22-year period (Jan 1983 - Dec 2004). Temperature values are for 10 meters above the surface of the earth.

Monthly Heating Degree Days
For the days of a given month,
sum the quantity [0 - (Tmin + Tmax) / 2]
when (Tmin + Tmax) / 2 < 0.

Units
degree days

Monthly Averaged Earth Skin Temperature

22-year Average
The monthly average of the earth's surface temperature for a given month, averaged for that month over the 22-year period (Jan 1983 - Dec 2004).

Units
degrees Celsius

Note
data over oceans is sea surface temperature

Average Minimum, Maximum and Amplitude Of The Daily Mean Earth Temperature

Minimum
The minimum of the daily mean earth's surface temperature for a given month, averaged over the 22-year period (Jan 1983 - Dec 2004).

Maximum
The maximum of the daily mean earth's surface temperature for a given month, averaged over the 22-year period (Jan 1983 - Dec 2004).

Amplitude
One half of the difference between the 22-year average minimum and 22-year average maximum.

Units
degrees Celsius

Monthly Averaged Frost days

22-year Average
The monthly average of the number of days for which the temperature falls below 0 degrees Celsius for a given month, averaged for that month over the 22-year period (Jan 1983 - Dec 2004). Temperature values are for 10 meters above the surface of the earth.

Units
days

Monthly Averaged Dew/Frost Point Temperature

22-year Average
The monthly average dew or frost point temperature for a given month, averaged for that month over the 22-year period (Jan 1983 - Dec 2004). The dew point of a given parcel of air is the temperature to which the parcel must be cooled, at constant barometric pressure, for the water vapor component to condense into water, called dew. When the dew point temperature falls below freezing it is called the frost point, instead creating frost. Dew/frost point temperature values are for 10 meters above the surface of the earth.

Units
degrees Celsius

Monthly Averaged Air temperature at 10 m Above The Surface Of The Earth For Indicated GMT Times

Average@GMT
The monthly average air temperature for 3-hour intervals of GMT during a given month, averaged for that month over the 22-year period (Jan 1983 - Dec 2004). Temperature values are for 10 meters above the surface of the earth.

Units
degrees Celsius

Meteorology (Wind):

Monthly Averaged Wind speed At 50 m Above The Surface Of The Earth

10-year Average
The monthly average wind speed for a given month, averaged for that month over the 10-year period (July 1983 - June 1993). Wind speed values are for 50 meters above the surface of the earth. Each monthly averaged value is evaluated as the numerical average of 3-hourly values for the given month.

Minimum And Maximum Difference From Monthly Averaged Wind Speed At 50 m
The minimum and maximum values for a given month indicate the percent difference between the year that has the least (minimum) or most (maximum) monthly averaged wind speed at 50 m and the 10-year monthly averaged wind speed at 50 m.

Units

- Monthly Averaged Wind speed in meters per second (m/s)
- Minimum and maximum values in percent

Reference
SSE Methodology

Monthly Averaged Percent Of Time The Wind Speed At 50 m Above The Surface Of The Earth Is Within The Indicated Range

Wind Speed Ranges
The monthly average percent of time that wind speed is within the indicated range for a given month, averaged for that month over the 10-year period (July 1983 - June 1993). Wind speed values are for 50 meters above the surface of the earth.

Units
percent

Monthly Averaged Wind Speed At 50 m Above The Surface Of The Earth For Indicated GMT Times

Average@GMT
The monthly average wind speed for 3-hour intervals of GMT during a given month, averaged for that month over the 10-year period (July 1983 - June 1993). Wind speed values are for 50 meters above the surface of the earth.

Units
meters per second (m/s)

Monthly Averaged Wind Direction At 50 m Above The Surface Of The Earth

10-year Average
The monthly average wind direction for a given month, averaged for that month over the 10-year period (July 1983 - June 1993). Wind direction values are for 50 meters above the surface of the earth.

Units
degrees

Notes

- measured clockwise from True North
- direction the wind is coming from

Monthly Averaged Wind Direction At 50 m Above The Surface Of The Earth For Indicated GMT Times

Average@GMT

The monthly average wind direction for 3-hour intervals of GMT during a given month, averaged for that month over the 10-year period (July 1983 - June 1993). Wind direction values are for 50 meters above the surface of the earth.

Units

degrees

Notes

- measured clockwise from True North
- direction the wind is coming from

Monthly Averaged Wind Speed At 10 m Above The Surface Of The Earth For Terrain Similar To Airports

10-year Average

The monthly average wind speed for a given month, averaged for that month over the 10-year period (July 1983 - June 1993) where the wind speed was evaluated at 10 m above the surface of the earth assuming the underlying terrain is similar to that typical of airports (e.g. "airport" flat rough grass category taken from Gipe; SSE Methodology).

Units

meters per second (m/s)

Reference

SSE Methodology

Difference Between The Average Wind Speed At 10 m Above The Surface Of The Earth And The Average Wind speed At 50 m Above The Surface Of The Earth

10-year Average

The percent difference between the 10-year monthly average of the wind speed at 10 m above the surface of the earth and the 10-year monthly average of the wind speed at 50 m above the surface of the earth.

Percent difference at 10 m = ((Wind Speed At 10 m - Wind Speed At 50 m) / Wind Speed At 50 m) * 100

Units

percent

Monthly Averaged Wind Speed Adjusted For Height And Vegetation Type

10-year Average

The monthly average wind speed for a given month, averaged for that month over the 10-year period (July 1983 - June 1993) where the wind speed is evaluated using the Gipe Power Law. The wind speed at 50 m above the surface of the earth and the surface roughness exponent based on the chosen vegetation type are used in the equation:

$$V = V_0 * (H / H_0)^{\alpha}$$

Where:

V_0 = wind speed at the original height
V = wind speed at the new height
H_0 = original height
H = new height
α = surface roughness exponent

Units

meters per second (m/s)

Reference

SSE Methodology, Reference: Gipe, 1999, *Wind Energy Basics*

Meteorology (Other):

Monthly Averaged Relative Humidity

22-year Average

The monthly average of relative humidity for a given month, averaged for that month over the 22-year period (Jan 1983 - Dec 2004). The relative humidity is calculated from the air temperature and specific humidity at 10 meters above the surface of the earth and the surface pressure.

Units percent

Reference

SSE Methodology

Monthly Averaged Specific Humidity

22-year Average

The monthly average of the specific humidity for a given month, averaged for that month over the 22-year period (Jan 1983 - Dec 2004). Specific humidity values are for 10 meters above the surface of the earth.

Units

kg/kg

Monthly Averaged Atmospheric Pressure

22-year Average
The monthly average of atmospheric pressure at the surface of the earth for a given month, averaged for that month over the 22-year period (Jan 1983 - Dec 2004).

Units
kPa

Reference
SSE Methodology

Monthly Averaged Total Column Precipitable Water

22-year Average
The monthly average of the total amount of atmospheric water vapor contained in a vertical column of unit cross-sectional area extending from the surface to the top of the atmosphere for a given month, averaged for that month over the 22-year period (Jul 1983 - Jun 2005).

Units
cm

Monthly Averaged Precipitation

22-year Average
The average daily rain rate based upon the total monthly averaged amount of rain for the given month divided by the number of days in the month, averaged for that month over the 22-year period (Jan 1983 - Dec 2004).

Units
mm/day

Reference
SSE Methodology

Supporting Information:

Monthly Averaged Top-of-atmosphere Insolation

22-year Average
The monthly average amount of the total solar radiation incident on the top-of-atmosphere for a given month, averaged for that month over the 22-year period (Jul 1983 - Jun 2005).

Units
$kWh/m^2/day$

Note
also referred to as extraterrestrial radiation (ETR)

Monthly Averaged Surface Albedo

22-year Average
The monthly average ratio of the solar energy reflected by the surface of the earth to monthly average solar energy incident on the surface of the earth for a given month, averaged for that month over the 22-year period (Jul 1983 - Jun 2005). (i.e. Fraction of insolation reflected by the surface of the earth.)

Units
dimensionless

Last modified 03/29/2016 19:41:52

Appendix D: Global irradiation of South Africa